CENTRO DE INVESTIGACIONES EN OPTICA, A.C.

“CERTIFICATION OF CONTINUOUS VARIABLE BIPARTITE AND TRIPARTITE QUANTUM ENTANGLEMENT AND STEERING IN A SYSTEM WITH A NONLINEAR INTERACTION”

Tesis que para obtener el grado de Doctora en Ciencias (Óptica)

Presenta: Patricia del Rocío Ornelas Cruces

Directora de Tesis: Dra. Laura Elena Casandra Rosales Zárate

León · Guanajuato · México
Octubre de 2024

Acknowledgments

Agradezco a **CONAHCYT** por el apoyo económico otorgado para la realización del posgrado y elaboración de este trabajo.

Al **Centro de Investigaciones en Óptica, A. C.**, por brindarme el apoyo para continuar mi formación académica.

Agradezco profundamente a mis padres, *Patricia* y *Marco*, por sus consejos y enseñanzas, por su apoyo incondicional para superarme y concluir este proyecto; por siempre creer en mí y estar presentes en cada etapa. No existen palabras que agradezcan todo el apoyo y cuidados que me brindaron en estos cuatro años.

Agradezco a mis hermanos por sus consejos y compañía. *Marco*, siempre serás un ejemplo para mí. *Valeria,* gracias por siempre motivarme con el fin de poder apoyarte cuando sea necesario.

Agradezco a *Fer* por todo su apoyo, compresión y cariño incondicional. Gracias por creer en mí desde el momento en que decidí empezar este proyecto. Por ayudarme y cuidarme cuando más lo necesité. No hay forma de agradecer el tiempo que me acompañaste mientras trabajaba en este proyecto.

Agradezco a mis amigos, *Paty Tavares* y *Gerardo Rodríguez* por acompañarme, escucharme y cuidarme. Por su apoyo incondicional y su invaluable amistad. *Paty*, gracias por todo el tiempo que compartimos. *Gerardo*, agradezco tu tiempo para escuchar mis ideas, por las gratas discusiones, observaciones y comentarios.

A mi directora de tesis, *Dr. Laura E. C. Rosales Zárate*, agradezco su tiempo, dedicación, esfuerzo y paciencia. Por compartir sus conocimientos conmigo y por todas las contribuciones realizadas a este trabajo. Gracias por siempre motivarme a mejorar. Agradezco su confianza y el apoyo incondicional brindado para concluir este proyecto.

Por último, agradezco a los sinodales, *Dr. Ricardo Gutiérrez Jáuregui*, *Dr. Carlos Herman Wiechers Medina*, *Dr. Roberto Ramírez Alarcón* y *Dra. Laura E. C. Rosales Zárate*, por su tiempo para leer este trabajo en detalle, así como las discusiones, correciones y observaciones realizadas.

Abstract

In recent years, there has been great interest and effort to develop quantum technologies which enable quantum communication. Such technologies utilize quantum nonlocal correlations, such as entanglement and steering, as a resource for quantum information protocols. It has been demonstrated that the systems that generate quantum entanglement and steering are those that are based on nonlinear processes such as spontaneous parametric down conversion, four wave mixing, sum/difference frequency generation, second harmonic generation, and third harmonic generation. Moreover, those systems can produce bipartite, tripartite or even multipartite quantum entanglement and steering. Recently, there have been proposals based on these nonlinear processes that takes place inside optical cavities which can also demonstrate the production of multipartite nonlocal correlations. In this work, we investigate quantum entanglement and steering generated by an intracavity down conversion process. We consider the interaction of three fields with a nonlinear medium inside an optical cavity. As a result, three down converted fields are obtained outside the cavity. We analyze this system by using the master equation, the phase-space methods and the linearized fluctuation formalisms. In particular, we consider the positive-P function and we obtain the intracavity spectrum in the frequency domain. We certify bipartite, tripartite and genuine tripartite entanglement, as well as bipartite one-way and two-way steering, and full tripartite two-way steering inseparability in quadrature operators in the frequency domain by using different entanglement and steering criteria. We also investigate the distribution of these quantum corrrelations among the different parties of the system through the monogamy relations for the entanglement and steering witnesses that we use throughout this work. Our results determine frequency values where these correlations are present in the system under consideration.

Contents

1 Introduction **1**

2 Criteria for the certification of quantum entanglement and steering **7**

2.1 Criteria for the certification of entanglement 8

2.1.1 Bipartite entanglement 8

2.1.2 Tripartite entanglement 10

2.2 Criteria for the certification of steering 11

2.2.1 Bipartite steering 11

2.2.2 Tripartite steering 11

3 Monogamy relations for quantum entanglement and steering witnesses **14**

3.1 Monogamy relations for quantum entanglement witnesses 15

3.2 Monogamy relations for quantum steering witness 16

4 Nonlinear Hamiltonian model and its master equation **17**

4.1 Nonlinear Hamiltonian model 18

4.2 Master equation of the system 20

5 Linearized fluctuation analysis **25**

5.1 Linearized fluctuation theory 25

5.2 Spectrum outside the cavity 26

6 Certification of quantum entanglement among the output fields **32**

6.1 Certification of bipartite entanglement 33

6.2 Certification of tripartite entanglement 35

7 Certification of quantum steering among the output fields 38

7.1 Certification of bipartite steering 38

7.2 Certification of full tripartite two-way steering inseparability 40

7.3 Certification of genuine tripartite steering 42

7.3.1 Certification of genuine tripartite steering: $g_i = 1$ 42

8 Distribution of entanglement and steering among the output fields 46

8.1 Distribution of entanglement between the output fields 46

8.2 Distribution of steering among the output fields 49

9 Conclusions 57

A Relation between the theoretical and experimental parameters of the system 59

Bibliography 62

Chapter 1

Introduction

Classical physics was able to describe the majority of the known phenomena until the end of the nineteenth century. It was the quantization of radiation, proposed by Max Planck, that led physics into a new era: the birth of the quantum mechanics. Since then, quantum mechanics has been playing a crucial role in the understanding of nature. Nonetheless, Einstein, Podolsky and Rosen (EPR) were not completely convinced that quantum mechanics was a complete theory [1]. In their seminal paper, they considered two systems which had interacted and had been spatially separated. Both parties, say A and B, are correlated in their positions and momenta. They considered the state of the system which is composed by parties A and B as:

$$\Psi(x_A, x_B) = \sum_{n=1}^{\infty} \psi_n(x_B)\phi_n(x_A) = \sum_{n=1}^{\infty} \varphi_n(x_B)\upsilon_n(x_A), \tag{1.1}$$

where $\phi_n(x_A)$ and $\upsilon_n(x_A)$ ($\psi_n(x_B)$ and $\varphi_n(x_B)$) are two set of eigenfunctions of A (B). If one performs a measurement in A by choosing $\phi_n(x_A)$ ($\upsilon_n(x_A)$), then B instantaneously projects onto $\psi_n(x_B)$ ($\varphi_n(x_B)$). Therefore, two different measurements performed in A implies that B may be projected into two different states and, in EPR words [1], "the two systems no longer interact, no real change can take place in the second system in consequence of anything that may be done to the first system". Thus, they concluded that this nonlocality was due to the incompleteness of the quantum theory.

Schrödinger, as a response to EPR, investigated the system proposed by EPR [2]. He remarked [2], "when two systems, of which we know the states by their respective representatives, enter into temporary physical interaction due to known forces between them, and when after a time of mutual influence the systems separate again, then they can no longer be described in the same way as before, viz. by endowing each of them with a representative of its own". In addition, he states [2]: "By the interaction the two representatives (or ψ-functions) have become entangled". So, here he introduced the term *entangled*. In [2], Schrödinger pointed out what entanglement is:

"Let x and y stand for all the coordinates of the first and second systems respectively and $\Psi(x, y)$ for the normalized representative of the state of the composed system, when the two have separated again, after the interaction has taken place. What constitutes the entanglement is that Ψ is not a product of a function of x and a function of y."

This leads to the following definition of entanglement: In the case of a pure state, it is said that the state $|\psi\rangle$ of a system composed by two spatially separated systems, A and B, is entangled if we cannot express $|\psi\rangle$ as a product of the states of A ($|\psi_A\rangle$) and B ($|\psi_B\rangle$) respectively. This can be expressed as [3, 4]

$$|\psi\rangle \neq |\psi_A\rangle\,|\psi_B\rangle\,. \tag{1.2}$$

While in the case of mixed states, which are described by a density operator ρ_{AB}, the definition of entanglement is given by [3]

$$\rho_{AB} \neq \sum_i p_i \rho_A^i \otimes \rho_B^i, \tag{1.3}$$

where p_i is the probability distribution and ρ_A^i (ρ_B^i) is the density operator of the system A (B).

In [2], Schrödinger also introduced the term *steer* where he mentioned that [2]: "It is rather discomforting that the theory should allow a system to be steered or piloted into one or the other type of state at the experimenter's mercy in spite of his having no access to it". That is, for a system composed by two parties, say A and B, A can steer the state on B into an eigenstate of either position or momentum, by choosing the measurements on A [5]. Notice that, the steerability of one of the systems, say B, depends on the measurements performed by A. While in the case that B steers A, is based on the measurements from B. Thus, steering has the property of being asymmetric.

Nowadays, these nonlocal effects are known as quantum entanglement and steering, respectively. Because of this nonlocal behaviour, quantum entanglement and steering are quantum nonlocal correlations. It is worth mentioning that the set of steerable states is a subset of the set of entangled states (see Figure 1.1). That is, not all entangled states are steerable [6, 7]. For instance, the parametrized Werner state, which is given by [6, 7]

$$W_d^\eta = \left(\frac{d-1+\eta}{d-1}\right)\frac{\boldsymbol{I}}{d^2} - \left(\frac{\eta}{d-1}\right)\frac{\boldsymbol{V}}{d}, \tag{1.4}$$

is entangled iff $\eta > 1/(d+1)$ [8], whereas W_d^η is steerable iff $(1-\eta)/d^2 < 1/d^3$. If the inequality $(1-\eta)/d^2 < 1/d^3$ is saturated, then $\eta_{steer} = 1 - 1/d$ and thus, the Werner state is unsteerable for $\eta \leqslant \eta_{steer}$ [6, 7]. Here, $\eta \in \mathbb{R}$ is the parameter, $\eta \in [0, 1]$, $\boldsymbol{I}$ and $\boldsymbol{V}$ are the identity and the flip operator ($\boldsymbol{V}\,|\phi, \psi\rangle = |\psi, \phi\rangle$), respectively, and d is

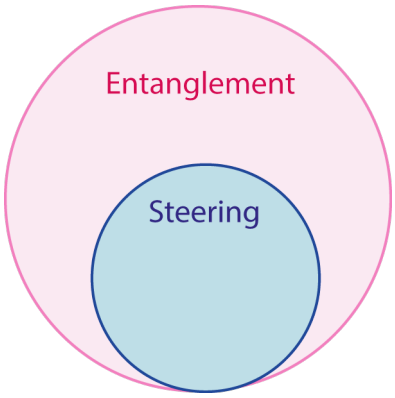

Figure 1.1: The set of steerable states is a subset of the set of entangled states: Quantum steering $\subseteq$ Quantum entanglement.

the dimension of the Hilbert space. For $d = 2$, W_d^η are entangled if $\eta > 1/\sqrt{2}$, while these are steerable if $\eta \geqslant 1/2$ [6, 7]. The one-way steerability of the Werner state has been demonstrated by Wollmann et al. [9]. In this work, the authors considered a parametrized Werner state with parameter $\mu \in [0, 1]$. They showed that if the Werner state is distributed through a lossy channel, then the Werner state is parametrized by probability p. They found that the relation between the parameter of the Werner state μ and the probability p must be $p > (2\mu+1)/3$ in order to be one-way steerable by one party, say Alice, and unsteerable by the other party, say Bob. Additionally, they proposed a steering inequality, which is based on Bob's choice of measurement setting and Alice outcomes. Experimentally, the authors demonstrated that one-way steering regime is parametrized by the value of μ of the Werner state and the loss p. Another example is the work of Händchen, V. et al. [10], where the authors experimentally generated two entangled Gaussian modes of light. They found that these modes are steerable (both two-way and one-way) or not steerable, depending on the contribution of the added vaccum to one of the modes.

Recently, these two quantum nonlocal correlations have been one of the main resource of quantum information (QI) protocols [3, 5, 11–18], and both have played a crucial role in the development of quantum technologies [19–21]. These emergent technologies take advantage of quantum principles to transform quantum states and utilize its properties. Therefore, the scientific community has focused on new research fields such as quantum communication [22], quantum computation [23], and quantum metrology [24]. There exist two main type of systems that these technologies use which are the discrete variable (DV) and the continuous variable (CV) system. The first one has a finite-dimensional Hilbert space with a discrete spectrum. While the second one has an infinite-dimensional Hilbert space and a continuous spectrum. Additionally, one can form bases for the infinite-dimensional Hilbert space with the eigenstates of the operators with continuous spectrum [25]. These operators are known as *quadrature operators.*

Currently, there has been great interest in CV quantum information protocols since the information is encoded in their quadrature operators [26, 27]. An example of these protocols is the CV Quantum Key Distribution (CV-QKD) [28–30] which is a protocol use to establish secure communication between two distant locations. Some CV-QKD protocols utilize the asymmetric property of steering to guarantee the security of the protocol [29, 31–33]. Another examples of CV QI protocols which take advantage of entanglement and steering are the CV quantum teleportation (CV-QT) [34–36] and the CV Quantum Secret Sharing (CV-QSS) [17, 37–39]. The former is an entanglement-based protocol which is utilized to teleport an unknown quantum state between a sender and a receiver, which are spatially separated and both share an entangled state. While the latter is a protocol in which the information is split into n parties that share an entangled state (securely encoded) and it can be reconstructed by a collaboration of the k number of parties where $k \leqslant n$. Additional security in CV-QSS [17] and CV-QT [36] is provided when quantum steering is also consider as a resource. Another way to guarantee the security of CV QI protocols is through the monogamy relations for entanglement (steering) [40, 41], which give information about the distribution of entanglement (steering) among the different parties of the system. That is, monogamy relations establish a bound on the entanglement (steering) that two parties (say A and B) of the system share and, if a third party (say C) interacts with A or B, the monogamy relations are violated. Thus, since both quantum nonlocal correlations are important resources for potential applications in QI protocols, in recent years, there have been theoretical and experimental investigation on the certification of quantum entanglement and steering, and also on the generation of these correlations [42–51]. In fact, it has been demonstrated that these correlations can be generated through nonlinear processes when the nonlinear medium is placed inside a cavity [45, 52–64]. One of the most important nonlinear process which can generate both correlations is the Spontaneous Parametric Down Conversion (SPDC) process.

In the SPDC process, a photon, known as the pump photon with energy ω_p, is converted into a pair of photons with lower energies, namely signal (ω_s) and idler (ω_i) photons [65]. The photons of the SPDC process must satisfy the phase-matching conditions, which are the conservation of the energy and momentum. These conditions are given by [65]

$$\hbar\omega_p = \hbar\omega_s + \hbar\omega_i, \tag{1.5}$$

$$\overrightarrow{k_p} = \overrightarrow{k_s} + \overrightarrow{k_i}, \tag{1.6}$$

where ω_j and $\vec{k_j}$ ($j = p,\ s,\ i$) are the energy and the wave vector, respectively, of the j photon in the SPDC process.

In this thesis we focus on a CV system which can generate both entanglement and steering. In particular, we consider three nonlinear processes inside an optical cavity. That is, three input fields interact with the nonlinear medium and, through SPDC,

three output fields are generated. We also investigate the certification of the different cases of entanglement and steering that this system can produce. Moreover, we study the distribution of both correlations among the different parties of the system under consideration.

This thesis is structured in the following way: In this Chapter 1, we give a brief introduction which contains the important concepts for the development of this work. Afterwards, the entanglement and steering criteria that we use for the certification of both correlations are summarized in Chapter 2. As we are also interested in investigating the distribution of both correlations among the different parties of the system, we have summarized the monogamy relations for different entanglement and steering criteria in Chapter 3. In Chapter 4, we describe the system that we propose for the generation of entanglement and steering, the Hamiltonian and the master equation of the system. While Chapter 5 contains the formalism to analyze the system under consideration in the frequency domain. In Chapter 6 and Chapter 7, we present our results which includes the certification of both correlations in the frequency domain. The distribution of entanglement and steering among the parties of the system is presented in Chapter 8. We discuss our results in Chapter 9. A block diagram of the structure of this thesis is shown in Figure 1.2.

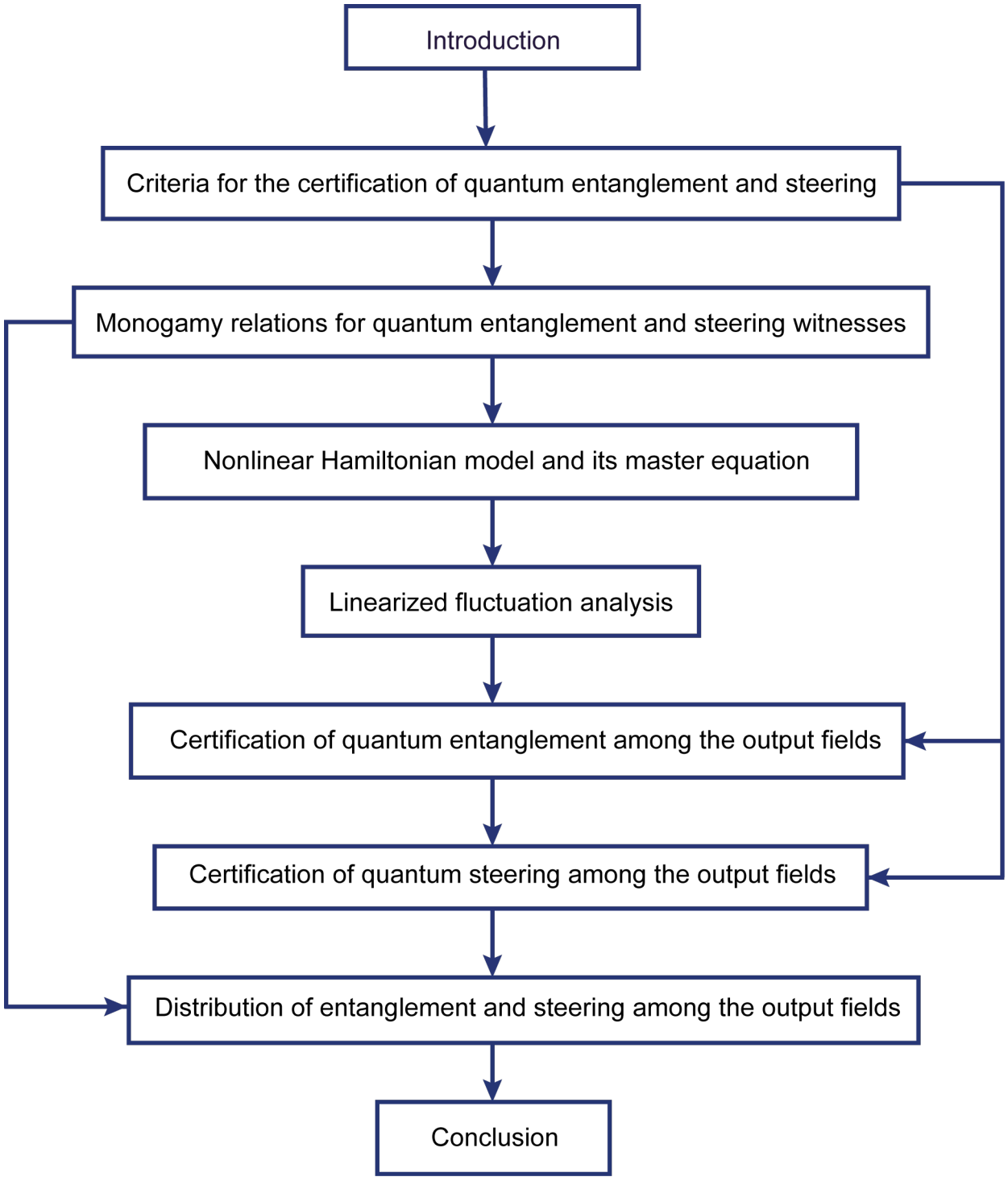

Figure 1.2: Block diagram of the structure of this thesis.

Chapter 2

Criteria for the certification of quantum entanglement and steering

Quantum nonlocal correlations such as quantum entanglement and steering are correlations that might be present in a system. A natural question that arises is: how to certify entanglement and steering in a system? That is, how can one identify which states are entangled or steerable and which are not? There are different criteria that provide the answer to these questions depending on the system under consideration.

In this chapter, we review different entanglement and steering criteria for continuous variable (CV) systems that certify these correlations in bipartite and multipartite systems. It is important to mention that we focus on the certification of quantum correlations, rather than their quantification.

In section 2.1 and section 2.2, we present the main criteria for the certification of entanglement and steering, respectively. These criteria include the bipartite and tripartite case.

We wish to emphasize that we have focused on the certification of entanglement and steering in quadrature operators. These operators are defined as a function of the creation ($\hat{a}^\dagger$) and annihilation ($\hat{a}$) bosonic operator:

$$\hat{X} = \frac{c}{2}\left(\hat{a} + \hat{a}^\dagger\right), \quad \hat{Y} = \frac{c}{2i}\left(\hat{a} - \hat{a}^\dagger\right).$$

Throughout this work we consider $c = 2$ [66, 67] such that the quadrature operators are given by

$$\hat{X} = \hat{a} + \hat{a}^\dagger, \quad \hat{Y} = -i\left(\hat{a} - \hat{a}^\dagger\right). \tag{2.1}$$

Thus, the commutator relation for this case is $\left[\hat{X},\hat{Y}\right]=2i$. These operators satisfy the uncertainty relation [68]

$$\left\langle (\Delta A)^2\right\rangle \left\langle (\Delta B)^2\right\rangle \geqslant \frac{1}{4}\left|\langle [A,B]\rangle\right|^2, \tag{2.2}$$

where $V(O)\equiv(\Delta O)^2$ is the variance of O ($O=A,B$). From our definition of the quadrature operators and the uncertainty relation (Equation 2.2), the Heisenberg realtion for $\hat{X}$ and $\hat{Y}$ is

$$V\left(\hat{X}\right)V\left(\hat{Y}\right)\geqslant 1. \tag{2.3}$$

The criteria that we use are expressed in terms of the variance $V\left(\hat{X}\right)$ ($V\left(\hat{Y}\right)$) and covariance $V\left(\hat{X},\hat{Y}\right)$ of our definition of the quadrature operators $\hat{X}$ and $\hat{Y}$ (Equation 2.1), which satisfy the aforementioned relations.

2.1 Criteria for the certification of entanglement

In order to certify entanglement in a quantum system, first we focus on the certification of bipartite entanglement utilizing the criteria developed by Tan, Duan-Giedke-Cirac-Zoller (DGCZ) and Simon [69–71], Giovannetti-Mancini-Vitali-Tombesi (GMVT) [72] and van Loock-Furusawa (VLF) [73]. Then, we describe the criteria derived by Teh and Reid [74] to investigate tripartite entanglement in a system.

2.1.1 Bipartite entanglement

Bipartite quantum entanglement is present between different parties of the system if any of the following inequalities are not satisfied:

Tan-Duan-Giedke-Cirac-Zoller-Simon criterion

The sum criterion, developed by Tan, Duan-Giedke-Cirac-Zoller and Simon (DGCZ) [69–71], certifies bipartite entanglement between different parties of a system. This is expressed in terms of sum of variances of the quadrature operators $\hat{X}_j$, $\hat{Y}_j$ ($j=1,2,\ldots$) in the following way:

$$DGCZ_{ij}=\frac{V\left(\hat{X}_i\pm\hat{X}_j\right)+V\left(\hat{Y}_i\mp\hat{Y}_j\right)}{4}\geqslant 1, \tag{2.4}$$

where the variance of the operators $\hat{X}_i$ and $\hat{X}_j$ is given by

$$V\left(\hat{X}_i\pm\hat{X}_j\right)=\left\langle\left(\hat{X}_i\pm\hat{X}_j\right)^2\right\rangle-\left\langle\hat{X}_i\pm\hat{X}_j\right\rangle^2.$$

Here, ij represent the different bipartitions of the system. For instance, in a tripartite system, we have $i, j = 1, 2, 3$ and we can investigate bipartite entanglement for the bipartitions 12, 23 and 13.

Giovannetti-Mancini-Vitali-Tombesi criterion

The product criteria (GMVT) derived in [72] considers a bipartite system and a couple of different observables $\hat{r}_j$ and $\hat{s}_j$ $(j = 1, 2)$ to define the operators

$$\hat{C}_j = i\left[\hat{r}_j, \hat{s}_j\right], \quad j = 1, 2.$$

Then, for the following operators

$$\hat{u} = a_1\hat{r}_1 + a_2\hat{r}_2,$$
$$\hat{v} = b_1\hat{s}_1 + b_2\hat{s}_2,$$

where a_j, b_j are arbitrary real parameters, the authors proved that a state that is separable must satisfy

$$\left\langle (\Delta\hat{u})^2 \right\rangle \left\langle (\Delta\hat{v})^2 \right\rangle \geqslant \tilde{O}^2, \tag{2.5}$$

where $\tilde{O} = \frac{1}{2}\left(|a_1 b_1|\,\tilde{O}_1 + |a_2 b_2|\,\tilde{O}_2\right)$ and $\tilde{O}_j \equiv \sum_k w_k \left|\left\langle \hat{C}_j \right\rangle_k\right|$ $(j = 1, 2)$. The violation of Equation 2.5 demonstrate bipartite entanglement.

van Loock-Furusawa criterion

The van Loock-Furusawa (VLF) criterion is expressed in terms of the sum of variances which are linear combinations of the quadrature operators $\hat{X}$ and $\hat{Y}$ of the different parties of the system [73]. Using the definition of the quadrature operators (Equation 2.1), the VLF inequality is expressed in the following way:

$$VLF_{ij} = \frac{V\left(\hat{X}_i - \hat{X}_j\right) + V\left(\hat{Y}_i + \hat{Y}_j + g_k\hat{Y}_k\right)}{4} \geqslant 1, \tag{2.6}$$

where $i \neq j \neq k$ and g_k is a real parameter. It is important to notice that ij represent different bipartitions of the system. For example, in a tripartite system we have different bipartitions and therefore three different inequalities. Also, according to van Loock and Furusawa [73], if at least two of the three inequalities are violated, then we can certify genuine tripartite entanglement (GTE) which is the type of entanglement that is present when all the parties of the system are inseparable from each other [73]. It is important to mention that this criterion is a necessary, but not sufficient condition to certify GTE.

In the next section, we summarize criteria that provide necessary and sufficient conditions to demonstrate that GTE is present in a system.

2.1.2 Tripartite entanglement

In order to certify tripartite entanglement, we will consider the following expressions that are defined in terms of the variances and covariances of the parties of a system:

$$\begin{aligned} B_I &= V\left(\hat{X}_i - \hat{X}_j\right) + V\left(\hat{Y}_i + \hat{Y}_j + g_k\hat{Y}_k\right), \\ B_{II} &= V\left(\hat{X}_j - \hat{X}_k\right) + V\left(g_i\hat{Y}_i + \hat{Y}_j + \hat{Y}_k\right), \\ B_{III} &= V\left(\hat{X}_i - \hat{X}_k\right) + V\left(\hat{Y}_i + g_j\hat{Y}_j + \hat{Y}_k\right), \end{aligned} \tag{2.7}$$

$$\begin{aligned} S_I &= \sqrt{V\left(\hat{X}_i - \hat{X}_j\right)V\left(\hat{Y}_i + \hat{Y}_j + g_k\hat{Y}_k\right)}, \\ S_{II} &= \sqrt{V\left(\hat{X}_i - \hat{X}_j\right)V\left(g_k\hat{Y}_k + \hat{Y}_i + \hat{Y}_j\right)}, \\ S_{III} &= \sqrt{V\left(\hat{X}_i - \hat{X}_j\right)V\left(\hat{Y}_i + g_k\hat{Y}_k + \hat{Y}_j\right)}, \end{aligned} \tag{2.8}$$

where g_l is a real parameter for $l = i$, j, k and $i \neq j \neq k$.

Criteria that certify genuine tripartite entanglement (GTE) in quadrature operators have been derived by Teh and Reid [74]. These are expressed in terms of B_α and S_α ($\alpha = I$, II, III) and state that if any of the following inequalities is violated, then GTE is present in the system:

1. $$B = B_I + B_{II} + B_{III} \geqslant 8, \tag{2.9}$$
   where $B_I \geqslant 4$, $B_{II} \geqslant 4$, and $B_{III} \geqslant 4$ are given in Equation 2.7.

2. $$S = S_I + S_{II} + S_{III} \geqslant 4, \tag{2.10}$$
   where $S_I \geqslant 2$, $S_{II} \geqslant 2$, and $S_{III} \geqslant 2$ are given in Equation 2.8.

3. $$\Delta^2 V \geqslant 2, \tag{2.11}$$
   where $\Delta^2 V \equiv V\left(\hat{X}_i - \frac{\hat{X}_j + \hat{X}_k}{\sqrt{2}}\right) + V\left(\hat{Y}_i + \frac{\hat{Y}_j + \hat{Y}_k}{\sqrt{2}}\right)$ for $i \neq j \neq k$.

4. $$\Delta V \geqslant 1, \tag{2.12}$$
   where $\Delta V \equiv \sqrt{V\left(\hat{X}_i - \frac{\hat{X}_j + \hat{X}_k}{\sqrt{2}}\right)V\left(\hat{Y}_i + \frac{\hat{Y}_j + \hat{Y}_k}{\sqrt{2}}\right)}$ for $i \neq j \neq k$.

We notice that Equation 2.10 and Equation 2.12 are the product version of the criteria given in Equation 2.9 and Equation 2.11, respectively.

2.2 Criteria for the certification of steering

In this section we summarize the different criteria that certify quantum steering in quadrature operators. We focus on the certification of bipartite and tripartite steering which include the cases of full tripartite two-way steering inseparability and genuine tripartite steering.

2.2.1 Bipartite steering

Criterion that certify bipartite steering was developed by Reid [75]. This states that bipartite steering is present in the system if the inequality

$$EPR_{i|j} = V_{\{inf|j\}}\left(\hat{X}_i\right) V_{\{inf|j\}}\left(\hat{Y}_i\right) \geqslant 1 \tag{2.13}$$

is violated. The inference variances $V_{\{inf|j\}}\left(\hat{X}_i\right)$ and $V_{\{inf|j\}}\left(\hat{Y}_i\right)$ are defined as [4]

$$V_{\{inf|j\}}\left(\hat{X}_i\right) = V\left(\hat{X}_i\right) - \frac{\left[V\left(\hat{X}_i, \hat{X}_j\right)\right]^2}{V\left(\hat{X}_j\right)}, \tag{2.14}$$

$$V_{\{inf|j\}}\left(\hat{Y}_i\right) = V\left(\hat{Y}_i\right) - \frac{\left[V\left(\hat{Y}_i, \hat{Y}_j\right)\right]^2}{V\left(\hat{Y}_j\right)}, \tag{2.15}$$

where $V\left(\hat{A}, \hat{B}\right)$ is the covariance of the operators $\hat{A}$ and $\hat{B}$ given by $\left\langle \frac{\hat{A}\hat{B}+\hat{B}\hat{A}}{2} \right\rangle - \left\langle \hat{A} \right\rangle \left\langle \hat{B} \right\rangle$. Here, $V_{\{inf|j\}}\left(\hat{O}_i\right)$ represent the inference variance of the operator $\hat{O}_i$ from measurement of $\hat{O}_j$. This criterion shows the asymmetric property of steering. Thus, $EPR_{i|j} < 1$ means that mode j steers mode i and there is no steering from i to j. This type of steering is known as **one-way steering**. If mode i also steers mode j, that is, if $EPR_{j|i} < 1$ and $EPR_{i|j} < 1$, then this case is known as **two-way steering**.

2.2.2 Tripartite steering

In the tripartite case, there are two types of steering that we consider which are **full tripartite two-way steering inseparability** and **genuine tripartite steering** (GTS). Both consider bipartitions of the system, however, these are different concepts [76].

In the case of *full tripartite two-way steering inseparability,* there exist a certification of steering in at least one direction, for each one of all bipartitions of the system [76]. On the other hand, *genuine tripartite steering* consider the bilocality of the system which can be described as the local behaviour of one party of the system with respect

to the system composed by other two parties [76]. This type of steering confirms that steering is present for all the different bipartitions in the system. Therefore, genuine tripartite steering is the strongest condition and, according to Teh, Gessner, Reid and Fadel [76], full tripartite two-way steering inseparability is the necessary condition for genuine tripartite steering.

Both full and genuine tripartite steering can be certified following the criteria derived in [76]. These are given in terms of B_α and S_α ($\alpha = I,\ II,\ III$) which were defined in Equation 2.7-Equation 2.8.

We can certify full tripartite two-way steering inseparability if any two of the three following inequalities are violated:

$$B_I \geqslant 2, \quad B_{II} \geqslant 2, \quad B_{III} \geqslant 2. \tag{2.16}$$

The criterion express in terms of S_α states that if any two of the inequalities

$$S_I \geqslant 1, \quad S_{II} \geqslant 1, \quad S_{III} \geqslant 1, \tag{2.17}$$

are not satisfied, then we can also certify full tripartite two-way steering inseparability.

For example, suppose that $B_I \geqslant 2$, $B_{II} < 2$ and $B_{III} < 2$. The simultaneous violation of B_{II} and B_{III} implies that we can certify full tripartite two-way steering inseparability in the system. Similarly for S_α. Thus, both criteria (Equation 2.16 and Equation 2.17) allow us to certify full tripartite two-way steering inseparability.

In the genuine tripartite steering case, two main criteria are considered. If either

$$B_I + B_{II} + B_{III} \geqslant 4, \tag{2.18}$$

or

$$S_I + S_{II} + S_{III} \geqslant 2, \tag{2.19}$$

is violated, then genuine tripartite steering is present in the system.

We also consider four criteria that certify GTS when $g_l = 1$ ($l = i,\ j,\ k$). These express that if either of the following inequalities are satisfied:

1.

$$B_\alpha + B_\beta < 2, \tag{2.20}$$

2.

$$S_\alpha + S_\beta < 1, \tag{2.21}$$

3.

$$B_I + B_{II} + B_{III} < 4, \tag{2.22}$$

4.

$$S_I + S_{II} + S_{III} < 2, \tag{2.23}$$

where $\alpha, \beta = I$, II, III and $\alpha \neq \beta$, then GTS is present in the system.

Chapter 3

Monogamy relations for quantum entanglement and steering witnesses

In a bipartite or multipartite system that generate quantum entanglement and steering, it is possible to investigate how these correlations are shared among the different parties of the system. One can determine the amount of entanglement and steering that each part of the system share with other parties through monogamy relations. These relations constrain the shareability of entanglement and steering among parties.

On one hand, the monogamy of entanglement was introduced by Coffman, Kundu and Wootters (CKW) [77]. This monogamy inequality is expressed in terms of the concurrence which is a measure of entanglement. Since then, a great deal of work has been done to develop monogamy inequalities for CV systems [78–80] which include the tripartite [81, 82] as well as the multipartite case [80, 83–87].

On the other hand, monogamy inequalities for bipartite steering were derived by Reid [88]. These relations constrain the distribution of steering among the different bipartitions of a system. In the case of multipartite systems, monogamy relations have been developed similar to monogamy CKW-type inequalities [89–92], and experimental demonstrations of these relations have been accomplished [91, 93, 94].

The study of the distribution of entanglement and steering is crucial for quantum information protocols such as Quantum Key Distribution (QKD) [31], which is a protocol between two distant parties of a system that utilize cryptography, in particular secret keys, to establish secure communication between the sender and the receiver. For instance, the monogamy of entanglement is essential to guarantee security in QKD protocols [95] and quantum cryptography [96–100]. Also, the steering monogamy relations allow secure communication between two distant parties even if only one of the parties is considered trusted [32, 101–103].

The following sections summarize the monogamy relations for entanglement and steering witnesses that we have described in chapter 2.

3.1 Monogamy relations for quantum entanglement witnesses

The monogamy of entanglement constrains the amount of entanglement that can be shared among different parties of a system. Monogamy relations for different entanglement witnesses have been derived in [41]. Below we describe the monogamy inequalities.

In a system that consist of three parties A, B and C, the monogamy relations for DGCZ and GMVT entanglement witnesses states that the following inequalities must hold:

$$D_{BA} + D_{BC} \geqslant 1, \tag{3.1}$$

$$D_{BA} + D_{BC} \geqslant max\left\{1, S_{B|\{AC\}}\right\}, \tag{3.2}$$

$$4G_{BA}G_{BC} \geqslant max\left\{1, S^2_{B|\{AC\}}\right\}, \tag{3.3}$$

where D_{ij} and G_{ij} $(i,\, j = A,\, B,\, C;\, i \neq j)$ are the DGCZ and GMVT witnesses respectively. Here, $S_{i|\{jk\}}$ $(i,\, j,\, k = A,\, B,\, C;\, i \neq j \neq k)$ is the steering parameter defined as the product of inference variances of the quadrature operators [88]

$$S_{i|\{jk\}} = V_{inf|\{jk\}}(\hat{X}_i)V_{inf|\{jk\}}(\hat{Y}_i), \tag{3.4}$$

where $V_{inf|\{jk\}}(\hat{O}_i)$ is the inference variance of part i from measurement of the combined parts $\{jk\}$ and is given by

$$V_{inf|\{jk\}}(\hat{X}_i) = V(\hat{X}_i) - \frac{\left[V(\hat{X}_i, \hat{X}_j \pm \hat{X}_k)\right]}{V(\hat{X}_j \pm \hat{X}_k)},$$

$$V_{inf|\{jk\}}(\hat{Y}_i) = V(\hat{Y}_i) - \frac{\left[V(\hat{Y}_i, \hat{Y}_j \pm \hat{Y}_k)\right]}{V(\hat{Y}_j \pm \hat{Y}_k)}.$$

The covariance of the operators $\hat{O}_i$, $\hat{O}_j$ and $\hat{O}_k$ is defined as [104]

$$V(\hat{O}_i, \hat{O}_j \pm \hat{O}_k) = \left\langle \frac{\hat{O}_i\left(\hat{O}_j \pm \hat{O}_k\right) \pm \left(\hat{O}_j \pm \hat{O}_k\right)\hat{O}_i}{2} \right\rangle - \left\langle \hat{O}_i \right\rangle \left\langle \hat{O}_j \pm \hat{O}_k \right\rangle.$$

Equation 3.1-Equation 3.3 show the distribution of entanglement among different bipartitions of a tripartite system.

3.2 Monogamy relations for quantum steering witness

The distribution of steering in a system composed of three different parties i, j and k, is constrained by the monogamy relations for the steering witness (Equation 2.13) [75]. These relations were derived by Reid [40] and quantify the amount of steering shared among i, j and k.

In a system where bipartite steering is present for different bipartitions, one can also consider bipartitions of the form $i - \{jk\}$, where $\{jk\}$ is the composed system of two parties j and k. The following monogamy relations for bipartite steering witness (Equation 2.13) must hold:

1. If party j steers party i, that is if $EPR_{i|j} < 1$, then the third party k cannot steer i and the monogamy relation is given by

$$EPR_{i|j}EPR_{i|k} \geqslant 1. \tag{3.5}$$

2. We consider the steering parameter given by $S_{i|\{jk\}}$ in Equation 3.4 [104, 105]. The monogamy inequality is expressed as

$$S_{i|\{jk\}} \leqslant EPR_{i|j}, \tag{3.6}$$

where $EPR_{i|j}$ is the bipartite steering between parties i and j ($i \neq j$).

3. For the three parties i, j, and k, the inequality

$$EPR_{i|j}EPR_{i|k} \geqslant S^2_{i|\{jk\}} \tag{3.7}$$

must hold.

4. The sum of the steering witness for the bipartitions ij and ik follows the monogamy relation

$$EPR_{i|j} + EPR_{i|k} \geqslant 2S_{i|\{jk\}}, \tag{3.8}$$

where $S_{i|\{jk\}}$ is the steering parameter given in Equation 3.4.

5. The product of EPR witness for the bipartitions ij and ik is constrained by either 1 or the steering parameter $S_{i|\{jk\}}$ as

$$EPR_{i|j}EPR_{i|k} \geqslant max\{1, S^2_{i|\{jk\}}\}. \tag{3.9}$$

where $S_{i|\{jk\}}$ has been described in Equation 3.4.

Chapter 4

Nonlinear Hamiltonian model and its master equation

Quantum entanglement and steering can be generated through different nonlinear processes such as triple photon generation (TPG) [42–44], third-harmonic generation (THG) [45, 46, 57, 64], spontaneous parametric down-conversion (SPDC) [47, 48, 61, 106–110], four-wave mixing (FWM) [49, 50, 111, 112], sum/difference frequency generation (SFG/DFG) [46, 55, 57, 113–116], or cascaded nonlinear processes [45, 49, 57, 58, 114, 115, 117, 118].

In recent years, there have been proposals that use the so called intracavity configurations which consist of a nonlinear medium inside an optical cavity. These configurations have the advantages of enhancing the nonlinear processes and minimizing losses. It has been demonstrated that intracavity nonlinear processes can generate bipartite, tripartite and multipartite entanglement [45, 52–64] as well as steering [53, 63, 107, 109, 110, 115–122] in the frequency domain.

For instance, in reference [45], the author investigated the nonlocal correlations that can be generated in two different intracavity configurations. One of these schemes consider the cascaded THG process which is generated by SHG cascaded with a SFG, while the other is a direct THG process. Both configurations produce CV bipartite entanglement and steering, in the frequency domain. However, the direct process shows a wide range of frequencies where the steering criterion is violated. While in the cascaded process, the three outputs present steering different frequencies.

In [119] an intracavity cascaded processes was considered. Here, two cascaded sum frequency processes occur inside an optical cavity. This system generates both bipartite and genuine tripartite quantum steering among pump, SHG, and THG in the frequency domain. The authors analyzed the changes that both bipartite and tripartite quantum steering exhibits when the values of the frequency or the nonlinear coupling coefficients are modified. The former analysis shows the violation of steering criteria across the whole range of the frequency under consideration. While

in the latter, the system cannot generate genuine tripartite steering for all values of the nonlinear coupling coefficients, whereas bipartite steering is present.

It has also been demonstrated that cavities which contain a nonlinear medium can generate higher correlations such as quadripartite quantum steering [115,118,123]. In reference [123], quadripartite quantum steering is generated by an optical parametric amplification cascaded with a sum-frequency process. While genuine quadripartite quantum steering, which is the steering that is shared among all 4-parties, has been confirmed in references [51, 115, 118]. In reference [115] a SPDC process cascaded with a sum-frequency process was used whereas in reference [118] a SPDC cascaded with two sum-frequency processes in an optical superlattice.

In this thesis, we focus on a system that can generate both quantum entanglement and steering. That is, we wish to investigate if bipartite and tripartite entanglement and steering can be certified in the frequency domain as well as in a wide range of frequencies.

The system consists of an optical cavity with a nonlinear medium inside. The cavity is pumped with three electromagnetic fields at frequency ω_i $(i = 1, 2, 3)$. Each field interacts with the nonlinear medium and, through SPDC process, each input field produce two down-converted fields at frequencies ω_j and ω_k $(j, k = 4, 5, 6;\ j \neq k)$ respectively as shown in Figure 4.1. It is worth pointing out that this system generates three fields at the output of the cavity through direct SPDC processes rather than cascaded. It is important to mention that this system had also been investigated by Bradley *et al.* [52] and Olsen and Corney [61].

In both references [52, 61] the system was analysed in the regime of below and above threshold with the condition of a doubly resonant Optical Parametric Oscillator (OPO). In [52], the authors demonstrated that the system can generate tripartite quantum entanglement and bipartite quantum steering in quadrature operators. While in [61], the authors also certified bipartite quantum entanglement as well as tripartite quantum steering, but they also extended the work of [52] in order to show that genuine tripartite entanglement can be generated as the value of the pump increases. Here, we investigate whether bipartite and tripartite entanglement and steering can be certified when there is no threshold condition of an OPO, and how these correlations are shared among the three output fields.

Below we describe the Hamiltonian which model the nonlinear processes inside the cavity and the master equation that describe the system of Figure 4.1.

4.1 Nonlinear Hamiltonian model

Nonlinear processes that occurs in intracavity configurations can be described by a Hamiltonian that models the interaction between the incident field and the nonlinear

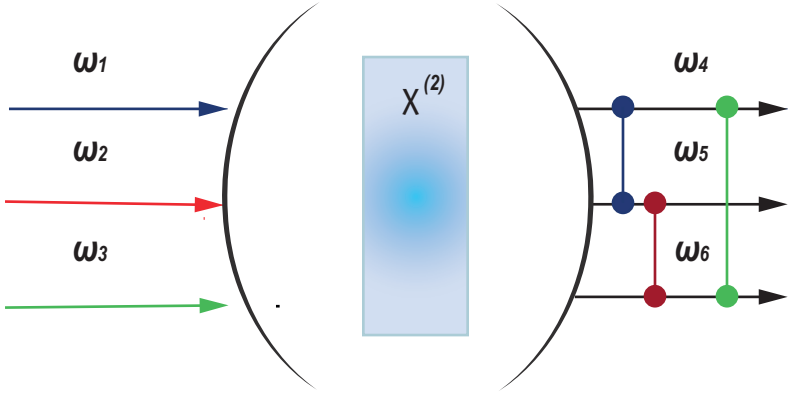

Figure 4.1: Triple SPDC process inside an optical cavity. Three input fields interact with the nonlinear medium and, through SPDC, generate three output fields with frequencies ω_4, ω_5, ω_6, respectively. The two down-converted fields are represented with the same color.

medium. The interaction Hamiltonian of the system (see Figure 4.1) is

$$\hat{H}_{int} = i\hbar \left[\chi_1 \hat{a}_1 \hat{a}_4^\dagger \hat{a}_5^\dagger + \chi_2 \hat{a}_2 \hat{a}_5^\dagger \hat{a}_6^\dagger + \chi_3 \hat{a}_3 \hat{a}_6^\dagger \hat{a}_4^\dagger\right] + H.C., \tag{4.1}$$

where each field is represented by bosonic operators $\hat{a}_i$ and $\hat{a}_i^\dagger$, χ_i $(i = 1, 2, 3)$ is the nonlinear coupling strength which is proportional to the nonlinear coefficient of the medium $\chi_i \propto \chi^{(2)}$ and $H.C.$ is the Hermitian conjugate of the former terms.

The input fields are described by the Hamiltonian, $\hat{H}_p$, which is given by

$$\hat{H}_p = i\hbar \sum_{i=1}^{3} \left(E_i \hat{a}_i^\dagger - E_i^* \hat{a}_i\right), \tag{4.2}$$

where E_i is the amplitude of the field. We also consider the cavity losses which can be included by the Liouvillian operator acting on the density matrix of the system $\hat{\rho}$ as

$$\mathcal{L}\hat{\rho} = \sum_{i=1}^{6} \left(2\gamma_i \hat{a}_i \hat{\rho} \hat{a}_i^\dagger - \gamma_i \hat{a}_i^\dagger \hat{a}_i \hat{\rho} - \gamma_i \hat{\rho} \hat{a}_i^\dagger \hat{a}_i\right), \tag{4.3}$$

where γ_k is the kth cavity loss.

We refer the reader to Appendix A for further details of the relation among the coupling strength, the cavity losses and the amplitude of the field with real parameters, such as length and volume of the nonlinear medium, and the power of the pump.

In order to analyse the dynamics of the system, we follow the formalism of the master equation which, in this case, includes the Liouvillian operator. This allows us to find an equation of motion for the density matrix of the system. In next section we present this formalism.

4.2 Master equation of the system

So far, we have described the parametric interaction inside the cavity as well as the cavity losses through the Hamiltonians, $\hat{H}_{int}$ and $\hat{H}_p$, and the Liouvillian, $\mathcal{L}\hat{\rho}$, respectively. Since we are interesting in investigate the dynamics of the system, we need to write an equation of motion for the density matrix of the system under consideration. This can be obtained by the so called master equation of the system.

The master equation of this model (see Figure 4.1) is expressed as the Lindblad form [124, 125]. That is, this includes the interaction Hamiltonian $\hat{H}_{int}$, the Hamiltonian of the pump field $\hat{H}_p$, and the cavity losses $\mathcal{L}\hat{\rho}$ as

$$\frac{\partial\hat{\rho}}{\partial t} = \frac{1}{i\hbar}\left[\hat{H}_{sys},\hat{\rho}\right] + \mathcal{L}\hat{\rho}, \tag{4.4}$$

where $\hat{H}_{sys} = \hat{H}_{int} + \hat{H}_p$.

In order to write the master equation for the density matrix of the system, first we calculate the corresponding commutator $\left[\hat{H}_{sys},\hat{\rho}\right] = \left[\hat{H}_{int} + \hat{H}_p,\hat{\rho}\right]$ with Equation 4.1 and Equation 4.2.

Next, we substitute the result of the commutator as well as Equation 4.3 into Equation 4.4. In this way, we obtain:

$$\begin{aligned}\frac{\partial\hat{\rho}}{\partial t} =& \chi_1\hat{a}_1\hat{a}_4^\dagger\hat{a}_5^\dagger\hat{\rho} + \chi_2\hat{a}_2\hat{a}_5^\dagger\hat{a}_6^\dagger\hat{\rho} + \chi_3\hat{a}_3\hat{a}_6^\dagger\hat{a}_4^\dagger\hat{\rho} - \chi_1\hat{a}_1^\dagger\hat{a}_4\hat{a}_5\hat{\rho} - \chi_2\hat{a}_2^\dagger\hat{a}_5\hat{a}_6\hat{\rho} - \chi_3\hat{a}_3^\dagger\hat{a}_6\hat{a}_4\hat{\rho}\\
&-\chi_1\hat{\rho}\hat{a}_1\hat{a}_4^\dagger\hat{a}_5^\dagger - \chi_2\hat{\rho}\hat{a}_2\hat{a}_5^\dagger\hat{a}_6^\dagger - \chi_3\hat{\rho}\hat{a}_3\hat{a}_6^\dagger\hat{a}_4^\dagger + \chi_1\hat{\rho}\hat{a}_1^\dagger\hat{a}_4\hat{a}_5 + \chi_2\hat{\rho}\hat{a}_2^\dagger\hat{a}_5\hat{a}_6 + \chi_3\hat{\rho}\hat{a}_3^\dagger\hat{a}_6\hat{a}_4\\
&+E_1\hat{a}_1^\dagger\hat{\rho} - E_1^*\hat{a}_1\hat{\rho} + E_2\hat{a}_2^\dagger\hat{\rho} - E_2^*\hat{a}_2\hat{\rho} + E_3\hat{a}_3^\dagger\hat{\rho} - E_3^*\hat{a}_3\hat{\rho} - E_1\hat{\rho}\hat{a}_1^\dagger + E_1^*\hat{\rho}\hat{a}_1\\
&-E_2\hat{\rho}\hat{a}_2^\dagger + E_2^*\hat{\rho}\hat{a}_2 - E_3\hat{\rho}\hat{a}_3^\dagger + E_3^*\hat{\rho}\hat{a}_3 + 2\gamma_1\hat{a}_1\hat{\rho}\hat{a}_1^\dagger - \gamma_1\hat{a}_1^\dagger\hat{a}_1\hat{\rho} - \gamma_1\hat{\rho}\hat{a}_1^\dagger\hat{a}_1\\
&+2\gamma_2\hat{a}_2\hat{\rho}\hat{a}_2^\dagger - \gamma_2\hat{a}_2^\dagger\hat{a}_2\hat{\rho} - \gamma_2\hat{\rho}\hat{a}_2^\dagger\hat{a}_2 + 2\gamma_3\hat{a}_3\hat{\rho}\hat{a}_3^\dagger - \gamma_3\hat{a}_3^\dagger\hat{a}_3\hat{\rho} - \gamma_3\hat{\rho}\hat{a}_3^\dagger\hat{a}_3 + 2\gamma_4\hat{a}_4\hat{\rho}\hat{a}_4^\dagger\\
&-\gamma_4\hat{a}_4^\dagger\hat{a}_4\hat{\rho} - \gamma_4\hat{\rho}\hat{a}_4^\dagger\hat{a}_4 + 2\gamma_5\hat{a}_5\hat{\rho}\hat{a}_5^\dagger - \gamma_5\hat{a}_5^\dagger\hat{a}_5\hat{\rho} - \gamma_5\hat{\rho}\hat{a}_5^\dagger\hat{a}_5 + 2\gamma_6\hat{a}_6\hat{\rho}\hat{a}_6^\dagger - \gamma_6\hat{a}_6^\dagger\hat{a}_6\hat{\rho}\\
&-\gamma_6\hat{\rho}\hat{a}_6^\dagger\hat{a}_6,\end{aligned} \tag{4.5}$$

which is the operator master equation of the system which describes the time evolution of $\hat{\rho}$.

Although, it is not always possible to solve the master equation, one way to do it is by using phase-space methods. These methods are quasi-probability representations that behave similarly to classical probabilities, although these may not always be non-negative. These representations transform the operator master equation of $\hat{\rho}$ into an equation of motion of the phase-space representation. One can use different representations such as the Glauber-Sudarshan P function [126, 127], the W Wigner function [128] or the positive-P function [129].

In this thesis, we use the positive-P function, $P(\boldsymbol{\alpha},\boldsymbol{\beta})$, which is a positive phase-space distribution defined as [129, 130]

$$\hat{\rho}=\int P(\boldsymbol{\alpha},\boldsymbol{\beta})\,\hat{\Lambda}(\boldsymbol{\alpha},\boldsymbol{\beta})\,d\mu(\boldsymbol{\alpha},\boldsymbol{\beta}), \tag{4.6}$$

where $d\mu(\boldsymbol{\alpha},\boldsymbol{\beta})=d^2\boldsymbol{\alpha}d^2\boldsymbol{\beta}$ and

$$\hat{\Lambda}(\boldsymbol{\alpha},\boldsymbol{\beta})=\frac{|\boldsymbol{\alpha}\rangle\langle\boldsymbol{\beta}^*|}{\langle\boldsymbol{\beta}^*|\boldsymbol{\alpha}\rangle}=\exp\left(\boldsymbol{\alpha}\hat{\boldsymbol{a}}^\dagger-\boldsymbol{\alpha}\boldsymbol{\beta}\right)|\mathbf{0}\rangle\langle\mathbf{0}|\exp(\boldsymbol{\beta}\hat{\boldsymbol{a}}), \tag{4.7}$$

is the projection operator of a pair of coherent states $\boldsymbol{\alpha}$ and $\boldsymbol{\beta}$. Here, $\boldsymbol{\alpha}=\boldsymbol{\alpha}_x+i\boldsymbol{\alpha}_y$ and $\boldsymbol{\beta}=\boldsymbol{\beta}_x+i\boldsymbol{\beta}_y$ stands for complex vectors.

The next step to solve Equation 4.5 is to transform the master equation into an equation of motion for the $P(\boldsymbol{\alpha},\boldsymbol{\beta})$ representation. This can be done by using the positive-P operator mappings which are given by [129]

$$\hat{a}\hat{\rho}\rightarrow\alpha P^+,\quad \hat{\rho}\hat{a}^\dagger\rightarrow\alpha^\dagger P^+,\quad \hat{\rho}\hat{a}\rightarrow\left(\alpha-\frac{\partial}{\partial\alpha^\dagger}\right)P^+,\quad \hat{a}^\dagger\hat{\rho}\rightarrow\left(\alpha^\dagger-\frac{\partial}{\partial\alpha}\right)P^+, \tag{4.8}$$

where we have defined $P^+\equiv P(\boldsymbol{\alpha},\boldsymbol{\beta})$.

We now apply the corresponding mappings of Equation 4.8, to transform Equation 4.5, and after some simplifications we obtain

$$\begin{aligned}
\frac{\partial P^+}{\partial t}=\Bigg[&-\frac{\partial}{\partial\alpha_1}\left(-\gamma_1\alpha_1-\chi_1\alpha_4\alpha_5+E_1\right)-\frac{\partial}{\partial\alpha_1^\dagger}\left(-\gamma_1\alpha_1^\dagger-\chi_1\alpha_4^\dagger\alpha_5^\dagger+E_1^*\right)\\
&-\frac{\partial}{\partial\alpha_2}\left(-\gamma_2\alpha_2-\chi_2\alpha_5\alpha_6+E_2\right)-\frac{\partial}{\partial\alpha_2^\dagger}\left(-\gamma_2\alpha_2^\dagger-\chi_2\alpha_5^\dagger\alpha_6^\dagger+E_2^*\right)\\
&-\frac{\partial}{\partial\alpha_3}\left(-\gamma_3\alpha_3-\chi_3\alpha_6\alpha_4+E_3\right)-\frac{\partial}{\partial\alpha_3^\dagger}\left(-\gamma_3\alpha_3^\dagger-\chi_3\alpha_6^\dagger\alpha_4^\dagger+E_3^*\right)\\
&-\frac{\partial}{\partial\alpha_4}\left(-\gamma_4\alpha_4+\chi_1\alpha_1\alpha_5^\dagger+\chi_3\alpha_3\alpha_6^\dagger\right)-\frac{\partial}{\partial\alpha_4^\dagger}\left(-\gamma_4\alpha_4^\dagger+\chi_1\alpha_1^\dagger\alpha_5+\chi_3\alpha_3^\dagger\alpha_6\right)\\
&-\frac{\partial}{\partial\alpha_5}\left(-\gamma_5\alpha_5+\chi_1\alpha_1\alpha_4^\dagger+\chi_2\alpha_2\alpha_6^\dagger\right)-\frac{\partial}{\partial\alpha_5^\dagger}\left(-\gamma_5\alpha_5^\dagger+\chi_1\alpha_1^\dagger\alpha_4+\chi_2\alpha_2^\dagger\alpha_6\right)\\
&-\frac{\partial}{\partial\alpha_6}\left(-\gamma_6\alpha_6+\chi_2\alpha_2\alpha_5^\dagger+\chi_3\alpha_3\alpha_4^\dagger\right)-\frac{\partial}{\partial\alpha_6^\dagger}\left(-\gamma_6\alpha_6^\dagger+\chi_2\alpha_2^\dagger\alpha_5+\chi_3\alpha_3^\dagger\alpha_4\right)\\
&+\frac{1}{2}\frac{\partial^2}{\partial\alpha_4\alpha_5}\left(2\chi_1\alpha_1\right)+\frac{1}{2}\frac{\partial^2}{\partial\alpha_5\alpha_6}\left(2\chi_2\alpha_2\right)+\frac{1}{2}\frac{\partial^2}{\partial\alpha_6\alpha_4}\left(2\chi_3\alpha_3\right)+\frac{1}{2}\frac{\partial^2}{\partial\alpha_4^\dagger\alpha_5^\dagger}\left(2\chi_1\alpha_1^\dagger\right)\\
&+\frac{1}{2}\frac{\partial^2}{\partial\alpha_5^\dagger\alpha_6^\dagger}\left(2\chi_2\alpha_2^\dagger\right)+\frac{1}{2}\frac{\partial^2}{\partial\alpha_6^\dagger\alpha_4^\dagger}\left(2\chi_3\alpha_3^\dagger\right)\Bigg]P^+,
\end{aligned} \tag{4.9}$$

which is the time evolution equation of the positive-P function. This can be expressed as a Fokker-Planck (FP) equation of the form [130, 131]

$$\frac{\partial P^{+}}{\partial t} = \left[-\sum_{i} \frac{\partial}{\partial x_i} A_i(\boldsymbol{x}) + \frac{1}{2} \sum_{ij} \frac{\partial^2}{\partial x_i \partial x_j} D_{ij}(\boldsymbol{x}) \right] P^{+}, \tag{4.10}$$

where $\boldsymbol{A}(\boldsymbol{x})$ is the drift matrix, $\boldsymbol{D}(\boldsymbol{x})$ is the diffusion matrix, $\boldsymbol{x}$ is the vector of N variables which, in this case, is $\boldsymbol{x} \equiv \boldsymbol{\alpha} = \alpha_1, \alpha_1^{\dagger}, \ldots, \alpha_6, \alpha_6^{\dagger}$.

As long as the diffusion matrix is positive semidefinite, and that it can be factorized as $\boldsymbol{D}(\boldsymbol{\alpha}) = \boldsymbol{B}(\boldsymbol{\alpha})\boldsymbol{B}^{T}(\boldsymbol{\alpha})$, one can map the FP equation (Equation 4.10) into a set of stochastic differential equations (SDEs) in the following form [125, 130]:

$$\frac{d\boldsymbol{\alpha}(t)}{dt} = \boldsymbol{A}(\boldsymbol{\alpha}) + \boldsymbol{B}(\boldsymbol{\alpha})\boldsymbol{\xi}_i(t), \tag{4.11}$$

where $\boldsymbol{\xi}_i(t)$ $(i = 1, 2, \ldots)$ is a real and independent Gaussian noise with $\langle \boldsymbol{\xi}_i(t) \rangle = 0$. An equivalent form of Equation 4.11 is given by

$$d\boldsymbol{\alpha}_i = \boldsymbol{A}_i(\boldsymbol{\alpha})dt + \boldsymbol{B}_{ij}(\boldsymbol{\alpha})dW_j, \tag{4.12}$$

where dW_j are the corresponding terms to real δ correlated Gaussian noise which satisfy

$$\langle dW_i(t) dW_j(t') \rangle = \delta_{ij}\delta(t - t'). \tag{4.13}$$

For our model, the drift matrix $\boldsymbol{A}(\boldsymbol{\alpha})$ and the diffusion matrix $\boldsymbol{D}(\boldsymbol{\alpha})$ are given by

$$\boldsymbol{A}(\boldsymbol{\alpha}) = \begin{pmatrix} -\gamma_1\alpha_1 - \chi_1\alpha_4\alpha_5 + E_1 \\ -\gamma_1\alpha_1^{\dagger} - \chi_1\alpha_4^{\dagger}\alpha_5^{\dagger} + E_1^{*} \\ -\gamma_2\alpha_2 - \chi_2\alpha_5\alpha_6 + E_2 \\ -\gamma_2\alpha_2^{\dagger} - \chi_2\alpha_5^{\dagger}\alpha_6^{\dagger} + E_2^{*} \\ -\gamma_3\alpha_3 - \chi_3\alpha_6\alpha_4 + E_3 \\ -\gamma_3\alpha_3^{\dagger} - \chi_3\alpha_6^{\dagger}\alpha_4^{\dagger} + E_3^{*} \\ -\gamma_4\alpha_4 + \chi_1\alpha_1\alpha_5^{\dagger} + \chi_3\alpha_3\alpha_6^{\dagger} \\ -\gamma_4\alpha_4^{\dagger} + \chi_1\alpha_1^{\dagger}\alpha_5 + \chi_3\alpha_3^{\dagger}\alpha_6 \\ -\gamma_5\alpha_5 + \chi_1\alpha_1\alpha_4^{\dagger} + \chi_2\alpha_2\alpha_6^{\dagger} \\ -\gamma_5\alpha_5^{\dagger} + \chi_1\alpha_1^{\dagger}\alpha_4 + \chi_2\alpha_2^{\dagger}\alpha_6 \\ -\gamma_6\alpha_6 + \chi_2\alpha_2\alpha_5^{\dagger} + \chi_3\alpha_3\alpha_4^{\dagger} \\ -\gamma_6\alpha_6^{\dagger} + \chi_2\alpha_2^{\dagger}\alpha_5 + \chi_3\alpha_3^{\dagger}\alpha_4 \end{pmatrix}, \tag{4.14}$$

$$\boldsymbol{D}(\boldsymbol{\alpha}) = \begin{pmatrix} 0_{6\times6} & 0_{6\times6} \\ 0_{6\times6} & d_{6\times6} \end{pmatrix}, \tag{4.15}$$

where

$$d = \begin{pmatrix} 0 & 0 & \chi_1\alpha_1 & 0 & \chi_3\alpha_3 & 0 \\ 0 & 0 & 0 & \chi_1\alpha_1^\dagger & 0 & \chi_3\alpha_3^\dagger \\ \chi_1\alpha_1 & 0 & 0 & 0 & \chi_2\alpha_2 & 0 \\ 0 & \chi_1\alpha_1^\dagger & 0 & 0 & 0 & \chi_2\alpha_2^\dagger \\ \chi_3\alpha_3 & 0 & \chi_2\alpha_2 & 0 & 0 & 0 \\ 0 & \chi_3\alpha_3^\dagger & 0 & \chi_2\alpha_2^\dagger & 0 & 0 \end{pmatrix}.$$

The matrix $\boldsymbol{B}(\boldsymbol{\alpha})$ which satisfies $\boldsymbol{D}(\boldsymbol{\alpha}) = \boldsymbol{B}(\boldsymbol{\alpha})\boldsymbol{B}^T(\boldsymbol{\alpha})$ is given by

$$\boldsymbol{B}(\boldsymbol{\alpha}) = \begin{pmatrix} 0_{6\times6} & 0_{6\times6} \\ 0_{6\times6} & b_{6\times6} \end{pmatrix},$$

where

$$b_{15} = -i\sqrt{i\frac{\chi_1\chi_3\alpha_1\alpha_3}{\chi_2\alpha_2}}, \qquad b_{16} = -\sqrt{i\frac{\chi_1\chi_3\alpha_1\alpha_3}{\chi_2\alpha_2}}, \qquad b_{23} = -\sqrt{\frac{\chi_1\chi_3\alpha_1^\dagger\alpha_3^\dagger}{2\chi_2\alpha_2^\dagger}},$$

$$b_{24} = -i\sqrt{\frac{\chi_1\chi_3\alpha_1^\dagger\alpha_3^\dagger}{2\chi_2\alpha_2^\dagger}}, \qquad b_{31} = -i\sqrt{i\frac{\chi_1\chi_2\alpha_1\alpha_2}{\chi_3\alpha_3}}, \qquad b_{35} = \sqrt{i\frac{\chi_1\chi_2\alpha_1\alpha_2}{\chi_3\alpha_3}},$$

$$b_{42} = -i\sqrt{\frac{2\chi_1\chi_2\alpha_1^\dagger\alpha_2^\dagger}{\chi_3\alpha_3^\dagger}}, \qquad b_{43} = -\sqrt{\frac{2\chi_1\chi_2\alpha_1^\dagger\alpha_2^\dagger}{\chi_3\alpha_3^\dagger}}, \qquad b_{51} = \sqrt{i\frac{\chi_2\chi_3\alpha_2\alpha_3}{\chi_1\alpha_1}},$$

$$b_{56} = i\sqrt{i\frac{\chi_2\chi_3\alpha_2\alpha_3}{\chi_1\alpha_1}}, \qquad b_{63} = -\sqrt{\frac{\chi_2\chi_3\alpha_2^\dagger\alpha_3^\dagger}{2\chi_1\alpha_1^\dagger}}, \qquad b_{64} = i\sqrt{\frac{\chi_2\chi_3\alpha_2^\dagger\alpha_3^\dagger}{2\chi_1\alpha_1^\dagger}}.$$

Finally, we obtain the set of SDEs

$$
\begin{aligned}
d\alpha_1 &= (-\gamma_1\alpha_1 - \chi_1\alpha_4\alpha_5 + E_1)\,dt,\\
d\alpha_1^\dagger &= \left(-\gamma_1\alpha_1^\dagger - \chi_1\alpha_4^\dagger\alpha_5^\dagger + E_1^*\right)dt,\\
d\alpha_2 &= (-\gamma_2\alpha_2 - \chi_2\alpha_5\alpha_6 + E_2)\,dt,\\
d\alpha_2^\dagger &= \left(-\gamma_2\alpha_2^\dagger - \chi_2\alpha_5^\dagger\alpha_6^\dagger + E_2\right)dt,\\
d\alpha_3 &= (-\gamma_3\alpha_3 - \chi_3\alpha_6\alpha_4 + E_3)\,dt,\\
d\alpha_3^\dagger &= (-\gamma_3\alpha_3 - \chi_3\alpha_6\alpha_4 + E_3^*)\,dt,\\
d\alpha_4 &= \left(-\gamma_4\alpha_4 + \chi_1\alpha_1\alpha_5^\dagger + \chi_3\alpha_3\alpha_6^\dagger\right)dt - \sqrt{i\frac{\chi_1\chi_3\alpha_1\alpha_3}{\chi_2\alpha_2}}\,(idW_{11} + dW_{12}),\\
d\alpha_4^\dagger &= \left(-\gamma_4\alpha_4^\dagger + \chi_1\alpha_1^\dagger\alpha_5 + \chi_3\alpha_3^\dagger\alpha_6\right)dt - \sqrt{\frac{\chi_1\chi_3\alpha_1^\dagger\alpha_3^\dagger}{2\chi_2\alpha_2^\dagger}}\,(dW_9 + idW_{10}),\\
d\alpha_5 &= \left(-\gamma_5\alpha_5 + \chi_1\alpha_1\alpha_4^\dagger + \chi_2\alpha_2\alpha_6^\dagger\right)dt + \sqrt{i\frac{\chi_1\chi_2\alpha_1\alpha_2}{\chi_3\alpha_3}}\,(dW_{11} - idW_7),\\
d\alpha_5^\dagger &= \left(-\gamma_5\alpha_5^\dagger + \chi_1\alpha_1^\dagger\alpha_4 + \chi_2\alpha_2^\dagger\alpha_6\right)dt - \sqrt{\frac{2\chi_1\chi_2\alpha_1^\dagger\alpha_2^\dagger}{\chi_3\alpha_3^\dagger}}\,(idW_8 + dW_9),\\
d\alpha_6 &= \left(-\gamma_6\alpha_6 + \chi_2\alpha_2\alpha_5^\dagger + \chi_3\alpha_3\alpha_4^\dagger\right)dt + \sqrt{i\frac{\chi_2\chi_3\alpha_2\alpha_3}{\chi_1\alpha_1}}\,(dW_7 + idW_{12}),\\
d\alpha_6^\dagger &= \left(-\gamma_6\alpha_6^\dagger + \chi_2\alpha_2^\dagger\alpha_5 + \chi_3\alpha_3^\dagger\alpha_4\right)dt - \sqrt{\frac{\chi_2\chi_3\alpha_2^\dagger\alpha_3^\dagger}{2\chi_1\alpha_1^\dagger}}\,(dW_9 - idW_{10}).
\end{aligned}
\tag{4.16}
$$

These SDEs can be solved numerically to obtain the dynamics of the system in the time domain. However, in this thesis we are interested in investigating the dynamics of the system in the frequency domain. This can be done by following the linearized fluctuation theory [130] which we will describe in the next chapter.

Chapter 5

Linearized fluctuation analysis

In this chapter, we present the formalism that we follow to obtain the variances and covariances of the quadrature operators, $\hat{X}$ and $\hat{Y}$, of each output field as a function of the frequency. This is known as the linearized fluctuation theory [132, 133] and it allows us to obtain fluctuations about the steady state in the frequency domain. This linearization has been widely used to investigate the output fluctuations that arise from the interaction between light and a nonlinear medium inside a cavity [45, 52–56, 58, 59, 62, 63, 107, 109, 110, 114, 115, 117, 119, 120, 123, 130, 134–137]. Below, we describe this formalism.

5.1 Linearized fluctuation theory

After a system has already reached its steady state (SS), one can characterize the fluctuations about the SS following the linearized fluctuation theory. This consist in adding small fluctuations around the steady-state solutions to obtain the output spectrum $S(\omega)$ [130].

We consider small fluctuations around the steady-state solutions of the system. That is, the variable α_i is expressed in terms of the steady-state solution $\bar{\alpha}_i$ and the fluctuation $\delta\alpha_i$ as

$$\alpha_i = \bar{\alpha}_i + \delta\alpha_i, \quad \alpha_i^\dagger = \bar{\alpha}_i^\dagger + \delta\alpha_i^\dagger, \tag{5.1}$$

where $\delta\alpha_i \ll \bar{\alpha}_i$ ($i = 1, 2, \ldots$).

This linearization allows one to obtain a set of motion equations for the fluctuations whenever one substitute Equation 5.1 into Equation 4.12. The set can be expressed in terms of matrices $\bar{\boldsymbol{A}}$ (drift) and $\bar{\boldsymbol{B}}$, and a vector $\boldsymbol{\delta\alpha} = \left[\delta\alpha_1, \delta\alpha_1^\dagger, \ldots, \delta\alpha_n, \delta\alpha_n^\dagger\right]$ such that

$$d\boldsymbol{\delta\alpha_i} = -\bar{\boldsymbol{A}}_i\boldsymbol{\delta\alpha}_i dt + \bar{\boldsymbol{B}}_{ij} d\boldsymbol{W}_j, \tag{5.2}$$

where both $\bar{\boldsymbol{A}}$ and $\bar{\boldsymbol{B}}$ contain the SS solutions. Here, $d\boldsymbol{W}_j$ is the vector

$$d\boldsymbol{W}_j = \left[\boldsymbol{\xi}_1(t), \boldsymbol{\xi}_1^\dagger(t), \ldots, \boldsymbol{\xi}_n(t), \boldsymbol{\xi}_n^\dagger(t)\right]^T dt. \tag{5.3}$$

The validity of this linearization can be checked by the positivity of the eigenvalue spectrum of the drift matrix $\bar{\boldsymbol{A}}$. This means that the real part of all the eigenvalues must be positive.

5.2 Spectrum outside the cavity

As long as the linearization of the fluctuations is valid, one can relate the fluctuations of the output spectrum in the following way [138–140]:

$$\boldsymbol{S}(\omega) = (\bar{\boldsymbol{A}} + i\omega\boldsymbol{I})^{-1}\boldsymbol{B}\boldsymbol{B}^T(\bar{\boldsymbol{A}}^T - i\omega\boldsymbol{I})^{-1}. \tag{5.4}$$

In addition, the variances and covariances can be obtained directly from the elements of $\boldsymbol{S}(\omega)$ utilizing the input-output relations as [141]

$$\begin{aligned} S_{\hat{X}_i}(\omega) &= 1 + 2\gamma_i S_{\hat{X}_i}(\omega), \\ S_{\hat{X}_i,\hat{X}_j}(\omega) &= 2\sqrt{\gamma_i\gamma_j} S_{\hat{X}_i,\hat{X}_j}(\omega). \end{aligned} \tag{5.5}$$

Next, we obtain the spectrum outside the cavity for our model.

First, we substitute Equation 5.1 for $i = 1 - 6$ into Equation 4.16 in order to get the following set of motion equations for the fluctuations:

$$
\begin{aligned}
d\delta\alpha_1 &= -\left(\gamma_1\delta\alpha_1 + \chi_1\overline{\alpha}_5\delta\alpha_4 + \chi_1\overline{\alpha}_4\delta\alpha_5\right)dt,\\
d\delta\alpha_1^\dagger &= -\left(\gamma_1\delta\alpha_1^\dagger + \chi_1\overline{\alpha}_5^\dagger\delta\alpha_4^\dagger + \chi_1\overline{\alpha}_4^\dagger\delta\alpha_5^\dagger\right)dt,\\
d\delta\alpha_2 &= -\left(\gamma_2\delta\alpha_2 + \chi_2\overline{\alpha}_6\delta\alpha_5 + \chi_2\overline{\alpha}_5\delta\alpha_6\right)dt,\\
d\delta\alpha_2^\dagger &= -\left(\gamma_2\delta\alpha_2^\dagger + \chi_2\overline{\alpha}_6^\dagger\delta\alpha_5^\dagger + \chi_2\overline{\alpha}_5^\dagger\delta\alpha_6^\dagger\right)dt,\\
d\delta\alpha_3 &= -\left(\gamma_3\delta\alpha_3 + \chi_3\overline{\alpha}_6\delta\alpha_4 + \chi_3\overline{\alpha}_4\delta\alpha_6\right)dt,\\
d\delta\alpha_3^\dagger &= -\left(\gamma_3\delta\alpha_3^\dagger + \chi_3\overline{\alpha}_6^\dagger\delta\alpha_4^\dagger + \chi_3\overline{\alpha}_4^\dagger\delta\alpha_6^\dagger\right)dt,\\
d\delta\alpha_4 &= -\left(-\chi_1\overline{\alpha}_5^\dagger\delta\alpha_1 - \chi_3\overline{\alpha}_6^\dagger\delta\alpha_3 + \gamma_4\delta\alpha_4 - \chi_1\overline{\alpha}_1\delta\alpha_5^\dagger - \chi_3\overline{\alpha}_3\delta\alpha_6^\dagger\right)dt\\
&\quad - \sqrt{i\frac{\chi_1\chi_3\overline{\alpha}_1\overline{\alpha}_3}{\chi_2\overline{\alpha}_2}}\left(idW_{11} + dW_{12}\right),\\
d\delta\alpha_4^\dagger &= -\left(-\chi_1\overline{\alpha}_5\delta\alpha_1^\dagger - \chi_3\overline{\alpha}_6\delta\alpha_3^\dagger + \gamma_4\delta\alpha_4^\dagger - \chi_1\overline{\alpha}_1^\dagger\delta\alpha_5 - \chi_3\overline{\alpha}_3^\dagger\delta\alpha_6\right)dt\\
&\quad - \sqrt{\frac{\chi_1\chi_3\overline{\alpha}_1^\dagger\overline{\alpha}_3^\dagger}{2\chi_2\overline{\alpha}_2^\dagger}}\left(dW_9 + idW_{10}\right),\\
d\delta\alpha_5 &= -\left(-\chi_1\overline{\alpha}_4^\dagger\delta\alpha_1 - \chi_2\overline{\alpha}_6^\dagger\delta\alpha_2 - \chi_1\overline{\alpha}_1\delta\alpha_4^\dagger + \gamma_5\delta\alpha_5 - \chi_2\overline{\alpha}_2\delta\alpha_6^\dagger\right)dt\\
&\quad + \sqrt{i\frac{\chi_1\chi_2\overline{\alpha}_1\overline{\alpha}_2}{\chi_3\overline{\alpha}_3}}\left(dW_{11} - idW_7\right),\\
d\delta\alpha_5^\dagger &= -\left(-\chi_1\overline{\alpha}_4\delta\alpha_1^\dagger - \chi_2\overline{\alpha}_6\delta\alpha_2^\dagger - \chi_1\overline{\alpha}_1^\dagger\delta\alpha_4 + \gamma_5\delta\alpha_5^\dagger - \chi_2\overline{\alpha}_2^\dagger\delta\alpha_6\right)dt\\
&\quad - \sqrt{\frac{2\chi_1\chi_2\overline{\alpha}_1^\dagger\overline{\alpha}_2^\dagger}{\chi_3\overline{\alpha}_3^\dagger}}\left(idW_8 + dW_9\right),\\
d\delta\alpha_6 &= -\left(-\chi_2\overline{\alpha}_5^\dagger\delta\alpha_2 - \chi_3\overline{\alpha}_4^\dagger\delta\alpha_3 - \chi_3\overline{\alpha}_3\delta\alpha_4^\dagger - \chi_2\overline{\alpha}_2\delta\alpha_5^\dagger + \gamma_6\delta\alpha_6\right)dt\\
&\quad + \sqrt{i\frac{\chi_2\chi_3\overline{\alpha}_2\overline{\alpha}_3}{\chi_1\overline{\alpha}_1}}\left(dW_7 + idW_{12}\right),\\
d\delta\alpha_6^\dagger &= -\left(-\chi_2\overline{\alpha}_5\delta\alpha_2^\dagger - \chi_3\overline{\alpha}_4\delta\alpha_3^\dagger - \chi_3\overline{\alpha}_3^\dagger\delta\alpha_4 - \chi_2\overline{\alpha}_2^\dagger\delta\alpha_5 + \gamma_6\delta\alpha_6^\dagger\right)dt\\
&\quad - \sqrt{\frac{\chi_2\chi_3\overline{\alpha}_2^\dagger\overline{\alpha}_3^\dagger}{2\chi_1\overline{\alpha}_1^\dagger}}\left(dW_9 - idW_{10}\right).
\end{aligned}
\tag{5.6}
$$

This can be expressed as a vector such that $d\boldsymbol{\delta\alpha} = -\bar{\boldsymbol{A}}\boldsymbol{\delta\alpha}dt + \bar{\boldsymbol{B}}\boldsymbol{dW}$, where

$$
\boldsymbol{\delta\alpha} = \left[\delta\alpha_1, \delta\alpha_1^\dagger, \delta\alpha_2, \delta\alpha_2^\dagger, \delta\alpha_3, \delta\alpha_3^\dagger, \delta\alpha_4, \delta\alpha_4^\dagger, \delta\alpha_5, \delta\alpha_5^\dagger, \delta\alpha_6, \delta\alpha_6^\dagger\right]^T. \tag{5.7}
$$

In this way, the drift matrix is given by

$$
\bar{\boldsymbol{A}} = \begin{pmatrix} \boldsymbol{A}_1 & \boldsymbol{A}_2 \\ -\boldsymbol{A}_2^\dagger & \boldsymbol{A}_3 \end{pmatrix}, \tag{5.8}
$$

where $\boldsymbol{A}_1 = diag\,(\gamma_1, \gamma_1, \gamma_2, \gamma_2, \gamma_3, \gamma_3)$,

$$\boldsymbol{A}_2 = \begin{pmatrix} \chi_1\overline{\alpha}_5 & 0 & \chi_1\overline{\alpha}_4 & 0 & 0 & 0 \\ 0 & \chi_1\overline{\alpha}_5^\dagger & 0 & \chi_1\overline{\alpha}_4^\dagger & 0 & 0 \\ 0 & 0 & \chi_2\overline{\alpha}_6 & 0 & \chi_2\overline{\alpha}_5 & 0 \\ 0 & 0 & 0 & \chi_2\overline{\alpha}_6^\dagger & 0 & \chi_2\overline{\alpha}_5^\dagger \\ \chi_3\overline{\alpha}_6 & 0 & 0 & 0 & \chi_3\overline{\alpha}_4 & 0 \\ 0 & \chi_3\overline{\alpha}_6^\dagger & 0 & 0 & 0 & \chi_3\overline{\alpha}_4^\dagger \end{pmatrix},$$

$$\boldsymbol{A}_3 = \begin{pmatrix} \gamma_4 & 0 & 0 & -\chi_1\overline{\alpha}_1 & 0 & -\chi_3\overline{\alpha}_3 \\ 0 & \gamma_4 & -\chi_1\overline{\alpha}_1^\dagger & 0 & -\chi_3\overline{\alpha}_3^\dagger & 0 \\ 0 & -\chi_1\overline{\alpha}_1 & \gamma_5 & 0 & 0 & -\chi_2\overline{\alpha}_2 \\ -\chi_1\overline{\alpha}_1^\dagger & 0 & 0 & \gamma_5 & -\chi_2\overline{\alpha}_2^\dagger & 0 \\ 0 & -\chi_3\overline{\alpha}_3 & 0 & -\chi_2\overline{\alpha}_2 & \gamma_6 & 0 \\ -\chi_3\overline{\alpha}_3^\dagger & 0 & -\chi_2\overline{\alpha}_2^\dagger & 0 & 0 & \gamma_6 \end{pmatrix},$$

and

$$\bar{\boldsymbol{B}} = \begin{pmatrix} 0_{6\times6} & 0_{6\times6} \\ 0_{6\times6} & b_{6\times6} \end{pmatrix}, \tag{5.9}$$

where the non-zero elements in the submatrix $b_{6\times6}$ are

$$b_{15} = -i\sqrt{i\frac{\chi_1\chi_3\bar{\alpha_1}\bar{\alpha_3}}{\chi_2\bar{\alpha_2}}}, \qquad b_{16} = -\sqrt{i\frac{\chi_1\chi_3\bar{\alpha_1}\bar{\alpha_3}}{\chi_2\bar{\alpha_2}}}, \qquad b_{23} = -\sqrt{\frac{\chi_1\chi_3\bar{\alpha}_1^\dagger\bar{\alpha}_3^\dagger}{2\chi_2\bar{\alpha}_2^\dagger}},$$

$$b_{24} = -\sqrt{\frac{\chi_1\chi_3\bar{\alpha}_1^\dagger\bar{\alpha}_3^\dagger}{2\chi_2\bar{\alpha}_2^\dagger}}, \qquad b_{31} = -i\sqrt{i\frac{\chi_1\chi_2\bar{\alpha}_1\bar{\alpha}_2}{\chi_3\bar{\alpha}_3}}, \qquad b_{35} = \sqrt{i\frac{\chi_1\chi_2\bar{\alpha}_1\bar{\alpha}_2}{\chi_3\bar{\alpha}_3}},$$

$$b_{42} = -i\sqrt{\frac{2\chi_1\chi_2\bar{\alpha}_1^\dagger\bar{\alpha}_2^\dagger}{\chi_3\bar{\alpha}_3^\dagger}}, \qquad b_{43} = -\sqrt{\frac{2\chi_1\chi_2\bar{\alpha}_1^\dagger\bar{\alpha}_2^\dagger}{\chi_3\bar{\alpha}_3^\dagger}}, \qquad b_{51} = \sqrt{i\frac{\chi_2\chi_3\bar{\alpha}_2\bar{\alpha}_3}{\chi_1\bar{\alpha}_1}},$$

$$b_{56} = i\sqrt{i\frac{\chi_2\chi_3\bar{\alpha}_2\bar{\alpha}_3}{\chi_1\bar{\alpha}_1}}, \qquad b_{63} = -\sqrt{\frac{\chi_2\chi_3\bar{\alpha}_2^\dagger\bar{\alpha}_3^\dagger}{2\chi_1\bar{\alpha}_1^\dagger}}, \qquad b_{64} = i\sqrt{\frac{\chi_2\chi_3\bar{\alpha}_2^\dagger\bar{\alpha}_3^\dagger}{2\chi_1\bar{\alpha}_1^\dagger}}.$$

As long as the real part of the eigenvalues of the drift matrix $\bar{\boldsymbol{A}}$ is positive, the results of the linearization are valid. The analytical expressions for eigenvalue spectrum of $\bar{\boldsymbol{A}}$ are not easily obtained. However, we investigate the particular case when

$$\alpha_i^{SS} = \begin{cases} E_i/\gamma_i, & i = 1,\, 2,\, 3, \\ 0, & j = 4,\, 5,\, 6, \end{cases} \tag{5.10}$$

where we have defined $\alpha_i^{SS} \equiv \bar{\alpha_i}$.

The eigenvalues of the drift matrix $\bar{\boldsymbol{A}}$ for α_i^{SS} are given by

$$
\begin{aligned}
\lambda_{1,2} &= \gamma_1, \\
\lambda_{3,4} &= \gamma_2, \\
\lambda_{5,6} &= \gamma_3, \\
\lambda_7 &= -\frac{\sqrt[3]{2}\zeta}{\xi_+} - \frac{\xi_+}{3\sqrt[3]{2}\gamma_1^2\gamma_2^2\gamma_3^2}, \\
\lambda_8 &= \frac{\left(1+\sqrt{3}i\right)\zeta}{\sqrt[3]{4}\xi_+} + \frac{\left(1-\sqrt{3}i\right)\xi_+}{6\sqrt[3]{2}\gamma_1^2\gamma_2^2\gamma_3^2}, \\
\lambda_9 &= \frac{\left(1-\sqrt{3}i\right)\zeta}{\sqrt[3]{4}\xi_+} + \frac{\left(1+\sqrt{3}i\right)\xi_+}{6\sqrt[3]{2}\gamma_1^2\gamma_2^2\gamma_3^2}, \\
\lambda_{10} &= -\frac{\sqrt[3]{2}\zeta}{\xi_-} - \frac{\xi_-}{3\sqrt[3]{2}\gamma_1^2\gamma_2^2\gamma_3^2}, \\
\lambda_{11} &= \frac{\left(1+\sqrt{3}i\right)\zeta}{\sqrt[3]{4}\xi_-} + \frac{\left(1-\sqrt{3}i\right)}{6\sqrt[3]{2}\gamma_1^2\gamma_2^2\gamma_3^2}\xi_-, \\
\lambda_{12} &= \frac{\left(1-\sqrt{3}i\right)\zeta}{\sqrt[3]{4}\xi_-} + \frac{\left(1+\sqrt{3}i\right)}{6\sqrt[3]{2}\gamma_1^2\gamma_2^2\gamma_3^2}\xi_-,
\end{aligned}
\tag{5.11}
$$

where

$$
\begin{aligned}
\zeta &= \chi_3^2 E_3^2\gamma_1^2\gamma_2^2 + \chi_2^2 E_2^2\gamma_1^2\gamma_3^2 + \chi_1^2 E_1^2\gamma_2^2\gamma_3^2, \\
\xi_\pm &= \sqrt[3]{\mp\xi_1 + \sqrt{\xi_2}}, \\
\xi_1 &= 54\chi_1\chi_2\chi_3 E_1 E_2 E_3\gamma_1^5\gamma_2^5\gamma_3^5, \\
\xi_2 &= 2916\chi_1^2\chi_2^2\chi_3^2 E_1^2 E_2^2 E_3^2\gamma_1^{10}\gamma_2^{10}\gamma_3^{10} - 108\gamma_1^6\gamma_2^6\gamma_3^6\zeta^3.
\end{aligned}
$$

For simplicity, here we consider $\gamma_i \equiv \gamma = 1$ and $\chi_i = \kappa = 0.01$. Since we are interested in real values of the SS solutions, we use the values $E_3 = 50$ and E_1, $E_2 \in [50, 100]$. For these values, the real part of all the eigenvalues are positive and thus the linearization is valid. While for the case $\gamma_j \equiv \gamma = 1$ ($j = 1 - 6$), $\chi_i = \kappa = 0.01$ and $E_i \equiv E \in [51, 100]$ ($i = 1,\ 2,\ 3$), we investigate the real part of all the eigenvalues obtaining that all of these are positive. Thus, the linearization is still valid for these values.

Next, we calculate the spectrum outside the cavity for $\gamma = 1$ ($j = 1 - 6$), $\kappa = 0.01$ and $E \in [51, 100]$ by using Equation 5.4. The elements of the matrix $\boldsymbol{S}(\omega)$ and the

input-output relations [141] are used to obtain the variances and covariances as [55]:

$$\begin{aligned} V\left(\widehat{X}_i\right) &= 1 + 2\gamma_i S_{\hat{X}_i}(\omega), \\ V\left(\widehat{X}_i, \widehat{X}_j\right) &= 2\sqrt{\gamma_i \gamma_j} S_{\hat{X}_i, \hat{X}_j}(\omega), \\ V\left(\widehat{Y}_i\right) &= 1 + 2\gamma_i S_{\hat{Y}_i}(\omega), \\ V\left(\widehat{Y}_i, \widehat{Y}_j\right) &= 2\sqrt{\gamma_i \gamma_j} S_{\hat{Y}_i, \hat{Y}_j}(\omega). \end{aligned} \tag{5.12}$$

We utilize these quantities to express the entanglement and steering criteria described in chapter 2 as a function of the frequency. The following chapters are focus on the certification of these correlations in the frequency domain. In Figure 5.1 we show the steps that we follow to obtain the spectrum outside the cavity in terms of the frequency and the parameters of the system (E, κ, γ).

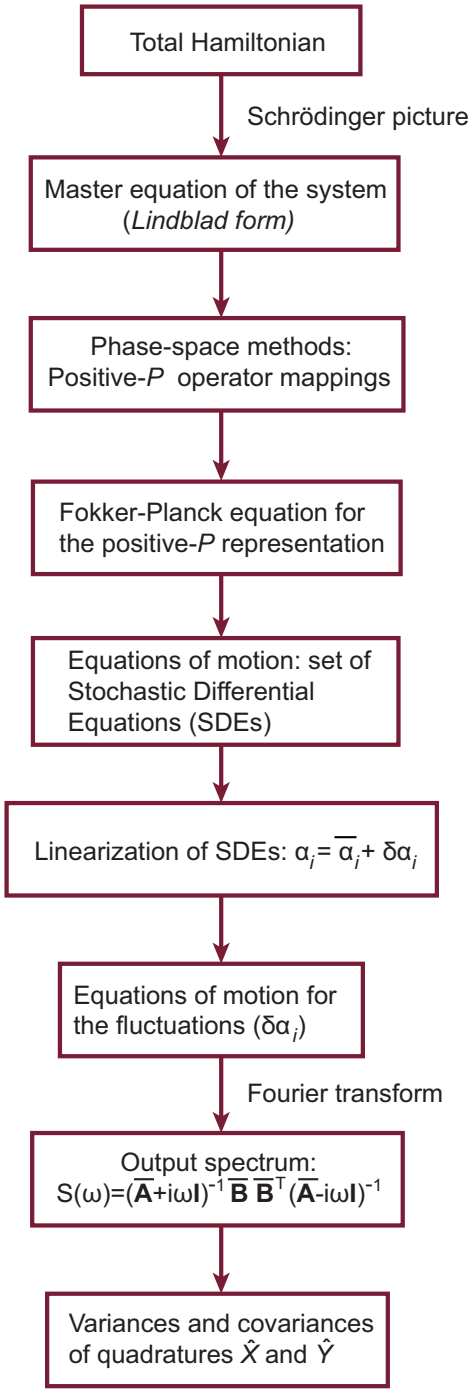

Figure 5.1: Block diagram of the steps to obtain the spectrum outside the cavity in the frequency domain.

Chapter 6

Certification of quantum entanglement among the output fields

In chapter 5, we have described the formalism to obtain the output spectrum $S(\omega)$ as a function of the frequency. This includes the steady-state solutions as well as the parameters of the system which are the amplitude of the incident fields E, the nonlinear coupling strength κ, and the intracavity losses γ. In order to certify quantum correlations, such as entanglement and steering, among the output fields we calculate the output spectrum $\boldsymbol{S}(\omega)$. Then, we utilize the elements of the matrix $\boldsymbol{S}(\omega)$ in the relations given in Equation 5.12 to obtain the variances and covariances of the output fields. Since these quantities depend on the value of the parameters of the system, we have performed simulations for different values of E, κ and γ.

Firstly, we consider that the input cavity losses (γ_{in}) are different to the output ones (γ_{out}). That is, $\gamma_1 = \gamma_2 = \gamma_3 \equiv \gamma_{in}$, $\gamma_4 = \gamma_5 = \gamma_6 \equiv \gamma_{out}$ and $\gamma_{in} \neq \gamma_{out}$. We recall that the subscript in refers to the input fields, while out corresponds to the output fields. We performed simulations for $\gamma_k \in [0.01, 1]$ ($k = in, out$), $E_i \equiv E = 100$ and $\chi_i \equiv \kappa = 0.01$ ($i = 1 - 3$). We find that bipartite quantum entanglement, genuine tripartite quantum entanglement, bipartite steering and full tripartite two-way steering inseparability can be certified whenever $\gamma_{in} = \gamma_{out}$ and $\gamma_{in}, \gamma_{out} > 0.81$. For $\gamma_{in} \leqslant 0.51$ and $\gamma_{out} \leqslant 0.91$, genuine tripartite steering cannot be certified. However, for $\gamma_{in} < 0.51$ and $\gamma_{out} < 0.91$, this correlation is certified at specific frequency intervals.

Secondly, we analyze both quantum entanglement and steering for $E_i \equiv E$ ($i = 1 - 3$). In this case, the cavity losses and the nonlinear coupling strength are $\gamma_j = 1$ ($j = 1 - 6$) and $\chi_i \equiv \kappa = 0.01$ ($i = 1 - 3$), respectively. We consider $E \in [51, 100]$ since the steady-state solutions must be real and different from zero. From the results of our simulations, we find that the interval of interest is $E \in [91, 105]$

since in this interval bipartite quantum entanglement, genuine tripartite quantum entanglement, bipartite steering and full tripartite two-way steering inseparability are certified simultaneously in a wide range of frequencies. It is important to mention that for values of the pump below $E = 91$, quantum entanglement and steering cannot be certified simultaneously. In addition, we find that the certification of both quantum correlations is related to the value of the pump amplitude.

Thirdly, for values of the nonlinear coupling strength $\chi_i \equiv \kappa \in [0.01, 0.3]$, with losses $\gamma_j = 1$ $(j = 1 - 6)$ and the amplitude of the fields $E_i \equiv E = 100$, we find that the certification of both quantum entanglement and steering holds, even if the value of κ increases.

Therefore, from our analysis of the different values of the parameters of the system and the results of our simulations, we determine that the optimal values of E, κ and γ to certify both quantum entanglement and steering in a wide range of frequencies are $E = 100$, $\kappa = 0.01$ and $\gamma = 1$. These values are considered throughout this thesis.

Therefore, in this chapter, we utilize the previously mentioned values and the criteria for the certification of entanglement, which have been described in section 2.1, to demonstrate whether bipartite and tripartite quantum entanglement in quadrature operators among the output fields exists or not. The following results are based on the published work by Ornelas-Cruces and Rosales-Zárate [142].

6.1 Certification of bipartite entanglement

We investigate bipartite entanglement between the output fields by using the Tan-Duan-Giedke-Cirac-Zoller-Simon (DGCZ), the Giovannetti-Mancini-Vitali-Tombesi (GMVT) and the van Loock-Furusawa (VLF) criteria described in subsection 2.1.1. As we have previously mentioned, these criteria consider two different parties of the system. Therefore, we analyze the bipartitions of the system $\{45\}$, $\{56\}$ and $\{46\}$ where each of them correspond to a pair of the down converted output fields (see Figure 4.1).

In the case of the VLF criterion, for each bipartition we obtain an inequality which depends on the real parameter g_l $(l = 4, 5, 6)$. That is,

$$
\begin{aligned}
VLF_{45} &= \frac{V\left(\hat{X}_4 - \hat{X}_5\right) + V\left(\hat{Y}_4 + \hat{Y}_5 + g_6\hat{Y}_6\right)}{4} \geqslant 1, \\
VLF_{56} &= \frac{V\left(\hat{X}_5 - \hat{X}_6\right) + V\left(\hat{Y}_5 + \hat{Y}_6 + g_4\hat{Y}_4\right)}{4} \geqslant 1, \\
VLF_{46} &= \frac{V\left(\hat{X}_4 - \hat{X}_6\right) + V\left(\hat{Y}_4 + \hat{Y}_6 + g_5\hat{Y}_5\right)}{4} \geqslant 1.
\end{aligned} \tag{6.1}
$$

In order to express g_l as a function of the variances of the quadrature operators $\hat{X}_i$ and $\hat{Y}_i$ ($i = 4, 5, 6$), we minimize the above equations with respect to the corresponding g_l.

In Figure 6.1 the DGCZ, GMVT and VLF criteria are shown. We observe that $DGCZ_{45} = DGCZ_{56} = DGCZ_{46}$, $GMVT_{45} = GMVT_{56} = GMVT_{46}$ and $VLF_{45} = VLF_{56} = VLF_{46}$. Therefore, we denote $DGCZ_{ij}$, $GMVT_{ij}$ and VLF_{ij} as the entanglement criteria for the different bipartitions where $i, j = 4, 5, 6$ and $i \neq j$. As mentioned in subsection 2.1.1, bipartite entanglement between the output fields in quadrature operators can be certified whenever the values of $DGCZ_{ij}$, $GMVT_{ij}$ and VLF_{ij} are below one (represented by the black solid line in Figure 6.1). We observe that the values for DGCZ criterion are below one for $\omega < 1.018$, while the values for GMVT criterion are below one for $\omega < 1.234$. On the other hand, the values for VLF criterion are below one for $\omega < 1.756$.

Even though, bipartite entanglement was certified by Bradley *et al* [52] using the VLF criterion, our results cannot be compared with the VLF values in [52] since the real parameters g_4, g_5 and g_6 were considered equal to one. Moreover, the matrix $\boldsymbol{B}(\boldsymbol{\alpha})$ is not the same as the one presented in [52]. We go further in the bipartite analysis by using two additional criteria and we demonstrate that VLF criterion is more robust than the DGCZ and GMVT criteria for this system. Therefore, we have certified bipartite entanglement in the low frequencies regime. Throughout this thesis, we consider the low frequencies regime for frequency values $\omega < 1$. We wish to mention that all quantities that we have plotted in this thesis are dimensionless.

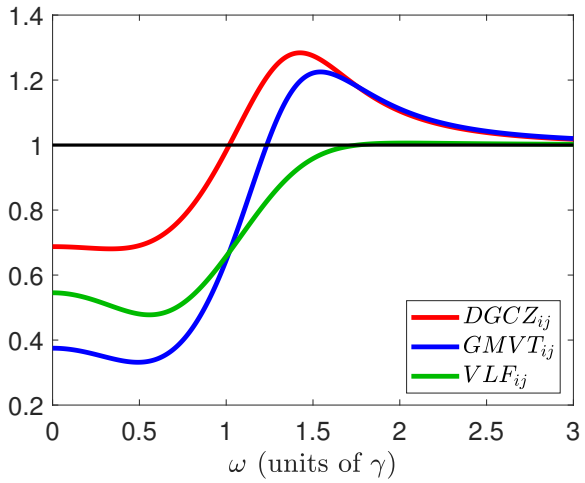

Figure 6.1: DGCZ, GMVT and VLF criteria for $E = 100$, $\kappa = 0.01$ and $\gamma = 1$. Bipartite entanglement for the bipartitions of the output fields $\{45\}$, $\{56\}$ and $\{46\}$ is certified whenever $DGCZ_{ij} < 1$, $GMVT_{ij} < 1$ and $VLF_{ij} < 1$ ($i, j = 4, 5, 6$, $i \neq j$). Here, the black solid line represents the bound of the DGCZ, GMVT and VLF criteria.

6.2 Certification of tripartite entanglement

In order to investigate tripartite entanglement among the output fields, we use the different criteria described in subsection 2.1.2. In the last section, we have demonstrated that the inequalities of the VLF criterion for the different bipartitions are violated for $\omega < 1.756$. The simultaneous violation of these inequalities implies that tripartite entanglement is present among the output fields [73]. However, this criterion is not sufficient to confirm genuine tripartite entanglement [74]. We determine whether tripartite entanglement among the output fields is genuine or not by checking the violation of the inequalities given in Equation 2.9-Equation 2.12.

For the criteria given in Equation 2.9 and Equation 2.10, we consider the bipartitions of the system $\{46\}-5$ and $\{56\}-4$ for $B_I\,(S_I)$, $\{45\}-6$ and $\{46\}-5$ for $B_{II}\,(S_{II})$, $\{45\}-6$ and $\{56\}-4$ for $B_{III}\,(S_{III})$, where

$$\begin{aligned} B_I &= V\left(\hat{X}_4 - \hat{X}_5\right) + V\left(\hat{Y}_4 + \hat{Y}_5 + g_6\hat{Y}_6\right) \geqslant 4, \\ B_{II} &= V\left(\hat{X}_5 - \hat{X}_6\right) + V\left(g_4\hat{Y}_4 + \hat{Y}_5 + \hat{Y}_6\right) \geqslant 4, \\ B_{III} &= V\left(\hat{X}_4 - \hat{X}_6\right) + V\left(\hat{Y}_4 + g_5\hat{Y}_5 + \hat{Y}_6\right) \geqslant 4, \end{aligned} \tag{6.2}$$

$$\begin{aligned} S_I &= \sqrt{V\left(\hat{X}_4 - \hat{X}_5\right) V\left(\hat{Y}_4 + \hat{Y}_5 + g_6\hat{Y}_6\right)} \geqslant 2, \\ S_{II} &= \sqrt{V\left(\hat{X}_5 - \hat{X}_6\right) V\left(g_4\hat{Y}_4 + \hat{Y}_5 + \hat{Y}_6\right)} \geqslant 2, \\ S_{III} &= \sqrt{V\left(\hat{X}_4 - \hat{X}_6\right) V\left(\hat{Y}_4 + g_5\hat{Y}_5 + \hat{Y}_6\right)} \geqslant 2. \end{aligned} \tag{6.3}$$

We minimize $B_I\,(S_I)$, $B_{II}\,(S_{II})$ and $B_{III}\,(S_{III})$ with respect to g_6, g_4 and g_5, respectively.

For the chosen values of the parameters of the system, the values of the set of inequalities given in Equation 6.2, and $B = B_I + B_{II} + B_{III}$ are shown in 6.2a. While the values of Equation 6.3 and $S = S_I + S_{II} + S_{III}$ are depicted in 6.2b. In 6.2a and 6.2b, we observe that $B_I = B_{II} = B_{III}$ and $S_I = S_{II} = S_{III}$, respectively. In addition, we notice that there exist frequencies where the conditions $B_\alpha < 4$ and $B < 8$, and $S_\alpha < 2$ and $S < 4$ ($\alpha = I, II, III$) are satisfied. We find that $B_\alpha < 4$ for $\omega < 1.756$ and $B < 8$ for $\omega < 1.013$, while $S_\alpha < 2$ for $\omega \in [0, 3]$ and $S < 4$ for $\omega < 1.079$. The simultaneous violation of Equation 6.2 and $B \geqslant 8$, as well as Equation 6.3 and $S \geqslant 4$, confirms genuine tripartite entanglement among the output fields. Therefore, we can certify genuine tripartite entanglement with the criteria given in Equation 2.9 and Equation 2.10 for $\omega < 1.013$ and $\omega < 1.079$, respectively. This demonstrates that the criterion given in Equation 2.10 certifies genuine tripartite entanglement over a wider range of frequencies than the criterion given in Equation 2.9.

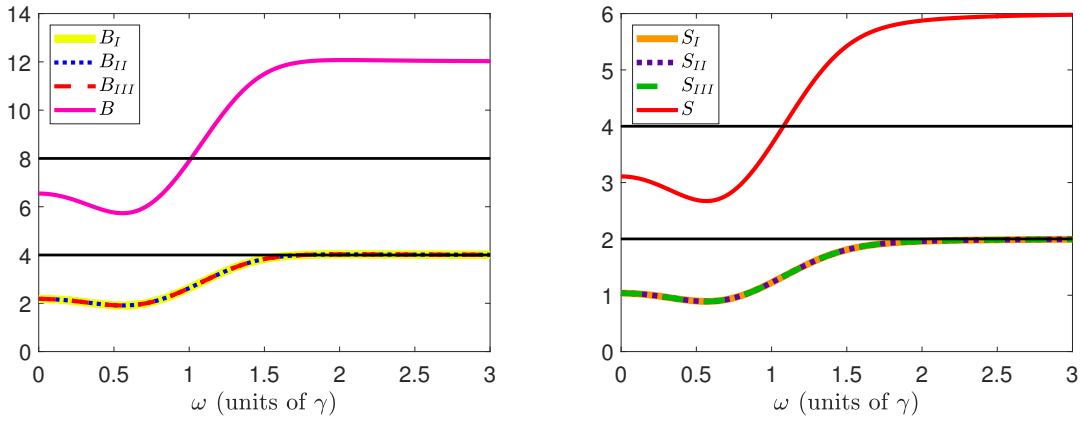

(a) (b)

Figure 6.2: Genuine tripartite entanglement among the output fields is certified whenever (a) $B_\alpha < 4$ and $B < 8$, or (b) $S_\alpha < 2$ and $S < 4$ ($\alpha = I, II, III$) for $E = 100$, $\kappa = 0.01$ and $\gamma = 1$. The black solid lines in (a) and (b) represent the bound for the entanglement criteria of Equation 2.9 and Equation 2.10, respectively.

In addition, we investigate the certification of genuine tripartite entanglement by using the criteria given in Equation 2.11 and Equation 2.12. For our system, these criteria can be written as

$$\Delta^2 V \equiv V\left(\hat{X}_4 - \frac{\hat{X}_5 + \hat{X}_6}{\sqrt{2}}\right) + V\left(\hat{Y}_4 + \frac{\hat{Y}_5 + \hat{Y}_6}{\sqrt{2}}\right) \geqslant 2, \tag{6.4}$$

$$\Delta V \equiv \sqrt{V\left(\hat{X}_4 - \frac{\hat{X}_5 + \hat{X}_6}{\sqrt{2}}\right) V\left(\hat{Y}_4 + \frac{\hat{Y}_5 + \hat{Y}_6}{\sqrt{2}}\right)} \geqslant 1. \tag{6.5}$$

The violation of any inequality, $\Delta^2 V \geqslant 2$ or $\Delta V \geqslant 1$, certifies genuine tripartite entanglement among the output fields.

In 6.3a and 6.3b, the values of $\Delta^2 V$ and ΔV are shown, respectively. We find that the violation of both inequalities, $\Delta^2 V < 2$ and $\Delta V < 1$, occurs for $\omega < 1.065$. We conclude that the certification of genuine tripartite entanglement with these criteria is also present at low frequencies.

So far, we have proved that genuine tripartite entanglement among the output fields is present in the system by using four different criteria. From our analysis, we find that the criterion given by Equation 6.3, is the one that certifies this type of entanglement in a wide range of frequencies which correspond to $\omega \in [0, 1.079)$.

In conclusion, we have certified bipartite, tripartite as well as genuine tripartite quantum entanglement among the output fields in the low frequency regime for $E = 100$,

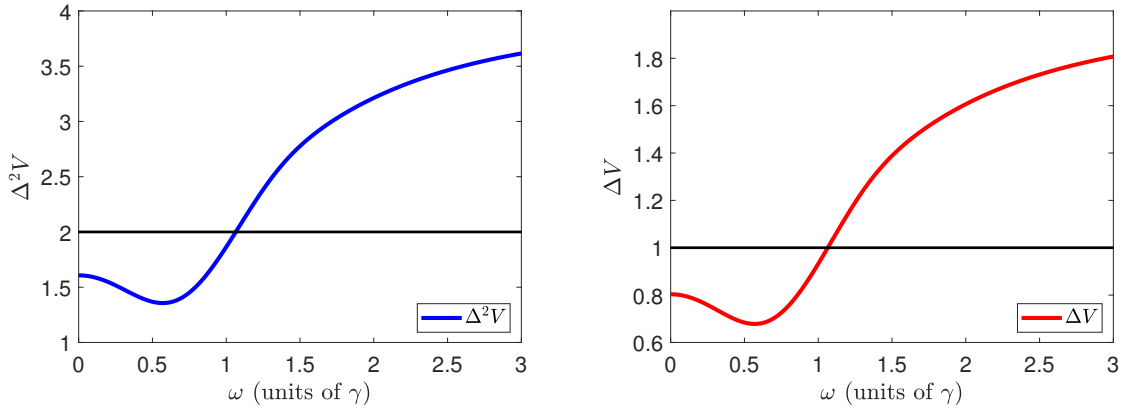

(a) (b)

Figure 6.3: If (a) $\Delta^2 V$ is below two (black solid line) or (b) ΔV is below one (black solid line) is sufficient to prove genuine tripartite entanglement among the output fields for $E = 100$, $\kappa = 0.01$ and $\gamma = 1$.

$\kappa = 0.01$ and $\gamma = 1$. In the case of bipartite entanglement, the VLF criterion certifies this type of entanglement for $\omega \in [0, 1.756)$. This criterion also demonstrates tripartite entanglement. While, in the case of genuine tripartite entanglement, the criterion given in Equation 6.3 certifies this correlation for $\omega < 1.079$. In reference [52], Bradley *et al* showed that this system generate tripartite entangled fields. However, the authors analyzed this system by considering both above and below the oscillation threshold of an OPO. We go further in the entanglement analysis, that is, we have investigated the system beyond threshold limits and we have demonstrated that this system produces both tripartite and genuine tripartite entangled fields.

In the next chapter we investigate whether the down converted fields can be steerable for the same values of the parameters of the system which are $E = 100$, $\kappa = 0.01$ and $\gamma = 1$.

Chapter 7

Certification of quantum steering among the output fields

In chapter 6, we have certified bipartite, tripartite and genuine tripartite entanglement among the output fields in the low frequency regime ($\omega < 1$). Although this correlation exists between the output fields, we are also interested in investigating another nonlocal correlation: quantum steering, which is a stronger correlation than quantum entanglement [6, 7]. It is important to mention that the certification of quantum entanglement in a system does not guarantee the certification of quantum steering [5–7].

In this chapter, we investigate whether the output fields can be steerable or not. In order to certify bipartite and tripartite quantum steering among the output fields, we use the output spectrum to obtain the variances and covariances of the quadrature operators. We utilize the criteria described in section 2.2 with the same values of the parameters of the system which are $E_i = E$=100, $\chi_i = \kappa$ =0.01 and $\gamma_j = \gamma$=1 ($i = 1, 2, 3$ and $j = 1 - 6$). The results presented in this chapter are based on the work by Ornelas-Cruces and Rosales-Zárate [143].

7.1 Certification of bipartite steering

Bipartite steering between the output fields can be certified with the criterion developed by Reid [4, 75]. As previously mentioned, steering has the property of being asymmetric. In this sense, it is important to investigate whether one party of the system j, can steer the party i, as well as the steerability of i from j. This criterion states that bipartite steering is present between two parties of the system whenever $EPR_{i|j} < 1$ is satisfied [4, 75]. For the output fields, $i, j = 4, 5, 6$ ($i \neq j$), this

criterion is expressed by the following inequalities:

$$EPR_{4|5} = V_{\{inf|5\}}\left(\hat{X}_4\right) V_{\{inf|5\}}\left(\hat{Y}_4\right) < 1, \tag{7.1}$$
$$EPR_{5|4} = V_{\{inf|4\}}\left(\hat{X}_5\right) V_{\{inf|4\}}\left(\hat{Y}_5\right) < 1, \tag{7.2}$$
$$EPR_{5|6} = V_{\{inf|6\}}\left(\hat{X}_5\right) V_{\{inf|6\}}\left(\hat{Y}_5\right) < 1, \tag{7.3}$$
$$EPR_{6|5} = V_{\{inf|5\}}\left(\hat{X}_6\right) V_{\{inf|5\}}\left(\hat{Y}_6\right) < 1, \tag{7.4}$$
$$EPR_{4|6} = V_{\{inf|6\}}\left(\hat{X}_4\right) V_{\{inf|6\}}\left(\hat{Y}_4\right) < 1, \tag{7.5}$$
$$EPR_{6|4} = V_{\{inf|4\}}\left(\hat{X}_6\right) V_{\{inf|4\}}\left(\hat{Y}_6\right) < 1. \tag{7.6}$$

The inference variances $V_{\{inf|j\}}\left(\hat{X}_i\right)$ and $V_{\{inf|j\}}\left(\hat{Y}_i\right)$ are explicitly given by [4]

$$V_{\{inf|5\}}\left(\hat{X}_4\right) = V\left(\hat{X}_4\right) - \frac{\left[V\left(\hat{X}_4, \hat{X}_5\right)\right]^2}{V\left(\hat{X}_5\right)},$$
$$V_{\{inf|5\}}\left(\hat{Y}_4\right) = V\left(\hat{Y}_4\right) - \frac{\left[V\left(\hat{Y}_4, \hat{Y}_5\right)\right]^2}{V\left(\hat{Y}_5\right)}, \tag{7.7}$$

$$V_{\{inf|4\}}\left(\hat{X}_5\right) = V\left(\hat{X}_5\right) - \frac{\left[V\left(\hat{X}_5, \hat{X}_4\right)\right]^2}{V\left(\hat{X}_4\right)},$$
$$V_{\{inf|4\}}\left(\hat{Y}_5\right) = V\left(\hat{Y}_5\right) - \frac{\left[V\left(\hat{Y}_5, \hat{Y}_4\right)\right]^2}{V\left(\hat{Y}_4\right)}, \tag{7.8}$$

$$V_{\{inf|6\}}\left(\hat{X}_5\right) = V\left(\hat{X}_5\right) - \frac{\left[V\left(\hat{X}_5, \hat{X}_6\right)\right]^2}{V\left(\hat{X}_6\right)},$$
$$V_{\{inf|6\}}\left(\hat{Y}_5\right) = V\left(\hat{Y}_5\right) - \frac{\left[V\left(\hat{Y}_5, \hat{Y}_6\right)\right]^2}{V\left(\hat{Y}_6\right)}, \tag{7.9}$$

$$V_{\{inf|5\}}\left(\hat{X}_6\right) = V\left(\hat{X}_6\right) - \frac{\left[V\left(\hat{X}_6, \hat{X}_5\right)\right]^2}{V\left(\hat{X}_5\right)},$$
$$V_{\{inf|5\}}\left(\hat{Y}_6\right) = V\left(\hat{Y}_6\right) - \frac{\left[V\left(\hat{Y}_6, \hat{Y}_5\right)\right]^2}{V\left(\hat{Y}_5\right)}, \tag{7.10}$$

$$V_{\{inf|6\}}\left(\hat{X}_4\right) = V\left(\hat{X}_4\right) - \frac{\left[V\left(\hat{X}_4, \hat{X}_6\right)\right]^2}{V\left(\hat{X}_6\right)},$$
$$V_{\{inf|6\}}\left(\hat{Y}_4\right) = V\left(\hat{Y}_4\right) - \frac{\left[V\left(\hat{Y}_4, \hat{Y}_6\right)\right]^2}{V\left(\hat{Y}_6\right)}, \tag{7.11}$$

$$V_{\{inf|4\}}\left(\hat{X}_6\right) = V\left(\hat{X}_6\right) - \frac{\left[V\left(\hat{X}_6, \hat{X}_4\right)\right]^2}{V\left(\hat{X}_4\right)},$$
$$V_{\{inf|4\}}\left(\hat{Y}_6\right) = V\left(\hat{Y}_6\right) - \frac{\left[V\left(\hat{Y}_6, \hat{Y}_4\right)\right]^2}{V\left(\hat{Y}_4\right)}, \tag{7.12}$$

where $V\left(\hat{X}_i, \hat{X}_j\right)$ and $V\left(\hat{Y}_i, \hat{Y}_j\right)$ is the covariance of the operators $\hat{X}_i$ and $\hat{X}_j$, and $\hat{Y}_i$ and $\hat{Y}_j$, respectively. These values are obtained from the output spectrum and the expressions given in Equation 5.12.

Figure 7.1 shows bipartite steering criterion between the output fields for $E = 100$, $\kappa = 0.01$ and $\gamma = 1$, where the product of the inference variances for the different bipartitions of the system are given by Equation 7.1-Equation 7.6. We observe that $EPR_{4|5} = EPR_{5|4}$, $EPR_{5|6} = EPR_{6|5}$ and $EPR_{4|6} = EPR_{6|4}$. Furthermore, the condition $EPR_{i|j} < 1$ is satisfied for i, $j = 4, 5, 6$ $(i \neq j)$. This demonstrate that each party j steers party i. Thus, the violation of $EPR_{i|j} \geqslant 1$ implies one-way steering for $\omega < 1.755$ between the output fields. Additionally, we notice that $EPR_{j|i} < 1$ is satisfied for $\omega < 1.755$ which shows that party i steers party j. The violation of both $EPR_{i|j} \geqslant 1$ and $EPR_{j|i} \geqslant 1$ implies two-way steering. Thus, for this system, both bipartite one-way and two-way steering are certified between the down-converted fields for the different bipartitions of the system in the low frequency regime.

7.2 Certification of full tripartite two-way steering inseparability

In this section, we investigate whether full tripartite two-way steering inseparability for the different bipartitions of the output fields exists or not. We use the criteria described in section 2.2 where B_α and S_α $(\alpha = I, II, III)$ are given by

$$B_I = V\left(\hat{X}_4 - \hat{X}_5\right) + V\left(\hat{Y}_4 + \hat{Y}_5 + g_6\hat{Y}_6\right),$$
$$B_{II} = V\left(\hat{X}_5 - \hat{X}_6\right) + V\left(g_4\hat{Y}_4 + \hat{Y}_5 + \hat{Y}_6\right),$$
$$B_{III} = V\left(\hat{X}_4 - \hat{X}_6\right) + V\left(\hat{Y}_4 + g_5\hat{Y}_5 + \hat{Y}_6\right), \tag{7.13}$$

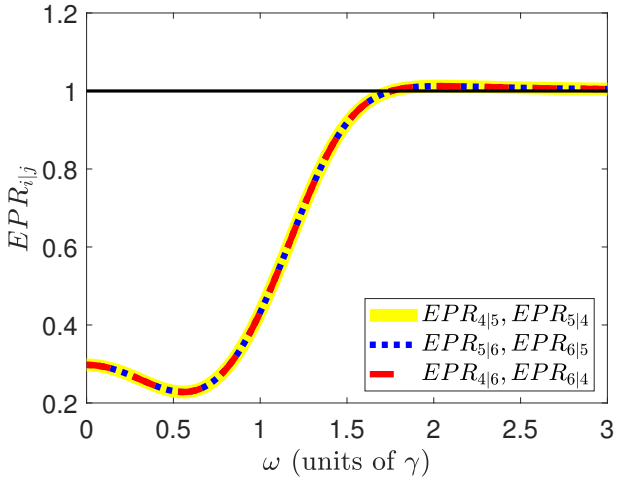

Figure 7.1: Bipartite quantum steering between the output fields for $E = 100$, $\kappa = 0.01$ and $\gamma = 1$. This is certified whenever $EPR_{i|j}$ is below one (black solid line). That is, $EPR_{i|j} < 1$ (i, $j = 4$, 5, 6, $i \neq j$).

$$S_I = \sqrt{V\left(\hat{X}_4 - \hat{X}_5\right) V\left(\hat{Y}_4 + \hat{Y}_5 + g_6\hat{Y}_6\right)},$$
$$S_{II} = \sqrt{V\left(\hat{X}_5 - \hat{X}_6\right) V\left(g_4\hat{Y}_4 + \hat{Y}_5 + \hat{Y}_6\right)},$$
$$S_{III} = \sqrt{V\left(\hat{X}_4 - \hat{X}_6\right) V\left(\hat{Y}_4 + g_5\hat{Y}_5 + \hat{Y}_6\right)}. \tag{7.14}$$

We minimize B_α and S_α ($\alpha = I$, II, III) with respect to g_6, g_4 and g_5, respectively. It is important to mention that B_I (S_I) is related to bipartitions $\{46\}-5$ and $\{56\}-4$, while B_{II} (S_{II}) corresponds to bipartitions $\{54\}-6$ and $\{64\}-5$, and B_{III} (S_{III}) to $\{45\}-6$ and $\{65\}-4$.

The criteria are shown in Figure 7.2 for the same values of the parameters of the system. First, we observe that $B_I = B_{II} = B_{III}$ and $S_I = S_{II} = S_{III}$, respectively. Second, full tripartite two-way steering inseparability is certified only for specific intervals of frequency. For instance, 7.2a shows that $B_\alpha < 2$ ($\alpha = I$, II, III) in the interval $\omega \in (0.363, 0.712)$. While in 7.2b, we observe that $S_\alpha < 1$ ($\alpha = I$, II, III) for $\omega \in (0.207, 0.808)$. Both criteria certify full tripartite two-way steering inseparability for different range of frequencies. That is, steering is present at least in one direction, for all bipartitions of the system which we have considered as $\{AB\}-C$ for A, B, $C = 4$, 5, 6 ($A \neq B \neq C$). However, the criterion $S_\alpha < 1$ ($\alpha = I$, II, III) certifies full tripartite two-way steering inseparability in a wide frequency interval.

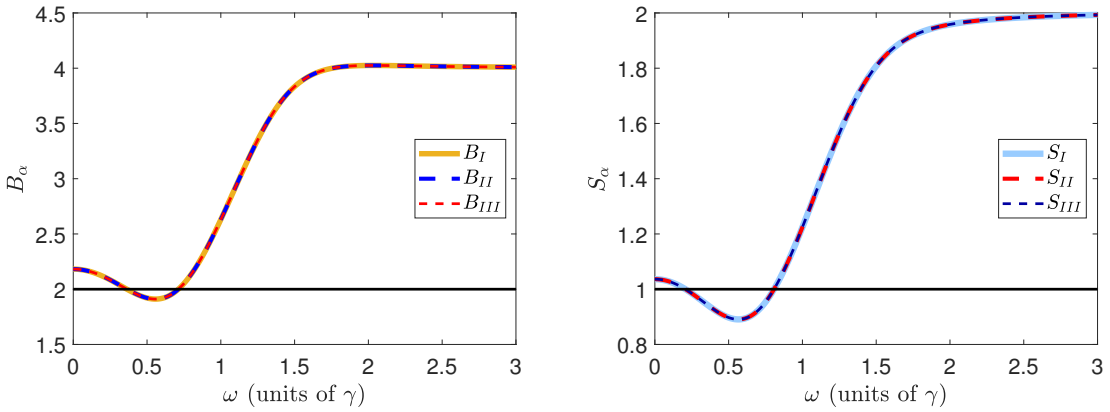

Figure 7.2: Full tripartite two-way steering inseparability among the output fields for $E = 100$, $\kappa = 0.01$ and $\gamma = 1$ is certified whenever (a) $B_\alpha < 2$ or (b) $S_\alpha < 1$. The black solid line represents the corresponding bound for B_α and S_α, respectively.

7.3 Certification of genuine tripartite steering

Once we have certified full tripartite two-way steering inseparability for the different bipartitions of the output fields, we wish to investigate if genuine tripartite steering is also present in the system.

We use the criteria given in Equation 2.18 and Equation 2.19, where B_α and S_α correspond to Equation 7.13 and Equation 7.14, respectively. As we have previously considered, B_α and S_α are minimized with respect to g_6, g_4 and g_5, respectively. Since this type of steering consider the bilocality of the system [76], we utilize the same bipartitions for $B_\alpha\,(S_\alpha)$ as we have described in the preceding section.The criteria are shown in Figure 7.3. We observe that there is no violation of either $B_I + B_{II} + B_{III} \geqslant 4$ or $S_I + S_{II} + S_{III} \geqslant 2$ for any value of frequency under consideration. This demonstrates that genuine tripartite steering is not present in the system for the chosen values of the parameters of the system.

7.3.1 Certification of genuine tripartite steering: $g_i = 1$

In the previous section, we have investigated whether genuine tripartite steering is present in the system by using different criteria which depend on the real parameter g_i $(i = 4, 5, 6)$. In that case, we have minimized B_α and S_α $(\alpha = I, II, III)$ with respect to g_6, g_4, and g_5, respectively, in order to obtain g_i $(i = 4, 5, 6)$ in terms of the variances and covariances of the quadrature operators of the output

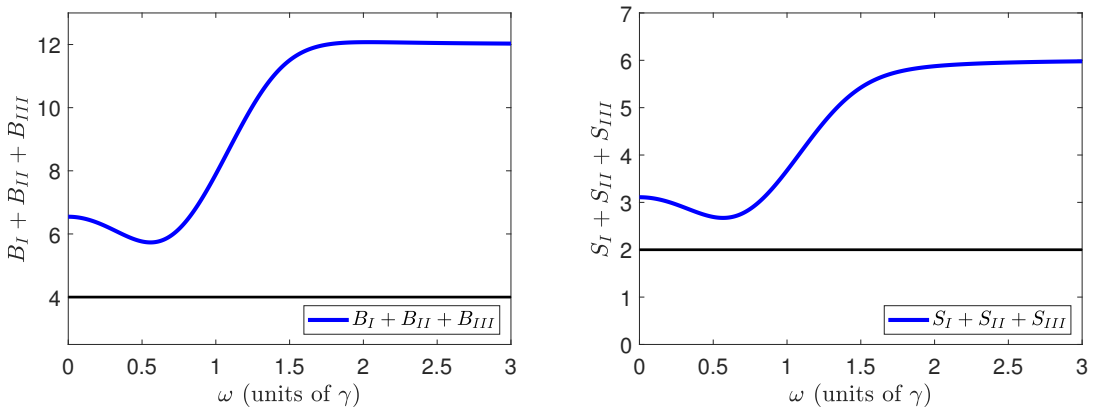

(a) (b)

Figure 7.3: Genuine tripartite steering among the output fields is certified whenever (a) $B_I + B_{II} + B_{III} < 4$ or (b) $S_I + S_{II} + S_{III} < 2$ for $E = 100$, $\kappa = 0.01$ and $\gamma = 1$. Here, neither of (a) or (b) are below the bound four or two (black solid lines), respectively.

fields $\hat{X}_j$, $\hat{Y}_j$ $(j = 4, 5, 6)$. However, it was not possible to certify genuine tripartite steering for any value of the frequency under consideration.

In this section, we investigate if genuine tripartite steering exists among the output fields by considering $g_i = 1$ $(i = 4, 5, 6)$. Figure 7.4 shows both criteria given in Equation 2.20 and Equation 2.21, while the criteria given in Equation 2.22 and Equation 2.23 are depicted in Figure 7.5. From these figures, we observe that neither of the criteria is satisfied for any value of the frequency for $g_i = 1$ $(i = 4, 5, 6)$. Therefore, genuine tripartite steering is not present in the system.

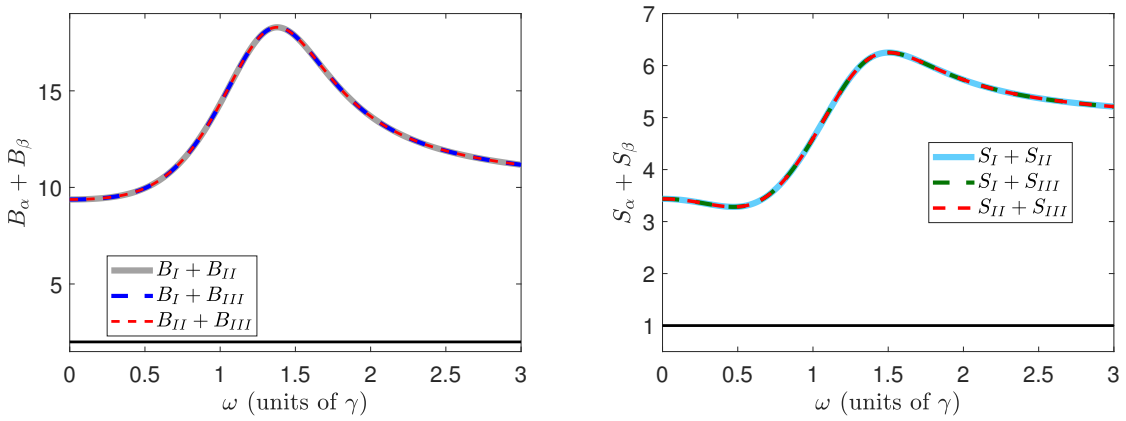

Figure 7.4: Genuine tripartite steering for $g_i = 1$ $(i = 4, 5, 6)$ is certified whenever (a) $B_\alpha + B_\beta < 2$ or (b) $S_\alpha + S_\beta < 1$ for $\alpha, \beta = I, II, III$ and $\alpha \neq \beta$. The values of the parameters of the system are $E = 100$, $\kappa = 0.01$ and $\gamma = 1$. The black solid lines in (a) and (b) represent the bound two and one, respectively.

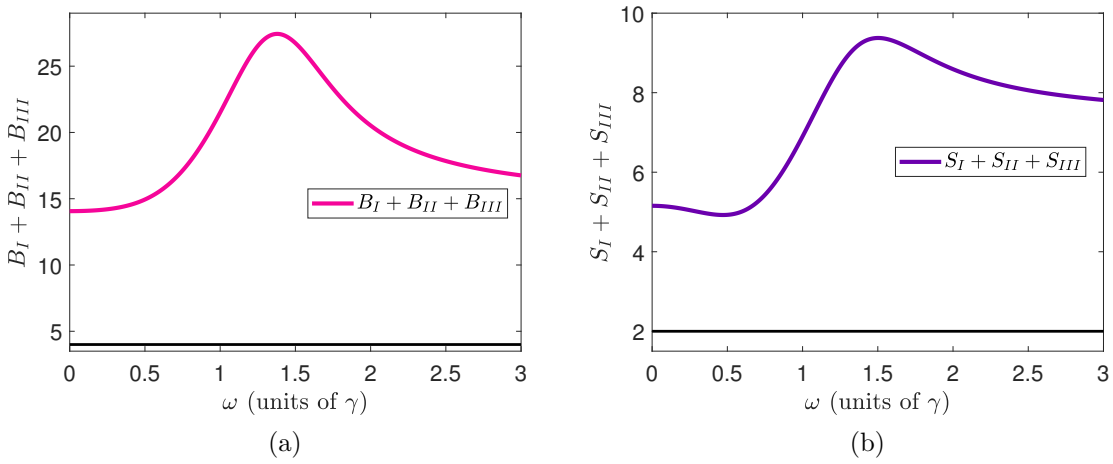

Figure 7.5: Genuine tripartite steering is present in the system if either (a) $B_I + B_{II} + B_{III} < 4$ or (b) $S_I + S_{II} + S_{III} < 2$ for $g_i = 1$ $(i = 4, 5, 6)$, $E = 100$, $\kappa = 0.01$, and $\gamma = 1$. In both (a) and (b) the black solid line represents the bound four and two, respectively.

In conclusion, for the chosen values of the parameters of the system we have certified bipartite one-way and two-way steering between the output fields in the low frequency regime. In addition, there exists full tripartite two-way steering inseparability among the output fields for specific frequency values. However, for the strongest type of

steering, which is the genuine tripartite case, it was not possible to certify for any value of the frequency.

In the next chapter, we investigate the distribution of both quantum entanglement and steering among the different parties of the system by using the monogamy relations. These relations are expressed in terms of the entanglement and steering witnesses which we have used throughout this thesis.

Chapter 8

Distribution of entanglement and steering among the output fields

In the preceding chapters, we have demonstrated that the output fields are entangled and these are also steerable in the low frequency regime. In particular, the entanglement that we have certified for the down-converted fields includes the bipartite, tripartite and genuine tripartite cases. While the steering cases are bipartite one-way and two-way steering, and full tripartite two-way steering inseparability. Although these correlations exist in the system, we have no knowledge about their distribution among the different parties of the system. In fact, the shareability of entanglement and steering among the three output fields is constrained. That is, the amount of entanglement (steering) that two parties parties, i and j, share limits the amount of entanglement (steering) that one of those parties (say i) can share with a third party k. It is worth mentioning that the monogamy relations presented in chapter 3 do not quantify the amount of entanglement (steering) that the parties share among them.

In this chapter, we investigate the distribution of these correlations by using the monogamy relations for entanglement and steering witnesses [41, 88], which we have described in chapter 3.

8.1 Distribution of entanglement between the output fields

In order to investigate the shareability of entanglement between the output fields, we utilize the monogamy relations for DGCZ and GMVT witnesses which we have described in section 3.1. For the system under consideration, the first monogamy

relations for DGCZ witness, for the different bipartitions, are given by

$$D_{45} + D_{46} \geqslant 1, \tag{8.1}$$
$$D_{54} + D_{56} \geqslant 1, \tag{8.2}$$
$$D_{64} + D_{65} \geqslant 1. \tag{8.3}$$

We can interpret these relations as follows. For instance, in Equation 8.1, the down-converted fields 4 and 5 share certain amount of entanglement which constrains the entanglement that 4 can share with 6. That is, the entanglement that 4 shares with 5 is not available to be shared with 6. In other words, as the amount of entanglement between 4 and 5 becomes maximum (which corresponds to $D_{45} \to 0$), the value of D_{46} increases, which can be expressed as $D_{46} \to \infty$. This relation does not measure the amount of entanglement, however, it provides a distribution of entanglement between the different bipartitions of the system. Equation 8.1-Equation 8.3 are depicted in Figure 8.1a. We observe that, for the different bipartitions, $D_{45}+D_{46} = D_{54}+D_{56} = D_{64} + D_{65}$ and this monogamy of entanglement for the DGCZ certifier is satisfied.

Another set of monogamy relations for DGCZ witness for the different bipartitions is given by

$$D_{45} + D_{46} \geqslant max\left\{1, S_{4|\{56\}}\right\}, \tag{8.4}$$
$$D_{54} + D_{56} \geqslant max\left\{1, S_{5|\{46\}}\right\}, \tag{8.5}$$
$$D_{64} + D_{65} \geqslant max\left\{1, S_{6|\{45\}}\right\}. \tag{8.6}$$

These relate the monogamy bound to a steering parameter $S_{B|\{AC\}}$, respectively. $S_{B|\{AC\}}$ certifies that the bipartition $\{AC\}$ steers B (A, B, $C = 4$, 5, 6) where

$$S_{4|\{56\}} = V_{inf|\{56\}}(\hat{X}_4)V_{inf|\{56\}}(\hat{Y}_4), \tag{8.7}$$
$$S_{5|\{46\}} = V_{inf|\{46\}}(\hat{X}_5)V_{inf|\{46\}}(\hat{Y}_5), \tag{8.8}$$
$$S_{6|\{45\}} = V_{inf|\{45\}}(\hat{X}_6)V_{inf|\{45\}}(\hat{Y}_6), \tag{8.9}$$

and

$$V_{inf|\{56\}}(\hat{X}_4) = V(\hat{X}_4) - \frac{\left[V(\hat{X}_4, \hat{X}_5 + \hat{X}_6)\right]}{V(\hat{X}_5 + \hat{X}_6)},$$
$$V_{inf|\{56\}}(\hat{Y}_4) = V(\hat{Y}_4) - \frac{\left[V(\hat{Y}_4, \hat{Y}_5 + \hat{Y}_6)\right]}{V(\hat{Y}_5 + \hat{Y}_6)}, \tag{8.10}$$

$$V_{inf|\{46\}}(\hat{X}_5) = V(\hat{X}_5) - \frac{\left[V(\hat{X}_5, \hat{X}_4 + \hat{X}_6)\right]}{V(\hat{X}_4 + \hat{X}_6)},$$
$$V_{inf|\{46\}}(\hat{Y}_5) = V(\hat{Y}_5) - \frac{\left[V(\hat{Y}_5, \hat{Y}_4 + \hat{Y}_6)\right]}{V(\hat{Y}_4 + \hat{Y}_6)}, \tag{8.11}$$

$$V_{inf|\{45\}}(\hat{X}_6) = V(\hat{X}_6) - \frac{\left[V(\hat{X}_6, \hat{X}_4 + \hat{X}_5)\right]}{V(\hat{X}_4 + \hat{X}_5)},$$
$$V_{inf|\{45\}}(\hat{Y}_6) = V(\hat{Y}_6) - \frac{\left[V(\hat{Y}_6, \hat{Y}_4 + \hat{Y}_5)\right]}{V(\hat{Y}_4 + \hat{Y}_5)}. \tag{8.12}$$

In Figure 8.1b, we show the monogamy relations given in Equation 8.4-Equation 8.6. We observe that $D_{45} + D_{46} = D_{54} + D_{56} = D_{64} + D_{65}$ and $S_{4|\{56\}} = S_{5|\{46\}} = S_{6|\{45\}}$. In addition, we notice that the amount of bipartite entanglement for the different bipartitions is always greater than the monogamy bound, either 1 or $S_{B|\{AC\}}$. These results also demonstrate that there exists steering of B by $\{AC\}$ for the different bipartitions of the system.

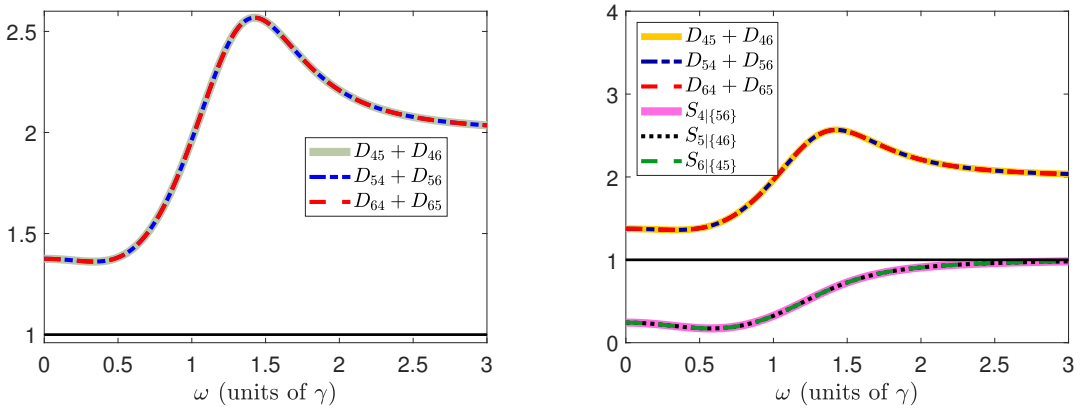

(a) (b)

Figure 8.1: Monogamy relations for the DGCZ witness. Both (a) $D_{BA}+D_{BC} \geqslant 1$ and (b) $D_{BA} + D_{BC} \geqslant max\left\{1, S_{B|\{AC\}}\right\}$ must satisfy for the bipartitions of the system {45}-{46}, {54}-{56}, and {64}-{65}, respectively. The black solid line represents the monogamy bound of (a) and (b), respectively.

For the GMVT witness, the monogamy relations for the different bipartitions are given by

$$4G_{54}G_{56} \geqslant max\left\{1, S^2_{5|\{46\}}\right\}, \tag{8.13}$$
$$4G_{45}G_{46} \geqslant max\left\{1, S^2_{4|\{56\}}\right\}, \tag{8.14}$$
$$4G_{64}G_{65} \geqslant max\left\{1, S^2_{6|\{45\}}\right\}, \tag{8.15}$$

where $S^2_{B|\{AC\}}(A, B, C = 4, 5, 6)$ is the steering parameter. These are shown in Figure 8.2 where we can observe that $4G_{54}G_{56} = 4G_{45}G_{46} = 4G_{64}G_{65}$ and $S^2_{5|\{46\}} = S^2_{4|\{56\}} = S^2_{6|\{45\}}$. We notice that the maximum between the steering parameter

$S^2_{B|\{AC\}}$ and one, for all the frequency interval under consideration, is one. In addition, the saturation of these monogamy relations, $4G_{BA}G_{BC} = 1$, occurs at $\omega_{sat} = 0.878$. Thus, this monogamy relation is valid for frequency values greater than ω_{sat}. This is due to the fact that there is no steering of the system B by the composite system $\{AC\}$ for all the frequency values in $\omega \in [0, \omega_{sat}]$. Actually, this is consistent with our results for the certification of full-tripartite two-way steering inseparability where we have certified steering at least in one direction for all bipartitions of the system only in the frequency interval $\omega \in (0.207, 0.808)$.

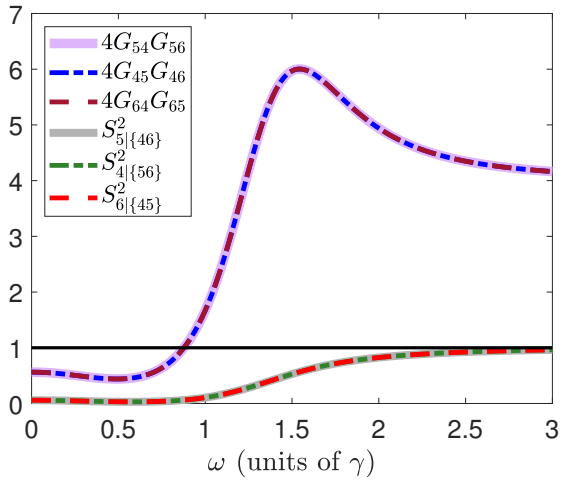

Figure 8.2: Monogamy relations for the GMVT witness. For the bipartitions {54}-{56}, {45}-{46}, and {64}-{65}, respectively, it must hold that $4G_{BA}G_{BC} \geqslant max\left\{1, S^2_{B|\{AC\}}\right\}$. Here, the one of this monogamy relation is represented by the black solid line.

8.2 Distribution of steering among the output fields

In chapter 7, we have certified three types of steering among the output fields for the different bipartitions of the system: one-way and two-way steering, and full tripartite two-way steering inseparability. Unfortunately, the strongest form of steering, which is the genuine tripartite steering, is not present in the system. In this section we investigate the distribution of steering for the different bipartitions of the system. We use the monogamy relations derived by Reid [40].

The first monogamy relation for steering witness that we consider is the one described in Equation 3.5. This monogamy relation states that if the criterion $EPR_{i|j}$ is violated between parties i and j such that j steers i, then the third party k cannot steer i. For the different bipartitions of the system, we obtain a set of monogamy relations given by

$$EPR_{4|5}EPR_{4|6} \geqslant 1, \tag{8.16}$$
$$EPR_{5|6}EPR_{5|4} \geqslant 1, \tag{8.17}$$
$$EPR_{6|5}EPR_{6|4} \geqslant 1. \tag{8.18}$$

These are shown in Figure 8.3, where we can observe clearly that neither of these are satisfied at any frequency value. That is, steering is not only shared between two parties of the system, but also occurs across different bipartitions of the system. This is due to fact that, for the different bipartitions of the system, full tripartite two-way steering inseparability is certified in the system.

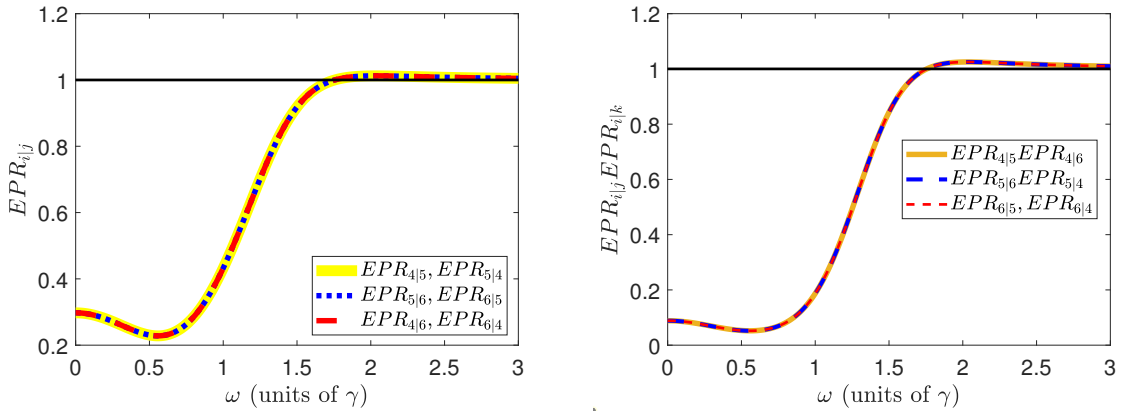

Figure 8.3: $EPR_{i|j}$ criterion and the monogamy relation for steering witness $EPR_{i|j}$. (a) Bipartite steering between two parties is certified whenever $EPR_{i|j} < 1$, and (b) monogamy relation $EPR_{i|j}EPR_{i|k} \geqslant 1$, for i, j, $k = 4$, 5, 6 ($i \neq j \neq k$). In both (a) and (b), the black solid line represents the bound of the $EPR_{i|j}$ criterion and the monogamy relation, respectively.

The second monogamy relation that we have investigated is given in Equation 3.6. This is related to the steering parameter $S_{i|\{jk\}}$ and it states that $S_{i|\{jk\}} \leqslant EPR_{i|j}$. For all the possible bipartitions of the system, this monogamy relation is given by

$$S_{4|\{56\}} \leqslant EPR_{4|5},\ S_{4|\{65\}} \leqslant EPR_{4|6}, \tag{8.19}$$
$$S_{5|\{46\}} \leqslant EPR_{5|4},\ S_{5|\{64\}} \leqslant EPR_{5|6}, \tag{8.20}$$
$$S_{6|\{45\}} \leqslant EPR_{6|4},\ S_{6|\{54\}} \leqslant EPR_{6|5}. \tag{8.21}$$

It is worth mentioning that Equation 8.19 corresponds to the bipartitions $\{45\}$ and $\{46\}$, while Equation 8.20 is related to the bipartitions $\{46\}$ and $\{56\}$, and Equation 8.21 to $\{45\}$ and $\{56\}$, respectively. In addition, $S_{i|\{jk\}} = S_{i|\{kj\}}$ since

$$S_{i|\{jk\}} = V_{inf|\{jk\}}(\hat{X}_i)V_{inf|\{jk\}}(\hat{Y}_i), \tag{8.22}$$

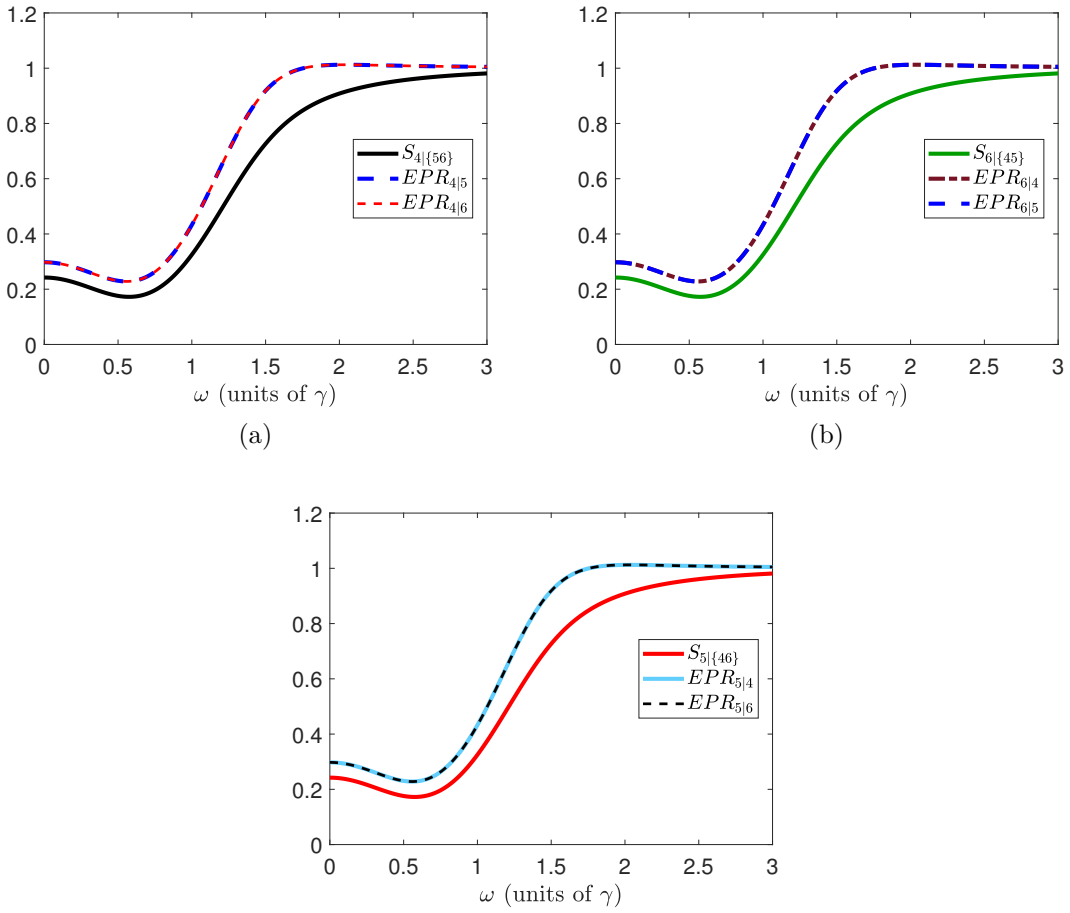

Figure 8.4: Monogamy relations for bipartite steering witness $EPR_{i|j}$ for the different bipartitions of the output fields. $S_{i|\{jk\}} \leqslant EPR_{i|j}$ is satisfied for $i, j, k = 4, 5, 6$ $(i \neq j \neq k)$, where (a) $S_{6|\{45\}} \leqslant EPR_{6|4}$ and $S_{6|\{45\}} \leqslant EPR_{6|5}$, (b) $S_{6|\{45\}} \leqslant EPR_{6|4}$ and $S_{6|\{45\}} \leqslant EPR_{6|5}$, and (c) $S_{5|\{46\}} \leqslant EPR_{5|4}$ and $S_{5|\{46\}} \leqslant EPR_{5|6}$.

where

$$V_{inf|\{jk\}}(\hat{X}_i) = V(\hat{X}_i) - \frac{\left[V(\hat{X}_i, \hat{X}_j + \hat{X}_k)\right]}{V(\hat{X}_j + \hat{X}_k)},$$
$$V_{inf|\{jk\}}(\hat{Y}_i) = V(\hat{Y}_i) - \frac{\left[V(\hat{Y}_i, \hat{Y}_j + \hat{Y}_k)\right]}{V(\hat{Y}_j + \hat{Y}_k)}, \tag{8.23}$$

and

$$S_{i|\{kj\}} = V_{inf|\{kj\}}(\hat{X}_i) V_{inf|\{kj\}}(\hat{Y}_i), \tag{8.24}$$

$$V_{inf|\{kj\}}(\hat{X}_i) = V(\hat{X}_i) - \frac{\left[V(\hat{X}_i, \hat{X}_k + \hat{X}_j)\right]}{V(\hat{X}_k + \hat{X}_j)},$$
$$V_{inf|\{kj\}}(\hat{Y}_i) = V(\hat{Y}_i) - \frac{\left[V(\hat{Y}_i, \hat{Y}_k + \hat{Y}_j)\right]}{V(\hat{Y}_k + \hat{Y}_j)}. \tag{8.25}$$

In Figure 8.4, we show Equation 8.19-Equation 8.21. First, we observe that $EPR_{i|j} = EPR_{i|k}$ for i, j, $k = 4, 5, 6$ $(i \neq j \neq k)$. Second, $EPR_{i|j} = EPR_{i|k}$ is always greater than the steering parameter $S_{i|\{jk\}}$. Thus, the steering of i from the bipartition $\{jk\}$, $S_{i|\{jk\}}$, cannot be better than the steering of i from j, $EPR_{i|j}$, since $EPR_{i|j}$ is only distributed between two parties.

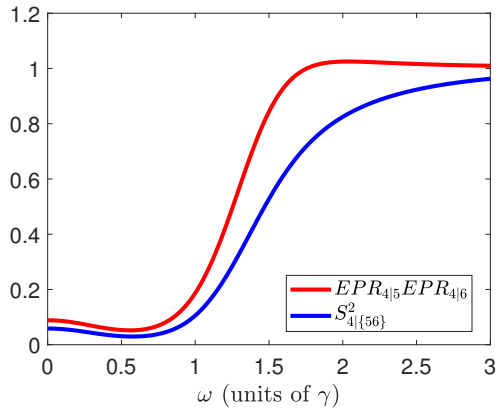

(a)

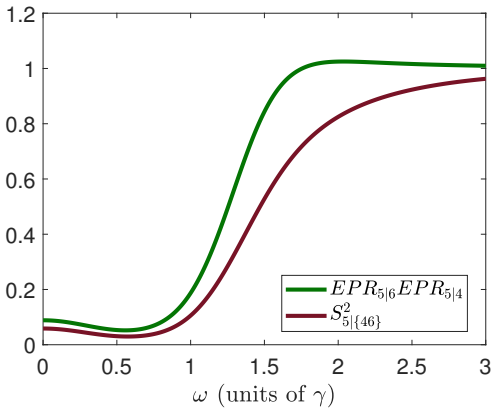

(b)

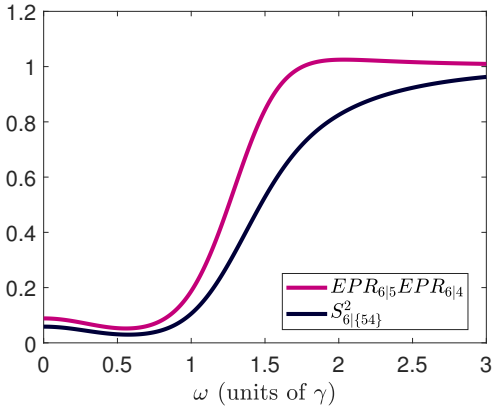

(c)

Figure 8.5: Monogamy relations for bipartite steering witness $EPR_{i|j}$ for the different bipartitions of the system states that $S^2_{i|\{jk\}} \leqslant EPR_{i|j}EPR_{i|k}$. This inequality is satisfied for (a) $EPR_{4|5}EPR_{4|6} \geqslant S^2_{4|\{56\}}$, (b) $EPR_{5|6}EPR_{5|4} \geqslant S^2_{5|\{46\}}$ and (c) $EPR_{6|5}EPR_{6|4} \geqslant S^2_{6|\{54\}}$.

Another monogamy relation for the steering witness $EPR_{i|j}$ is the one which relates the product of bipartite steering for the different bipartitions of the system, $EPR_{i|j}EPR_{i|k}$, and the square of the steering parameter, $S^2_{i|\{jk\}}$. This is given in section 3.2 and states that $EPR_{i|j}EPR_{i|k} \geqslant S^2_{i|\{jk\}}$. For all the possible bipartitions of the system and the square of the steering parameter, we have the following set of monogamy relations

$$EPR_{4|5}EPR_{4|6} \geqslant S^2_{4|\{56\}}, \tag{8.26}$$
$$EPR_{5|4}EPR_{5|6} \geqslant S^2_{5|\{46\}}, \tag{8.27}$$
$$EPR_{6|4}EPR_{6|5} \geqslant S^2_{6|\{45\}}, \tag{8.28}$$

which are shown in Figure 8.5. We notice that for the different bipartitions of the system, the inequality $EPR_{i|j}EPR_{i|k} \geqslant S^2_{i|\{jk\}}$ is always satisfied for i, j, $k = 4$, 5, 6 and $i \neq j \neq k$. That is, once steering is shared between the bipartitions $\{ij\}$ and $\{ik\}$, the steering for the bipartition $i - \{jk\}$ will certainly decrease.

We also consider the monogamy relation which relates the sum of two EPR criterion for different bipartitions of the system as $EPR_{i|j} + EPR_{i|k} \geqslant 2S_{i|\{jk\}}$. For the different bipartitions of the system, this monogamy relation gives the following inequalities

$$EPR_{4|5} + EPR_{4|6} \geqslant 2S_{4|\{56\}}, \tag{8.29}$$
$$EPR_{5|4} + EPR_{5|6} \geqslant 2S_{5|\{46\}}, \tag{8.30}$$
$$EPR_{6|4} + EPR_{6|5} \geqslant 2S_{6|\{45\}}. \tag{8.31}$$

These are shown in Figure 8.6 where we observe that for the different bipartitions of the system, it is always true that $EPR_{i|j} + EPR_{i|k} \geqslant 2S_{i|\{jk\}}$. That is, the individual steering of $\{ij\}$ and $\{ik\}$ is bounded by the steering from the bipartition $\{jk\}$ over i ($S_{i|\{jk\}}$).

Finally, we consider the monogamy relation for the steering witness $EPR_{i|j}$ given by $EPR_{i|j}EPR_{i|k} \geqslant max\{1, S^2_{i|\{jk\}}\}$, which gives as a bound, either 1 or $S^2_{i|\{jk\}}$. For the different bipartitions of the system, we obtain the following set of monogamy relations which are shown in Figure 8.7:

$$EPR_{4|5}EPR_{4|6} \geqslant max\{1, S^2_{4|\{56\}}\}, \tag{8.32}$$
$$EPR_{5|4}EPR_{5|6} \geqslant max\{1, S^2_{5|\{46\}}\}, \tag{8.33}$$
$$EPR_{6|4}EPR_{6|5} \geqslant max\{1, S^2_{6|\{45\}}\}. \tag{8.34}$$

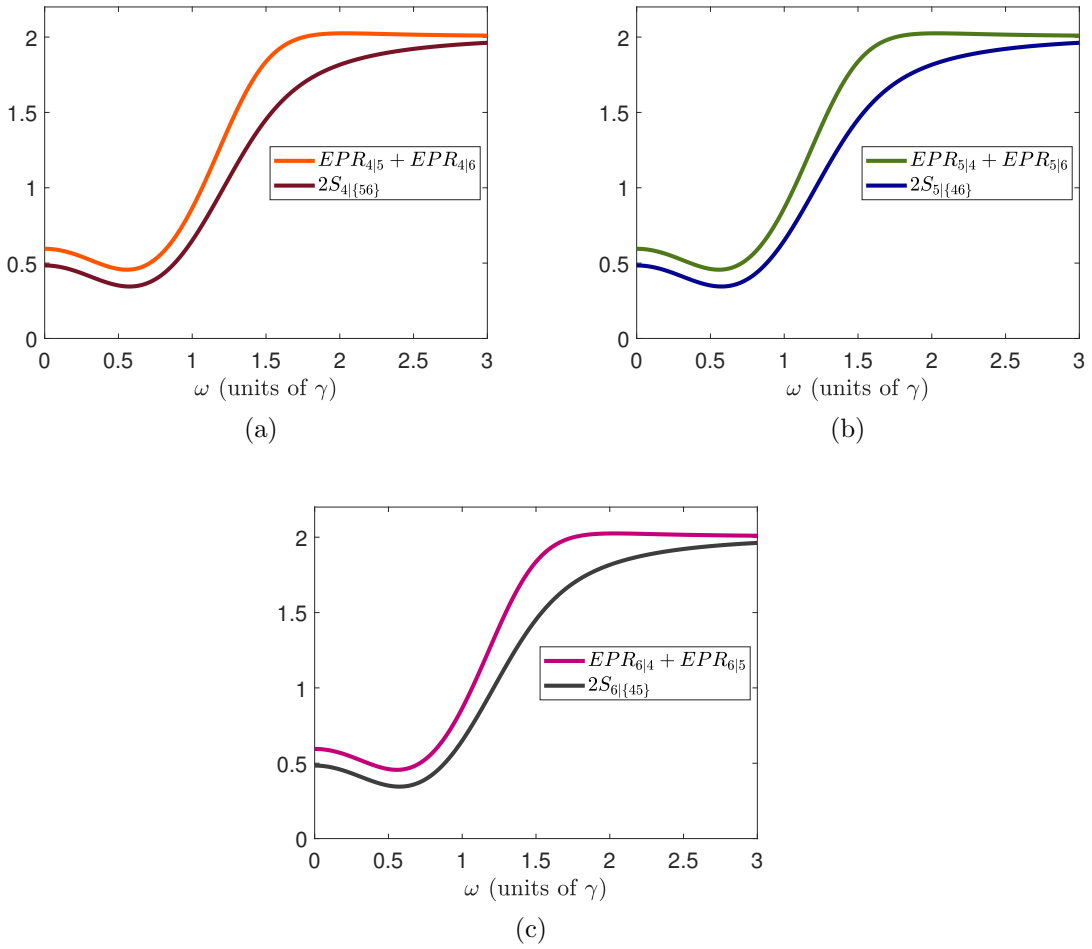

Figure 8.6: Monogamy relation for bipartite steering witness $EPR_{i|j}$ for the different bipartitions of the system: $EPR_{i|j}+EPR_{i|k} \geqslant 2S_{i|\{jk\}}$. This inequality is satisfied for (a) $EPR_{4|5} + EPR_{4|6} \geqslant 2S_{4|\{56\}}$, (b) $EPR_{5|4} + EPR_{5|6} \geqslant 2S_{5|\{46\}}$ and (c) $EPR_{6|4} + EPR_{6|5} \geqslant 2S_{6|\{45\}}$.

Each monogamy relation, depicted in figures 8.7a- 8.7c, shows important behaviour which is worth mentioning. Firstly, we observe that the maximum between 1 and the steering parameter $S^2_{i|\{jk\}}$ is always 1. Secondly, from our results we find that the saturation occurs at $\omega_{sat} = 1.756$ for each $EPR_{i|j}EPR_{i|k}$ for i, j, $k = 4, 5, 6$ $(i \neq j \neq k)$. Thirdly, for any frequency value that satisfies $\omega > \omega_{sat}$, the monogamy relation holds. While below this value, ω_{sat}, we can observe that neither of these monogamy relations are satisfied at any frequency value. Lastly, the violation of these monogamy relations is consistent with the violation of Equation 8.16-Equation 8.18 due to the fact that we have certified another type of steering which is full tripartite two-way steering inseparability.

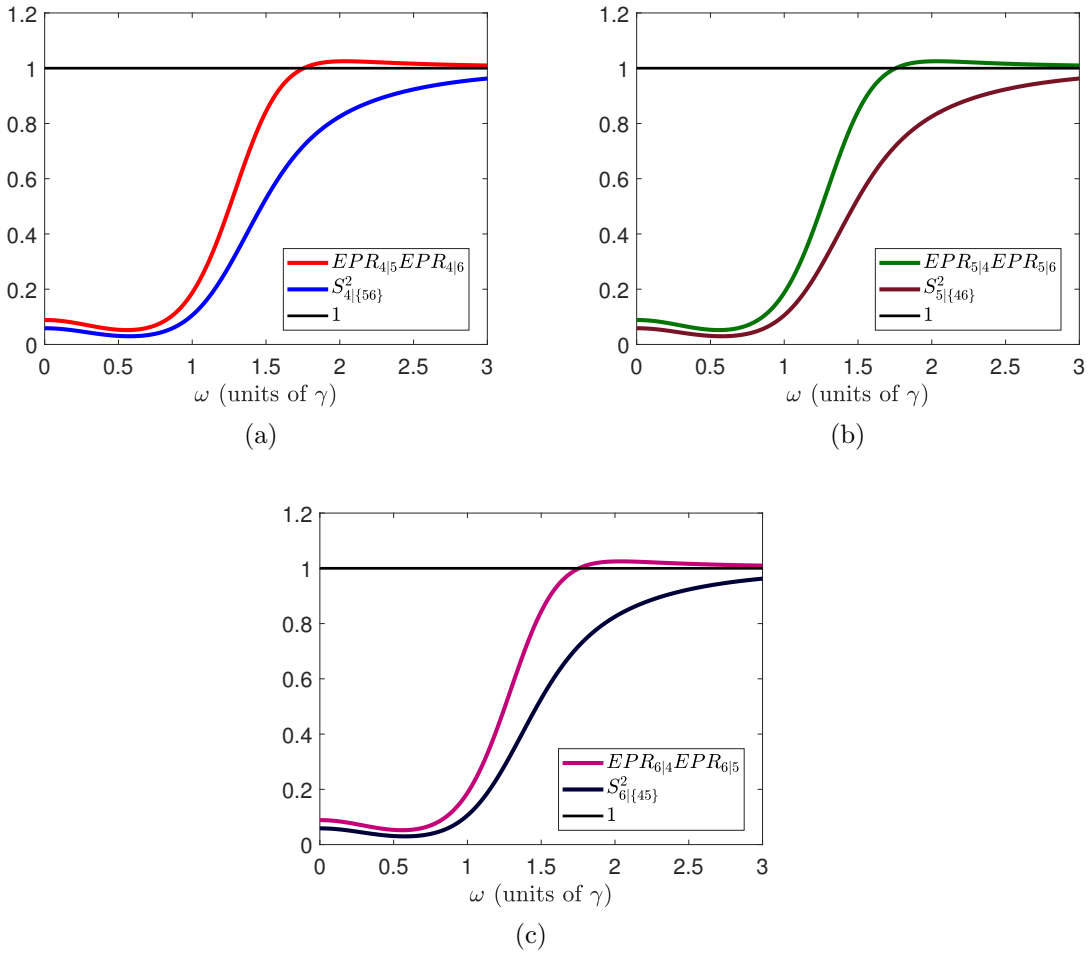

Figure 8.7: Monogamy relations for bipartite steering witness $EPR_{i|j}$ for the different bipartitions of the system states that $EPR_{i|j}EPR_{i|k} \geqslant max\{1, S^2_{i|\{jk\}}\}$. (a) $EPR_{4|5}EPR_{4|6} \geqslant max\{1, S^2_{4|\{56\}}\}$, (b) $EPR_{5|4}EPR_{5|6} \geqslant max\{1, S^2_{5|\{46\}}\}$ and (c) $EPR_{6|4}EPR_{6|5} \geqslant max\{1, S^2_{6|\{45\}}\}$. In (a), (b) and (c), the bound of one is represented by the black solid line.

In conclusion, in order to investigate the distribution of both correlations, entanglement and steering, among the different parties of the system, we have used the monogamy relations for different entanglement and steering witnesses. From our results, we conclude that if these relations are satisfied, then the distribution of the correlations between different bipartitions is constrained. That is, once the correlation is distributed in a bipartition of the system, then for the other bipartition, the correlation is reduced and it is also bounded.

We claim that the monogamy relations may be considered as a form of conservation law since if these are not satisfied, then there exist other type of correlation in

the system. We have demonstrated this in the cases of the monogamy relation for GMVT entanglement witness, $4G_{BA}G_{BC} \geqslant max\left\{1, S^2_{B|\{AC\}}\right\}$, where the relation is violated for frequency values $\omega < 0.878$, while for steering, $EPR_{i|j}EPR_{i|k} \geqslant 1$ and $EPR_{i|j}EPR_{i|k} \geqslant max\{1, S^2_{i|\{jk\}}\}$, both are violated for $\omega < 1.757$ and $\omega < 1.756$, respectively. The violation of the three monogamy relations confirms the existence of full tripartite two-way steering inseparability in the system.

Chapter 9

Conclusions

In this thesis, we have investigated the generation of quantum entanglement and steering by an intracavity down conversion process. That is, we have considered the interaction of three fields with a nonlinear medium inside an optical cavity. As a result, three down converted fields are obtained outside the cavity.

We analyzed this system by following three main formalisms: the master equation, the phase-space methods and the linearized fluctuation theory. In particular, we have used the positive-P function and we have obtained the intracavity spectrum in the frequency domain. This methodology allowed us to obtain the variances and covariances of the quadrature operators of the down-converted fields in the frequency domain, which are completely determined by the parameters of the system: the nonlinear coupling strength χ_i, the intracavity losses γ_i and the amplitude of the field E_i. Throughout this work, we consider the simplest case which corresponds to the symmetric case of the parameters of the system. That is $\chi_i \equiv \kappa$, $\gamma_i \equiv \gamma$ and $E_i \equiv E$. In addition, we have performed simulations in order to obtain the values of these parameters that can certify simultaneously quantum entanglement and steering. The values are $\kappa = 0.01$, $\gamma = 1$ and $E = 100$.

We utilized different entanglement and steering criteria to investigate the presence of these correlations in the frequency domain for the system under consideration. We have certified bipartite, tripartite and genuine tripartite entanglement as well as bipartite one-way and two-way steering, and full tripartite two-way steering inseparability in quadrature operators among the output fields. In the case of bipartite entanglement, we have showed that the VLF criterion certifies this type of entanglement for $\omega \in [0, 1.756)$. For these frequency values, this criterion also certifies tripartite entanglement. While, in the case of genuine tripartite entanglement, the criterion given in Equation 6.3 certifies this correlation for $\omega < 1.079$. For steering, we have determined that the output fields are steerable. In particular, we have certified bipartite one-way and two-way steering between the output fields for $\omega < 1.755$. We have also showed that there exists full tripartite two-way steering inseparability for $\omega \in (0.207, 0.808)$. In addition, we have investigated the distribution of

these quantum correlations among the different parties of the system by using the monogamy relations for the entanglement and steering witnesses. The monogamy relations are valid and these also confirm the existence of full tripartite two-way steering inseparability among the output fields. Our results determine frequency values where both correlations, entanglement and steering, are present in the system under consideration. These may be used for applications in quantum information protocols, such as Quantum Key Distribution (QKD) and Quantum Secret Sharing (QSS). For instance, since the system under consideration presents both one-way and two-way steerable EPR-like states, it can be used for a secure QSS protocol [17, 37, 38].

Future work consist of extending this model to a multipartite system and investigating if both, entanglement and steering, are still present in the system, as well as whether it is possible to certify them in a wider range of frequency values rather than in the low frequency regime. Additionally, we wish to examine the existence of other correlations, such as genuine tripartite steering in the multipartite case.

Appendix A

Relation between the theoretical and experimental parameters of the system

In section 4.1, the system was described by a nonlinear Hamiltonian model which considers the interaction Hamiltonian $\hat{H}_{int}$, the Hamiltonian of the input fields $\hat{H}_p$ and the Liouvillian operator $\mathcal{L}\hat{\rho}$ which includes the cavity losses. Our model considers theoretical parameters such as the field amplitude E_i, the coupling strength χ_i and the cavity losses γ_i which can be related to experimental parameters. This can be done by following the works of Yariv and Louisell [144] and Cassedy and Jain [145]. In both references [144,145] the Optical Parametric Oscillator (OPO) is analysed. In the former [144], the authors derived the oscillation threshold condition, the power output, and the relation between the loss parameters and the Q-cavity factor. While in [145] the authors analysed the injection tuning of an OPO where they generalised the theory developed in reference [144], and they also derived analytical expressions for N-modes.

In this Appendix we include an analysis between the theoretical parameters, which are considered in the nonlinear Hamiltonian model (section 4.1), and the experimental parameters, but this is beyond the scope of this work. As we have described in chapter 4, the system under consideration consists of three nonlinear interactions inside an optical resonant cavity (see Figure 4.1). Each input field (a_{p_i}) creates two down-converted fields (a_{n_s} and a_{n_i}) via SPDC such that the dynamics can be

described by the following three coupled nonlinear equations [144, 145]

$$\begin{aligned}
\frac{da_p}{dt} &= -i\omega_p a_p - \frac{\omega_p}{2Q_p}a_p - \sum_{n=1}^{N}\kappa_n a_{n_i}a_{n_s} + i\lambda_p \exp\left(-i\omega_p t\right), \\
\frac{da_{n_s}}{dt} &= -i\omega_{n_s} a_{n_s} - \frac{\omega_{n_s}}{2Q_s}a_{n_s} + \kappa_n a^*_{n_i}a_p, \\
\frac{da_{n_i}}{dt} &= -i\omega_{n_i} a_{n_i} - \frac{\omega_{n_i}}{2Q_i}a_{n_i} + \kappa_n a^*_{n_s}a_p,
\end{aligned} \tag{A.1}$$

where $n_s\,(n_i)$ is the nth signal (idler) mode which arise from the nonlinear process and both satisfy the condition $\omega_p = \omega_{n_s} + \omega_{n_i}$. $Q_s\,(Q_i)$ is the cavity-Q factor of the signal (idler) mode, κ_n is the nonlinear coupling strength and λ_p is the pumping parameter which are define as [144–146]

$$Q_j = \frac{\omega_j \epsilon_j}{2\sigma_j}, \tag{A.2}$$

$$\lambda_p = \frac{1}{2}\sqrt{\frac{\omega_p}{2\epsilon}}\int \bar{E}_p \cdot \bar{P}' dv, \tag{A.3}$$

Here, σ_j is the volume conductivity which consider the losses in the cavity, $\bar{E}_p$, $\bar{P}'$ and ω_p are the electric field, polarization and frequency of the pump respectively.

Also,

$$\kappa_n = \frac{1}{2}\sqrt{\omega_p\omega_{n_i}\omega_{n_s}}\frac{d_{ijk}}{\epsilon^{3/2}V^{1/2}}F\left(\Delta k_n L\right), \tag{A.4}$$

where ω_j $(j = p,\, n_s,\, n_i)$ is the frequency of field, d_{ijk} is the nonlinear coefficient of the medium, V and L are the volume and length of the cavity, respectively, and $F\left(\Delta k_n L\right)$ is a function defined by

$$F\left(\Delta k_n L\right) = \frac{\sin\left(\frac{1}{2}\Delta k_n L\right)}{\frac{1}{2}\Delta k_n L}, \tag{A.5}$$

where the phase-matching is $\Delta k_n = k_p - k_{n_s} - k_{n_i}$.

For $\Delta k_n = 0$,

$$F\left(\Delta k_n L\right) = \frac{\sin\left(\frac{1}{2}\Delta k_n L\right)}{\frac{1}{2}\Delta k_n L} = 1,$$

and thus

$$\kappa_n = \frac{1}{2}\sqrt{\omega_p\omega_{n_i}\omega_{n_s}}\frac{d_{ijk}}{\epsilon^{3/2}V^{1/2}}. \tag{A.6}$$

Also, the power of the input field is given by [144]

$$P_j = \frac{\omega_j^2}{Q_j} E_j^* E_j = \frac{\omega_j^2}{Q_p} |E_j|^2, \tag{A.7}$$

where E_j is the amplitude of the field (pump, signal or idler). It is worth pointing out that it has been demonstrated that the efficiency of an OPO is directly related to the pump intensity [147, 148].

Furthermore, the cavity losses can be related to the effective reflectances R and the length of the cavity L by [144]

$$\gamma_j = \frac{c\,(1-R)}{2L} \quad (j = 1 - N). \tag{A.8}$$

However, there exist other type of losses to take into account.

So far, we have expressed the theoretical parameters, which are the amplitude of the field E_j, the nonlinear coupling κ_n and the cavity losses γ_j, in terms of experimental parameters such as the power of the pump P_j (Equation A.7), the nonlinear coefficient d_{ijk}, the volume of the cavity V (Equation A.6), the effective reflectances R and the length of the cavity L (Equation A.8). Further considerations for cavity-enhanced SPDC can be found in [149].

Additionally, we wish to mention that there exist other parameters and properties to describe a cavity. For instance, for a linear cavity, the parameters are the optical path length for one round, the distance between the input and the output mirror, the intensity transmission and reflectivity of the input (output) mirror. While the properties of the cavity include the free spectral range or the finesse. More details can be found in [150].

Bibliography

[1] A. Einstein, B. Podolsky, and N. Rosen. Can quantum-mechanical description of physical reality be considered complete? *Phys. Rev.*, 47:777–780, 1935.

[2] E. Schrödinger. Discussion of probability relations between separated systems. *Math. Proc. Cambridge Philos. Soc*, 31(4):555, 1935.

[3] R. Horodecki, P. Horodecki, M. Horodecki, and K. Horodecki. Quantum entanglement. *Rev. Mod. Phys.*, 81:865–942, 2009.

[4] M. D. Reid, P. D. Drummond, W. P. Bowen, E. G. Cavalcanti, P. K. Lam, H. A. Bachor, U. L. Andersen, and G. Leuchs. Colloquium: The Einstein-Podolsky-Rosen paradox: From concepts to applications. *Rev. Mod. Phys.*, 81:1727–1751, 2009.

[5] R. Uola, A. C. S. Costa, H. C. Nguyen, and O. Gühne. Quantum steering. *Rev. Mod. Phys.*, 92:015001, 2020.

[6] S. J. Jones, H. M. Wiseman, and A. C. Doherty. Entanglement, Einstein-Podolsky-Rosen correlations, Bell nonlocality, and steering. *Phys. Rev. A*, 76:052116, 2007.

[7] H. M. Wiseman, S. J. Jones, and A. C. Doherty. Steering, Entanglement, Nonlocality, and the Einstein-Podolsky-Rosen Paradox. *Phys. Rev. Lett.*, 98:140402, 2007.

[8] R. F. Werner. Quantum states with Einstein-Podolsky-Rosen correlations admitting a hidden-variable model. *Phys. Rev. A*, 40:4277–4281, 1989.

[9] S. Wollmann, N. Walk, A. J. Bennet, H. M. Wiseman, and G. J. Pryde. Observation of Genuine One-Way Einstein-Podolsky-Rosen Steering. *Phys. Rev. Lett.*, 116:160403, 2016.

[10] V. Händchen, T. Eberle, S. Steinlechner, A. Samblowski, T. Franz, R. F. Werner, and R. Schnabel. Observation of one-way Einstein-Podolsky-Rosen steering. *Nature Photonics*, 6(9):596–599, 2012.

[11] H. Bechmann-Pasquinucci and W. Tittel. Quantum cryptography using larger alphabets. *Phys. Rev. A*, 61:062308, 2000.

[12] N. J. Cerf, M. Bourennane, A. Karlsson, and N. Gisin. Security of quantum key distribution using d-level systems. *Phys. Rev. Lett.*, 88:127902, 2002.

[13] Y.-H. Luo, H.-S. Zhong, M. Erhard, X.-L. Wang, L.-C. Peng, M. Krenn, X. Jiang, L. Li, N.-L. Liu, C.-Y. Lu, A. Zeilinger, and J.-W. Pan. Quantum teleportation in high dimensions. *Phys. Rev. Lett.*, 123:070505, 2019.

[14] X.-M. Hu, C. Zhang, B.-H. Liu, Y. Cai, X.-J. Ye, Y. Guo, W.-B. Xing, C.-X. Huang, Y.-F. Huang, C.-F. Li, and G.-C. Guo. Experimental high-dimensional quantum teleportation. *Phys. Rev. Lett.*, 125:230501, 2020.

[15] M. Erhard, M. Krenn, and A. Zeilinger. Advances in high-dimensional quantum entanglement. *Nat. Rev. Phys.*, 2:365–381, 2020.

[16] C.-Y. Lu, Y. Cao, C.-Z. Peng, and J.-W. Pan. Micius quantum experiments in space. *Rev. Mod. Phys.*, 94:035001, 2022.

[17] C. Wilkinson, M. Thornton, and N. Korolkova. Quantum steering as a resource for secure tripartite quantum state sharing. *Phys. Rev. A*, 107(6):062401, 2023.

[18] H. Wang, D. Liao, D. Guo, J. Xin, and J. Kong. Continuous-variable (3, 3)-threshold quantum secret sharing based on one-sided device-independent security. *Phys. Lett. A*, 462:128650, 2023.

[19] J. P. Dowling and G. J. Milburn. Quantum technology: the second quantum revolution. *Philosophical Transactions of the Royal Society of London. Series A: Mathematical, Physical and Engineering Sciences*, 361(1809):1655–1674, 2003.

[20] I. A. Walmsley. Quantum optics: Science and technology in a new light. *Science*, 348(6234):525–530, 2015.

[21] A. Acín, I. Bloch, H. Buhrman, T. Calarco, C. Eichler, J. Eisert, D. Esteve, N. Gisin, S. J. Glaser, F. Jelezko, et al. The quantum technologies roadmap: a european community view. *New J. Phys.*, 20(8):080201, 2018.

[22] N. Gisin and R. Thew. Quantum communication. *Nature Photonics*, 1(3):167–171, 2007.

[23] M. A. Nielsen and I. L. Chuang. *Quantum computation and quantum information*, volume 2. Cambridge University Press, 2001.

[24] E. Polino, M. Valeri, N. Spagnolo, and F. Sciarrino. Photonic quantum metrology. *AVS Quantum Sci.*, 2(2), 2020.

[25] G. Adesso, S. Ragy, and A. R. Lee. Continuous variable quantum information: Gaussian states and beyond. *Open Systems & Information Dynamics*, 21(01n02):1440001, 2014.

[26] F. Grosshans and P. Grangier. Continuous Variable Quantum Cryptography Using Coherent States. *Phys. Rev. Lett.*, 88:057902, 2002.

[27] F. Grosshans, G. Van Assche, J. Wenger, R. Brouri, N. J. Cerf, and P. Grangier. Quantum key distribution using gaussian-modulated coherent states. *Nature*, 421(6920):238–241, 2003.

[28] M. D. Reid. Quantum cryptography with a predetermined key, using continuous-variable Einstein-Podolsky-Rosen correlations. *Phys. Rev. A*, 62:062308, 2000.

[29] F. Xu, X. Ma, Q. Zhang, H. K. Lo, and J. W. Pan. Secure quantum key distribution with realistic devices. *Rev. Mod. Phys.*, 92:025002, 2020.

[30] Y. Zhang, Z. Chen, S. Pirandola, X. Wang, C. Zhou, B. Chu, Y. Zhao, B. Xu, S. Yu, and H. Guo. Long-Distance Continuous-Variable Quantum Key Distribution over 202.81 km of Fiber. *Phys. Rev. Lett.*, 125:010502, 2020.

[31] V. Scarani, H. Bechmann-Pasquinucci, N. J. Cerf, M. Dušek, N. Lütkenhaus, and M. Peev. The security of practical quantum key distribution. *Rev. Mod. Phys.*, 81:1301–1350, 2009.

[32] C. Branciard, E. G. Cavalcanti, S. P. Walborn, V. Scarani, and H. M. Wiseman. One-sided device-independent quantum key distribution: Security, feasibility, and the connection with steering. *Phys. Rev. A*, 85:010301, 2012.

[33] E. Diamanti and A. Leverrier. Distributing Secret Keys with Quantum Continuous Variables: Principle, Security and Implementations. *Entropy*, 17(9):6072–6092, 2015.

[34] H. Yonezawa, T. Aoki, and A. Furusawa. Demonstration of a quantum teleportation network for continuous variables. *Nature*, 431:430–433, 2004.

[35] S. Pirandola and S. Mancini. Quantum teleportation with continuous variables: A survey. *Laser Physics*, 16:1418–1438, 2004.

[36] Q. He, L. Rosales-Zárate, G. Adesso, and M. D. Reid. Secure Continuous Variable Teleportation and Einstein-Podolsky-Rosen Steering. *Phys. Rev. Lett.*, 115:180502, 2015.

[37] A. M. Lance, T. Symul, W. P. Bowen, B. C. Sanders, and P. K. Lam. Tripartite quantum state sharing. *Phys. Rev. Lett.*, 92(17):177903, 2004.

[38] A. M. Lance, T. Symul, W. P. Bowen, B. C. Sanders, T. Tyc, T. C. Ralph, and P. K. Lam. Continuous-variable quantum-state sharing via quantum disentanglement. *Phys. Rev. A*, 71:033814, 2005.

[39] I. Kogias, Y. Xiang, Q. He, and G. Adesso. Unconditional security of entanglement-based continuous-variable quantum secret sharing. *Phys. Rev. A*, 95:012315, 2017.

[40] M. D. Reid. Monogamy inequalities for the Einstein-Podolsky-Rosen paradox and quantum steering. *Phys. Rev. A*, 88:062108, 2013.

[41] L. Rosales-Zárate, R. Y. Teh, B. Opanchuk, and M. D. Reid. Monogamy inequalities for certifiers of continuous-variable Einstein-Podolsky-Rosen entanglement without the assumption of Gaussianity. *Phys. Rev. A*, 96:022313, 2017.

[42] J. Douady and B. Boulanger. Experimental demonstration of a pure third-order optical parametric downconversion process. *Opt. Lett.*, 29(23):2794–2796, 2004.

[43] D. R. Hamel, L. K. Shalm, H. Hübel, A. J. Miller, F. Marsili, V. B. Verma, R. P. Mirin, S. W. Nam, K. J. Resch, and T. Jennewein. Direct generation of three-photon polarization entanglement. *Nature Photonics*, 8:801–807, 2014.

[44] E. A. Rojas González, A. Borne, B. Boulanger, J. A. Levenson, and K. Bencheikh. Continuous-variable triple-photon states quantum entanglement. *Phys. Rev. Lett.*, 120:043601, 2018.

[45] M. K. Olsen. Third-harmonic entanglement and Einstein-Podolsky-Rosen steering over a frequency range of more than an octave. *Phys. Rev. A*, 97:033820, 2018.

[46] T. Peña Armendáriz, R. Ramírez-Alarcón, and L. E. C. Rosales-Zárate. Continuous variable tripartite entanglement and steering using a third-order nonlinear optical interaction. *J. Opt. Soc. Am. B*, 38(2):371–378, 2021.

[47] A. T. Avelar and S. P. Walborn. Genuine tripartite continuous-variable entanglement with spatial degrees of freedom of photons. *Phys. Rev. A*, 88:032308, 2013.

[48] A. Gatti. Multipartite spatial entanglement generated by concurrent nonlinear processes. *Phys. Rev. A*, 104:052430, 2021.

[49] Y. Liu, Y. Cai, B. Luo, J. Yan, M. Niu, F. Li, and Y. Zhang. Collective multipartite Einstein-Podolsky-Rosen steering via cascaded four-wave mixing of rubidium atoms. *Phys. Rev. A*, 104:033704, 2021.

[50] Y. Liang, R. Yang, J. Zhang, and T. Zhang. Hexapartite steering based on a four-wave-mixing process with a spatially structured pump. *Opt. Express*, 31(7):11775–11787, 2023.

[51] Y. R. Shen, Y. X. Jiang, X. Y. Cheng, J. W. Lv, Y. B. Yu, G. R. Jin, and A. X. Chen. Quadripartite quantum steering generated by single-pass cascaded nonlinear processes. *Europhysics Letters*, 146(1), 2024.

[52] A. S. Bradley, M. K. Olsen, O. Pfister, and R. C. Pooser. Bright tripartite entanglement in triply concurrent parametric oscillation. *Phys. Rev. A*, 72:053805, 2005.

[53] M. K. Olsen. Bright entanglement in the intracavity nonlinear coupler. *Phys. Rev. A*, 73:053806, 2006.

[54] M. K. Olsen and A. S. Bradley. Continuous variable tripartite entanglement from twin nonlinearities. *J. Phys. B: At. Mol. Opt. Phys.*, 39(1):127, 2005.

[55] C. Pennarun, A. S. Bradley, and M. K. Olsen. Tripartite entanglement and threshold properties of coupled intracavity down-conversion and sum-frequency generation. *Phys. Rev. A*, 76:063812, 2007.

[56] S. L. W. Midgley, A. S. Bradley, O. Pfister, and M. K. Olsen. Quadripartite continuous-variable entanglement via quadruply concurrent down-conversion. *Phys. Rev. A*, 81:063834, 2010.

[57] Y. B. Yu, H. J. Wang, M. Xiao, and S. N. Zhu. Directly produced three-color entanglement by quasi-phase-matched third-harmonic generation. *Opt. Express*, 19(15):13949–13956, 2011.

[58] Y. Yu and H. Wang. Bright three-color continuous-variable entanglement generated by a cascaded sum-frequency process in an optical cavity. *J. Opt. Soc. Am. B*, 28(8):1899–1904, 2011.

[59] Y. B. Yu, H. J. Wang, and J. W. Zhao. Analysis of directly produce pump, signal, and idler three-color continuous-variable entanglement. *Eur. Phys. J. D*, 66:18, 2012.

[60] Y. B. Yu, H. J. Wang, and J. W. Zhao. Analysis of directly produce pump, signal, and idler three-color continuous-variable entanglement. *The European Physical Journal D*, 66, 2012.

[61] M. K. Olsen and J. F. Corney. Bipartite entanglement in continuous-variable tripartite systems. *Opt. Commun.*, 378:49–57, 2016.

[62] G. He, Y. Sun, L. Hu, R. Zhang, X. Chen, and J. Wang. Five-partite entanglement generation between two optical frequency combs in a quasi-periodic $\chi^{(}2)$ nonlinear optical crystal. *Sci. Rep.*, 7:9054, 2017.

[63] J. Li and M. K. Olsen. Quantum correlations across two octaves from combined up- and down-conversion. *Phys. Rev. A*, 97:043856, 2018.

[64] M. D. E. Denys, M. K. Olsen, L. S. Trainor, H. G. L. Schwefel, and A. S. Bradley. Steady states, squeezing, and entanglement in intracavity triplet down conversion. *Opt. Commun.*, 484:126699, 2021.

[65] C. Couteau. Spontaneous parametric down-conversion. *Contemporary Physics*, 59(3):291–304, 2018.

[66] G. Adesso, A. Serafini, and F. Illuminati. Entanglement, purity, and information entropies in continuous variable systems. *Open Systems & Information Dynamics*, 12:189–205, 2005.

[67] G. Adesso and F. Illuminati. Entanglement in continuous-variable systems: recent advances and current perspectives. *J. Phys. A: Math. Theor.*, 40:7821, 2007.

[68] J. J. Sakurai and J. Napolitano. *Modern quantum mechanics*. Cambridge University Press, 2020.

[69] S. M. Tan. Confirming entanglement in continuous variable quantum teleportation. *Phys. Rev. A*, 60:2752–2758, 1999.

[70] R. Simon. Peres-Horodecki separability criterion for continuous variable systems. *Phys. Rev. Lett.*, 84:2726–2729, 2000.

[71] L. M. Duan, G. Giedke, J. I. Cirac, and P. Zoller. Inseparability criterion for continuous variable systems. *Phys. Rev. Lett.*, 84:2722–2725, 2000.

[72] V. Giovannetti, S. Mancini, D. Vitali, and P. Tombesi. Characterizing the entanglement of bipartite quantum systems. *Phys. Rev. A*, 67:022320, 2003.

[73] P. van Loock and A. Furusawa. Detecting genuine multipartite continuous-variable entanglement. *Phys. Rev. A*, 67:052315, 2003.

[74] R. Y. Teh and M. D. Reid. Criteria for genuine N-partite continuous-variable entanglement and Einstein-Podolsky-Rosen steering. *Phys. Rev. A*, 90:062337, 2014.

[75] M. D. Reid. Demonstration of the Einstein-Podolsky-Rosen paradox using nondegenerate parametric amplification. *Phys. Rev. A*, 40:913–923, 1989.

[76] R. Y. Teh, M. Gessner, M. D. Reid, and M. Fadel. Full multipartite steering inseparability, genuine multipartite steering, and monogamy for continuous-variable systems. *Phys. Rev. A*, 105:012202, 2022.

[77] V. Coffman, J. Kundu, and W. K. Wootters. Distributed entanglement. *Phys. Rev. A*, 61:052306, 2000.

[78] G. Adesso and F. Illuminati. Continuous variable tangle, monogamy inequality, and entanglement sharing in gaussian states of continuous variable systems. *New J. Phys.*, 8(1):15, 2006.

[79] T. Hiroshima, G. Adesso, and F. Illuminati. Monogamy Inequality for Distributed Gaussian Entanglement. *Phys. Rev. Lett.*, 98:050503, 2007.

[80] G. Adesso and F. Illuminati. Strong Monogamy of Bipartite and Genuine Multipartite Entanglement: The Gaussian Case. *Phys. Rev. Lett.*, 99:150501, 2007.

[81] G. Adesso, A. Serafini, and F. Illuminati. Multipartite entanglement in three-mode gaussian states of continuous-variable systems: Quantification, sharing structure, and decoherence. *Phys. Rev. A*, 73:032345, 2006.

[82] X. N. Zhu, G. Bao, Z. X. Jin, and S. M. Fei. Monogamy of entanglement for tripartite systems. *Phys. Rev. A*, 107:052404, 2023.

[83] A. Khan, J. ur Rehman, K. Wang, and H. Shin. Unified monogamy relations of multipartite entanglement. *Sci. Rep.*, 9:16419, 2019.

[84] Y. Guo and L. Zhang. Multipartite entanglement measure and complete monogamy relation. *Phys. Rev. A*, 101:032301, 2020.

[85] X. L. Zong, H. H. Yin, W. Song, and Z. L. Cao. Monogamy of quantum entanglement. *Frontiers in Physics*, 10, 2022.

[86] B. Xie, M. J. Zhao, and B. Li. General monogamy and polygamy properties of quantum systems. *Quantum Inf. Process.*, 22:124, 2023.

[87] X. Zhang, N. Jing, M. Liu, and H. Ma. On monogamy and polygamy relations of multipartite systems. *Phys. Scr.*, 98:035106, 2023.

[88] M. D. Reid. Monogamy inequalities for the Einstein-Podolsky-Rosen paradox and quantum steering. *Phys. Rev. A*, 88:062108, 2013.

[89] S.-W. Ji, M. S. Kim, and H. Nha. Quantum steering of multimode Gaussian states by Gaussian measurements: monogamy relations and the Peres conjecture. *J. Phys. A: Math. Theor.*, 48(13):135301, 2015.

[90] Y. Xiang, I. Kogias, G. Adesso, and Q. He. Multipartite Gaussian steering: Monogamy constraints and quantum cryptography applications. *Phys. Rev. A*, 95:010101, 2017.

[91] X. Deng, Y. Xiang, C. Tian, G. Adesso, Q. He, Q. Gong, X. Su, C. Xie, and K. Peng. Demonstration of monogamy relations for Einstein-Podolsky-Rosen steering in gaussian cluster states. *Phys. Rev. Lett.*, 118:230501, 2017.

[92] B. Paul and K. Mukherjee. Shareability of quantum steering and its relation with entanglement. *Phys. Rev. A*, 102:052209, 2020.

[93] M. Wang, Y. Xiang, H. Kang, D. Han, Y. Liu, Q. He, Q. Gong, X. Su, and K. Peng. Deterministic distribution of multipartite entanglement and steering in a quantum network by separable states. *Phys. Rev. Lett.*, 125:260506, 2020.

[94] Z. Y. Hao, K. Sun, Y. Wang, Z. H. Liu, M. Yang, J. S. Xu, C. F. Li, and G. C. Guo. Demonstrating shareability of multipartite Einstein-Podolsky-Rosen steering. *Phys. Rev. Lett.*, 128:120402, 2022.

[95] J. Singh, K. Bharti, and Arvind. Quantum key distribution protocol based on contextuality monogamy. *Phys. Rev. A*, 95:062333, 2017.

[96] A. K. Ekert. Quantum cryptography based on Bell's theorem. *Phys. Rev. Lett.*, 67:661–663, 1991.

[97] H. K. Lo and H. F. Chau. Unconditional security of quantum key distribution over arbitrarily long distances. *Science*, 283(5410):2050–2056, 1999.

[98] M. P. Seevinck. Monogamy of correlations versus monogamy of entanglement. *Quantum Inf. Process.*, 9:273–294, 2010.

[99] M. Pawłowski. Security proof for cryptographic protocols based only on the monogamy of Bell's inequality violations. *Phys. Rev. A*, 82:032313, 2010.

[100] M. Tomamichel, S. Fehr, J. Kaniewski, and S. Wehner. A monogamy-of-entanglement game with applications to device-independent quantum cryptography. *New J. Phys.*, 15:103002, 2013.

[101] Y. Wang, W.-s. Bao, H.-w. Li, C. Zhou, and Y. Li. Finite-key analysis for one-sided device-independent quantum key distribution. *Phys. Rev. A*, 88:052322, 2013.

[102] B. Opanchuk, L. Arnaud, and M. D. Reid. Detecting faked continuous-variable entanglement using one-sided device-independent entanglement witnesses. *Phys. Rev. A*, 89:062101, 2014.

[103] N. Walk, S. Hosseini, J. Geng, O. Thearle, J. Y. Haw, S. Armstrong, S. M. Assad, J. Janousek, T. C. Ralph, T. Symul, H. M. Wiseman, and P. K. Lam. Experimental demonstration of Gaussian protocols for one-sided device-independent quantum key distribution. *Optica*, 3(6):634–642, 2016.

[104] M. K. Olsen, A. S. Bradley, and M. D. Reid. Continuous variable tripartite entanglement and Einstein-Podolsky-Rosen correlations from triple nonlinearities. *J. Phys. B: At. Mol. Opt. Phys.*, 39:2515, 2006.

[105] Q. Y. He and M. D. Reid. Genuine multipartite Einstein-Podolsky-Rosen steering. *Phys. Rev. Lett.*, 111:250403, 2013.

[106] A. S. Villar, M. Martinelli, C. Fabre, and P. Nussenzveig. Direct production of tripartite pump-signal-idler entanglement in the above-threshold optical parametric oscillator. *Phys. Rev. Lett.*, 97:140504, 2006.

[107] M. K. Olsen. Controlled Asymmetry of Einstein-Podolsky-Rosen Steering with an Injected Nondegenerate Optical Parametric Oscillator. *Phys. Rev. Lett.*, 119:160501, 2017.

[108] H. S. Qureshi, S. Ullah, and F. Ghafoor. Bipartite Gaussian quantum steering, entanglement, and discord and their interconnection via a parametric down-converter. *Appl. Opt.*, 59(9):2701–2708, 2020.

[109] T. H. Chen, K. Y. Pan, C. Xiao, Y. B. Yu, and A. X. Chen. Asymmetric quantum steering generated by triple-photon down-conversion process with injected signals. *Frontiers in Physics*, 10, 2022.

[110] T. H. Chen, Y. B. Yu, and A. X. Chen. Genuine quadripartite steering in three-photon spontaneous parametric down-conversion. *Phys. Rev. A*, 106:L060601, 2022.

[111] S. Liu, Y. Zheng, Z. Fang, X. Ye, Y. Cheng, and X. Chen. Effective four-wave mixing in the lithium niobate on insulator microdisk by cascading quadratic processes. *Opt. Lett.*, 44(6):1456–1459, 2019.

[112] G. Misra and A. Kumar. Continuous variable multipartite entanglement in cascaded nonlinearities. *Journal of Optics*, 24(7):074004, 2022.

[113] M. K. Olsen and A. S. Bradley. Bright bichromatic entanglement and quantum dynamics of sum frequency generation. *Phys. Rev. A*, 77:023813, 2008.

[114] Y. Yu, F. Ji, Z. Shi, H. Wang, J. Zhao, and Y. Wang. Three-color entanglement generated by single-pass cascaded sum-frequency processes. *Laser Physics Letters*, 14(3):035202, 2017.

[115] S. L. Liang, Y. Liu, Y. B. Yu, J. Y. Lan, X. B. He, and K. X. Guo. Genuine quadripartite quantum steering generated by an optical parametric oscillation cascaded with a sum-frequency process. *Europhysics Letters*, 131(1):10001, 2020.

[116] Y. Liu, S. L. Liang, G. R. Jin, Y. B. Yu, and A. X. Chen. Einstein-Podolsky-Rosen steering in spontaneous parametric down-conversion cascaded with a sum-frequency generation. *Phys. Rev. A*, 102:052214, 2020.

[117] S. L. Liang, G. R. Jin, Y. B. Yu, and A. X. Chen. Asymmetric quantum steering in cascaded nonlinear process. *Results in Physics*, 28:104636, 2021.

[118] Y. R. Shen, T. H. Chen, S. L. Liang, X. Y. Cheng, J. W. Lv, Y. X. Jiang, L. Cheng, Y. B. Yu, G. R. Jin, and A. X. Chen. The generation of genuine quadripartite Einstein-Podolsky-Rosen steering in an optical superlattice. *Sci. Rep.*, 13:21196, 2023.

[119] Y. Liu, S. L. Liang, G. R. Jin, and Y. B. Yu. Genuine tripartite Einstein-Podolsky-Rosen steering in the cascaded nonlinear processes of third-harmonic generation. *Opt. Express*, 28(3):2722–2731, 2020.

[120] Y. Liu, S. L. Liang, G. R. Jin, Y. B. Yu, J. Y. Lan, X. B. He, and K. X. Guo. Generation of tripartite Einstein-Podolsky-Rosen steering by cascaded nonlinear process. *Chin. Phys. B*, 29(5):050301, 2020.

[121] K. Y. Pan, T. H. Chen, C. Xiao, Y. B. Yu, and A. X. Chen. Multi-color quantum steering frequency comb produced by enhanced Raman scattering. *Results in Physics*, 37:105518, 2022.

[122] Z. Li, S. Zhai, L. Kong, and X. Kang. Three-color and tripartite steering generated by intracavity cascaded processes. *Optical Engineering*, 62(2):028101, 2023.

[123] C. Xiao, X. Y. Cheng, J. W. Lv, Y. R. Shen, Y. X. Jiang, L. Cheng, Y. B. Yu, G. R. Jin, and A. X. Chen. One to many one-way control in quadripartite asymmetric Einstein-Podolsky-Rosen steering. *New J. Phys.*, 26(1):013049, 2024.

[124] G. Lindblad. On the generators of quantum dynamical semigroups. *Commun. Math. Phys.*, 48(2):119–130, 1976.

[125] H. Carmichael. *Statistical Methods in Quantum Optics 1: Master Equations and Fokker-Planck Equations*. Physics and astronomy online library. Springer, 1999.

[126] R. J. Glauber. Coherent and incoherent states of the radiation field. *Phys. Rev.*, 131:2766–2788, 1963.

[127] E. C. G. Sudarshan. Equivalence of semiclassical and quantum mechanical descriptions of statistical light beams. *Phys. Rev. Lett.*, 10:277–279, 1963.

[128] E. Wigner. On the quantum correction for thermodynamic equilibrium. *Phys. Rev.*, 40:749–759, 1932.

[129] P. D. Drummond and C. W. Gardiner. Generalised P-representations in quantum optics. *J. Phys. A: Math. Gen.*, 13(7):2353, 1980.

[130] P. Drummond and M. Hillery. *The quantum theory of nonlinear optics*. Cambridge University Press, 2014.

[131] H. Risken. *The Fokker-Planck Equation: Methods of Solution and Applications*. Springer series in synergetics. Springer-Verlag, 1989.

[132] D.F. Walls and G.J. Milburn. *Quantum Optics*. Springer Berlin Heidelberg, 2008.

[133] C. Fabre, J. M. Courty, E. Giacobino, A. Heidmann, L. Hilico, P. Mandel, N. Pettiaux, and S. Reynaud. *Semi-Classical Input-Output Linearization Techniques for Quantum Fluctuations and Beyond*, pages 211–220. Springer US, Boston, MA, 1992.

[134] P. D. Drummond and D. F. Walls. Quantum theory of optical bistability. I. Nonlinear polarisability model. *J. Phys. A: Math. Gen.*, 13(2):725, 1980.

[135] C. Fabre, E. Giacobino, A. Heidmann, L. Lugiato, S. Reynaud, M. Vadacchino, and Wang Kaige. Squeezing in detuned degenerate optical parametric oscillators. *Quantum Optics: Journal of the European Optical Society Part B*, 2(2):159, 1990.

[136] M. K. Olsen and A. S. Bradley. Asymmetric polychromatic tripartite entanglement from interlinked $\chi^{(2)}$ parametric interactions. *Phys. Rev. A*, 74:063809, 2006.

[137] S. L. W. Midgley, M. K. Olsen, A. S. Bradley, and O. Pfister. Analysis of a continuous-variable quadripartite cluster state from a single optical parametric oscillator. *Phys. Rev. A*, 82:053826, 2010.

[138] S. Chaturvedi, C. W. Gardiner, I. S. Matheson, and D. F. Walls. Stochastic analysis of a chemical reaction with spatial and temporal structures. *J. Stat. Phys.*, 17(6):469–489, 1977.

[139] M. J. Collett and D. F. Walls. Squeezing spectra for nonlinear optical systems. *Phys. Rev. A*, 32:2887–2892, 1985.

[140] C. Gardiner. *Stochastic methods*, volume 4. Springer Berlin, 2009.

[141] C. W. Gardiner and M. J. Collett. Input and output in damped quantum systems: Quantum stochastic differential equations and the master equation. *Phys. Rev. A*, 31:3761–3774, 1985.

[142] P. Ornelas-Cruces and L. Rosales-Zárate. Monogamy relations for bipartite and tripartite entanglement via intracavity spontaneous parametric down-conversion. *Phys. Lett. A*, 492:129227, 2023.

[143] P. Ornelas-Cruces and L. Rosales-Zárate. Bipartite and tripartite steering by a nonlinear medium in a cavity. *J. Opt. Soc. Am. B*, 40(9):2441–2449, 2023.

[144] A. Yariv and W. H. Louisell. 5a2–theory of the optical parametric oscillator. *IEEE Journal of Quantum Electronics*, 2(9):418–424, 1966.

[145] E. Cassedy and M. Jain. A theoretical study of injection tuning of optical parametric oscillators. *IEEE Journal of Quantum Electronics*, 15(11):1290–1301, 1979.

[146] M. Oshman and S. Harris. Theory of optical parametric oscillation internal to the laser cavity. *IEEE Journal of Quantum Electronics*, 4(8):491–502, 1968.

[147] A. E. Siegman. Nonlinear optical effects: an optical power limiter. *Applied Optics*, 1(101):127–132, 1962.

[148] J Bjorkholm. Some effects of spatially nonuniform pumping in pulsed optical parametric oscillators. *IEEE Journal of Quantum Electronics*, 7(3):109–118, 1971.

[149] O. Slattery, L. Ma, K. Zong, and X. Tang. Background and review of cavity-enhanced spontaneous parametric down-conversion. *Journal of Research of the National Institute of Standards and Technology*, 124:1, 2019.

[150] H. A. Bachor and T. C. Ralph. *A guide to experiments in quantum optics*. John Wiley & Sons, 2019.